Alma Mater Studiorum – Università di Bologna

DOTTORATO DI RICERCA IN

SCIENZE CHIRURGICHE: Progetto n.1 METODOLOGIE DI RICERCA NELLE MALATTIE VASCOLARI"

Ciclo XXIV

Settore Concorsuale di afferenza: MED/22

Evaluation of cardiovascular disease markers in patients submitted to carotid artery stenting or endarterectomy.

Presentata da: Silvia Fittipaldi

Coordinatore Dottorato

Chiar.mo Prof. Andrea Stella

Relatore

Chiar.mo Prof Gianandrea Pasquinelli

Esame finale anno 2012

ABSTRACT

Introduction. Microembolization during the carotid artery revascularization procedure may cause cerebral lesions. Elevated C-Reactive Protein (hsCRP), Vascular endothelial growth factor (VEGF) and serum amyloid A protein (SAA) exert inflammatory activities thus promoting carotid plaque instability. Neuron specific enolase (NSE) is considered a marker of cerebral injury. Neoangiogenesis represents a crucial step in atherosclerosis, since neovessels density correlates with plaque destabilization. However their clinical significance on the outcome of revascularization is unknown. This study aims to establish the correlation between palque vulnerabilty, embolization and histological or serological markers of inflammation and neoangiogenesis.

Methods. Serum hsCRP, SAA, VEGF, NSE mRNA, PAPP-A mRNA levels were evaluated in patients with symptomatic carotid stenosis who underwent filter-protected CAS or CEA procedure. Cerebral embolization, presence of neurologicals symptoms, plaque neovascularization were evaluated testing imaging, serological and histological methods. Results were compared by Fisher's, Student T test and Mann-Whitney U test.

Results. Patients with hsCRP<5 mg/l, SAA<10mg/L and VEGF<500pg/ml had a mean PO of 21.5% versus 35.3% (p<0.05). In either group, embolic material captured by the filter was identified as atherosclerotic plaque fragments. Cerebral lesions increased significantly in all patients with hsCRP>5mg/l and SAA>10mg/l (16.5 vs 2.8 mean number, 3564.6 vs 417.6 mm^3 mean volume).

Discussion. High hsCRP, SAA and VEGF levels are associated with significantly greater embolization during CAS and to the vulnerabiliy of the plaque. This data suggest CAS might not be indicated as a method of revascularization in this specific group of patients.

Keywords: atherosclerosis, vasa vasorum, cerebral lesion, SAA

LIST OF ORIGINAL PUBLICATIONS

The data presented in this thesis ar based on the following original articles

Faggioli G*, Fittipaldi S*, Pini R., Beltrandi E, Mauro R, Freyrie A, Rapezzi C, Stella A, Pasquinelli G. C-Reactive protein and embolization during carotid artery stenting. A serological and morphological study. Histol Histopathol (2011) 26: 843-853. *first author.

Faggioli G, Pini R, Mauro R, Pasquinelli G, Fittipaldi S, Freyrie A, Serra C, Stella A. Identification of Carotid:'Vulnerable Plaque' by Contrast-enhanced Ultrasonography: correlation with Plaque Histology, Symptoms And Cerebral Computed Tomography. Eur J Vasc Endovasc Surg (2011) Feb;41(2):238-48.

Vasuri F, Resta L, Fittipaldi S, Malvi D, Pasquinelli G. RUNX-1 and CD44 as markers of resident stem cell derivation in undifferentiated intimal sarcoma of pulmonary artery. A case report Histopathology. In press.

Vasuri F*, Fittipaldi S*, Buzzi M, Degiovanni A, Stella A, D'Errico-Grigioni A, Pasquinelli G. Nestin and WT1 expression in small-sized vasa vasorum from human normal arteries. Histology and Histopathology. *first author, in press.

Stella A*, Fittipaldi S*, Pini R, Pasquinelli G, Mauro R, Beltrandi E, Freyrie A, Gargiulo M, Faggioli G. High Sensitivity C-Reactive Protein and Vascular Endothelial Growth Factor as Indicators of Carotid Plaque Vulnerability, In revision to Atherosclerosis. *first author.

Some unpublished data are also presented

Overview of the PhD project and data obtained

The main objective of our research project is the cellular and morphological characterization of carotid plaque vulnerability using different approaches; clinical analysis, immunohistochemical and molecular assays. The principal physiopathologic processes studied are inflammation, neoangiogenesis and calcification (osteogenic differentiation).

Clinical study

First we evaluated serological marker of cardiovascular disease in patients submitted to carotid artery stenting (CAS) or endarterectomy (CEA); 84 patients with >70% carotid artery stenosis were preferentially submitted to CEA (50) or CAS (34). On CAS we showed a direct positive correlation between post procedural cerebral lesions, the quantity of thromboembolic material retrieved on the filter and pre-operatory serum levels of inflammation markers. Patients with high hsCRP (>5mg/l), SAA (>10 mg/L) and VEGF (>500pg/ml) are associated with significantly greater embolization during CAS procedure and particularly in dishomogenous plaque. Volume and number of total cerebral lesions post procedural increased significantly in all patients having high hsCRP and SAA values. These data suggest that CAS might not be indicated in this specific group of patients with plaque prone to rupture. Secondly we compared different histological parameters of plaque vulnerability with the Contrast-enhanced Ultrasonography. An increase of dB-E was associated significantly with thinner fibrous cap (TFC <200 um, dB-E: 5.96 vs 3), greater inflammatory infiltrate (7.4 vs 3.2) and greater microvessels density (5.5 vs 2.5). We observed that either in symptomatic patients or in presence of pre-operative cerebral ipsilateral embolic lesions, dB-E values increased significantly (respectively 7.4 vs 3.5 and 5.96 vs 3.0) (3). In addition we observed that patients having neurological symptoms pre-operatively and vulnerable plaque had also high VEGF and hsCRP serum levels compared with

patients with non vulnerable. There was an inverse linear correlation between VEGF serum concentration and fibrous cap thickness. All patients presented an increase of 32% of neuronal specific enolase mRNA level expression after the CAS procedure compared to patients submitted to CEA procedure.

Study on vasculogenic niche

Another aspects of the research project is the vasa vasorum (VV) neovasculogenic potential and involvement in atherosclerosis. We studied Nestin, WT1, dPAPP-A and SAA4 expression in vasa vasorum in human normal arteries (n°20). We saw that Nestin and WT1 in adult VV are expressed in adult VV, especially in VV <50 μm diameter and gathered in "hot spots". The cytoplasmic colocalization of WT1 and nestin straightens the role of WT1 as a post-transcriptional activator of nestin protein. In our series WT1 was mainly cytoplasmic in the larger vessels, while nuclear expression increased in the smaller vessels ("second-order" VV). The nuclear localization of WT1 could express an increasing transcriptional activity in progenitor-committed Nestin-positive cells. We want to compare WT1/Nestin mRNA and protein hot-spots sub-cellular localization in normal arteries versus pathological arteries to assess a correlation with neovascularization during atherogenesis. The "hot spot" could therefore represent a valid model for the vasculogenic niche and the main source for neovasculogenesis during atherosclerosis. We are now performing the same analysis in atheroma lesions. We saw that dPAPP-A and SAA4 are specific histological and serological markers of atheromasic lesions presence. We also studied (data not presented) a case of pulmonary artery undifferentiated intimal sarcoma that expresses previously unreported markers; RUNX-1, Nestin, WT1 and CD44, commonly seen in different stages of the vascular differentiation hierarchy. These findings raise the question whether this neoplasm derives from a vessel wall-resident stem cell, like the hemangioblast or an embryonic-like stem cell.

Für meine Oma…

ABBREVIATIONS

ACAS: Asymptomatic carotid artherosclerosis study

ACST: Asymptomatic carotid surgery trial

AHA: American Heart Association

APO: Apolipoprotein

ASA: Acetylsalicylic acid

ATIR: Angiotensin type1 receptor

BAV: Bicuspid aortic valves

BNP: Brain natriuretic peptide

BMP2: Bone Morphogenetic Protein 2

BSA: Bovin serum albumine

CAD: Coronary artery disease

CAS: Carotid artery stenting

CCD: Charge-coupled device

CCP: Cathepsin cystein protease

cDNA: complementary DNA

CEA: Carotid endarterectomy

CEUS: Contrast-enhanced Ultrasound

CRP: C-reactive protein

CT: Computerized tomography

DAPI: Pro long anti-fade reagent

dB-E: db-Enhanced

DWI-MR: Diffusion weight resonance magnetic imaging

ECs: Endothelial cells

ELISA: Enzyme-linked immunosorbent assay

ESVS: European Society for Vascular Surgery

FBG: Fibrinogen

FFA: Free fatty acid

FLT: FMS-like tyrosine kinase

GSM: Gray Scale Measurement

HDL: High-density lipoprotein

HE: Hematoxylin-eosin

HMDS: Hexamethyldisilazene

HsCRP: highsensitivity C-reactive Protein

ICAM: intercellular adhesion molecule

IGF: Insulin-like growth factor

IHC: immunohistochemical

IL: interleukin

IMA: ischemia modified albumi

LDL: Low-density lipoprotein

LM: Light microscope

LOX1: Lectin-like oxidized low-density lipoprotein receptor 1

Lp-PLA2: lipoprotein-associated phospholipase A2

MBP: Eosinophil major basic protein

MCP-1: Monocytechemoattractant protein-1

miRNA: micro RNA

MMP: Matrix metalloproteinases

MPO: Myeloperoxidase

MR: Magnetic Resonance

mRNA: Messenger RNA

MYG: Myoglobin

NO: Nitric oxide

NSE: Neuron specific enolase

NT-proBNP: N-terminal prohormone of brain natriuretic peptide

OP: Occluded pore

Ox-LDL: oxidized low-density lipoprotein

PAD: Peripheral artery disease

PAI-1: Plasminogen activator inhibitor

PAPP-A: pregnancy-associated plasma protein-A

PCR: Polymerase chain reaction

PlGF: Placental growth factor

PO: Pore occluded

PTX3: Pentraxin-related protein

RBC: Red blood cells

RNA: Ribonucleic acid

ROI: Region of interest

RT: Room temperature

SAA: Serum amyloid A protein

SAA4: Serum amyloid A isoform 4

sCD163: soluble haemoglobin scavenger receptor

sCD40L: soluble CD40 ligand

SD: Standard deviation

SEM: Scanning electron microscopy

SI: Surface involvement

SMC: Smooth muscle cell

sPLA2: Secretory phopholipase A2

sTREM-1: soluble triggering receptor expressed on myeloid cells

SVS: Society of vascular surgeons

TF: Tissue factor

TFC: Thinner fibrous cap

TG: Triglyceride

TGF: Tumour growth factor

TIA: Transient ischemic attack

TIMP: Tissue inhibitors of metallo-proteinases

TNF: Tumour necrosis factor

TNI: Troponin I

TNT: Troponin T

VCAM: Vascular cell adhesion molecule

VEGF: Vascular endothelial growth factor

VV: Vasa Vasorum

VWFC: von Willebrand factor

WT1: Wilm's tumour suppressor

TABLE OF CONTENTS   Page

ABSTRACT

LIST OF ORIGINAL PUBLICATIONS

ABBREVIATIONS

Overview of the PHD project & data obtained

Patients CAS

Drug therapy CAS

Distribution and description of the material covering the filter

      Filter analysis by light microscopy

      Filter analysis by scanning electron microscopy

Evaluation of microvessel density with an ocular micrometer in
 carotid plaque at IHC

Markers levels pre-procedural, amounts of debris and
 cerebral lesions post-procedural

Patients

CEUS evaluation, inflammation and plaque vulnerability

VEGF, hsCRP serum levels and histological plaque vulnerability

Thin fibrous cap

CD31 and CD34

Nestin and WT1

Comparison between IHC and vessel morphology

Localization of Nestin and WT1 at immunofluorescence

INTRODUCTION

INTRODUCTION

Atherosclerosis

In 1628 William Harvey, St. Bartholomew's Hospital, London, describes the function of the heart, arteries and veins. It is considered to be one of the greatest advances in medicine. Between 1783 and 1793 Edward Jenner, a British country physician who created the smallpox vaccine, while doing an autopsy accidentally discovered coronary arteries disease. He was probably the first to associate angina pectoris with hardening of the arteries **(Fig 1)**.
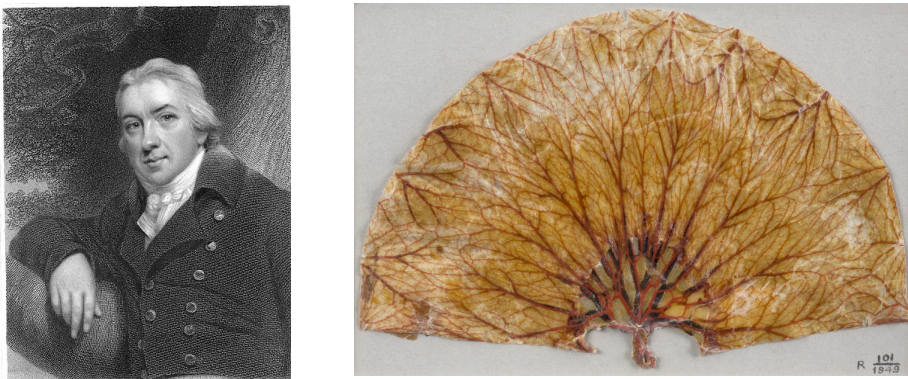
Figure 1: Edward Jenner and a stomach flattened and injected with wax to show the veins and arteries.

Highlights of the introduction

Nowadays, in occidental countries cardiovascular events, such as stroke, are the leading causes of death, thus the priority of primary and secondary

prevention (Rosamond et al., 2007). Even if selected patients with acute ischemic stroke are treated with promising experimental therapies, such as tissue plasminogen activator, the best approach to reduce stroke remains still prevention. An early diagnosis allows individuals at higher risk or prone to stroke to be identified and targeted for specific therapies or interventions (Goldstein et al., 2001). The presence of atherosclerotic lesions at the carotid bifurcation and the presence of ischemic cerebral lesions are the main factors leading to cardiovascular events. In fact, the presence of recent focal neurological symptoms ipsilateral to a carotid stenosis is a powerful predictor of 'high risk' carotid atherosclerosis. Especially, the risk of major events such as death or stroke, is further increased in patients presenting vulnerable plaque (Wang et al., 2010). The degree of stenosis is still the gold standard to assess stroke risk and subsequent indication to revascularization (R Rosamond et al., 2007). In symptomatic or asymptomatic patients with a stenosis greater than 60%, carotid endoarterectomy procedure (CEA) results respectively in a 56% and 34.5% reduction of the development of major events, thus proving the efficacy of the CEA intervention (ACAS 1991). However waiting time between diagnosis and CEA intervention can result in an interval stroke rate of 9%-15%. The aim of the early intervention is to avoid embolization caused by a vulnerable lesion at the carotid district, nevertheless there is a big issue to recognize "young" vulnerable plaque non-invasively before an acute clinical event occurs. (Setacci, et al., 2008). Different studies estimate the individual risk of stroke such as the Framingham risk score or the ABCD2 score system. The prognostic value of all these score systems improves if completed with clinical information, vascular imaging data and brain imaging data of patients. (A. Bhatt et al., 2011). Cerebro-ischemic symptoms, as transient ischemic attacks or amaurosis fugax, increased the risk of major events such as death or stroke (Liapis et al., 2001). In a magnetic resonance imaging prospective assessment study, it has been

3

shown, that the occurrence of cerebrovascular events in asymptomatic patients is associated with the characteristics of carotid plaque; thinned or ruptured fibrous caps, intraplaque hemorrhage, larger lipid-rich necrotic cores and larger maximum wall thickness. (Takaya 2006).

Stroke risk prediction based only on conventional risk factors is not enough; hence research is oriented on predictive biological biomarkers. Previous studies demonstrated the correlation between serological and structural markers of inflammation and neoangiogenesis related to the risk of cardiovascular events in the coronary district (Ferri et al., 2006). Thus biomarkers knowledge is necessary to allow primary prevention of coronary events (Muller et al., 2006). However there is yet no standard value for biomarkers able to identify a vulnerable plaque in the carotid district.

Evaluation of the silent atheroma non-invasively is only possible through recent imaging approaches and computed analysis such as pixel density analysis and elastography at Duplex examination, local temperature probe (Setacci, et al., 2008); these techniques allow to evaluate echostructural alterations, such as ulcers, typical of vulnerable plaque but not molecular composition. Thus, in addition to structural plaque analysis and inflammation protein, particular attention is given to molecular pathway involved in the atherosclerotic lesions development.

Studies related to the discovery of novel biomarkers signature involved in plaque destabilization and stroke are of fundamental importance .

Carotid plaque: pathogenesis

Atherosclerosis is characterized by intimal lesions, the atheromas, which are protrusions within the vascular lumen that can determine alterations in the normal blood flow and direct damage to the vessel structure. At first,

these lesions present a focal distribution in the artery; however, they rapidly begin to increase in number as the disease advances, until affecting the whole circumference of the vessel walls that are more severely damaged **(Fig 2)**.

The structure of the basic lesion consists in a plaque localised in the intima presenting a central lipid core (cholesterol and its esters) covered by a fibrous cap.
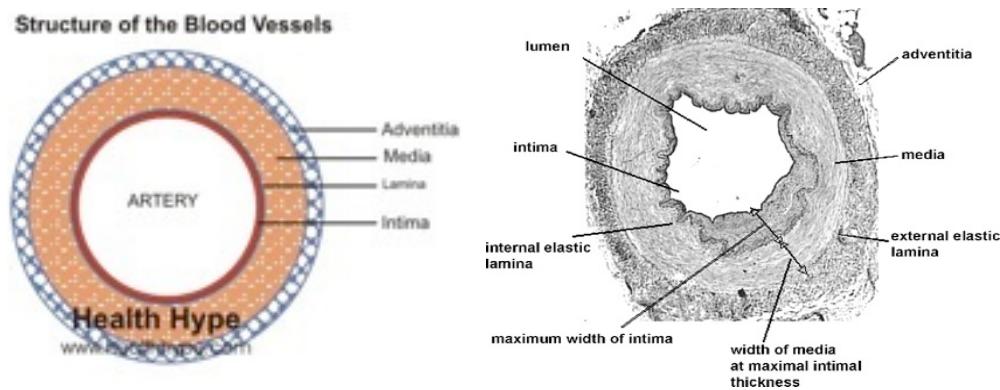
Figure 2: Structure of a blood vessel (right: healthy type, left: atheromasic vessels)

Atherosclerotic plaques are mainly composed of cellular elements: smooth-muscle cells, macrophages and leukocytes, connective tissue of extracellular matrix – collagen, elastic fibres and proteoglycans – and intra- and extracellular lipid deposits. **(Fig 3).** The relative proportion of these components varies depending on the different plaques, which results in a wide spectrum of lesions with different degrees of instability. The overlaying fibrous cap is composed of smooth-muscle cells, few leukocytes and relatively dense connective tissue. The cellular area which is below and

adjacent to the fibrous cap – the "shoulder" of the fibrous cap – is composed of macrophages, smooth-muscle cells and T lymphocytes. The deep necrotic core presents a disorganised mass of lipid material, which is composed of cholesterol crystals, cellular debris, thrombi undergoing organization and other plasma proteins. Lipids are mainly composed of cholesterol and its esters. There are cells that have phagocytized this lipid material: they are called "foam cells" and they are, in particular circulating monocytes activated in macrophages, and activated smooth-muscle cells. Finally, especially at the periphery of the lesions, frequent aspects of neovascularization can be detected and they are represented by the proliferation of blood vessels that can be more or less mature. The variations in the histological characteristics of the plaques depend on the number of smooth-muscle cells and macrophages, the amount of collagen and other extracellular components, besides the lipid contents (Cotran et al., VI Ed)

The pathogenic development of these lesions is still unclear; the endothelium is believed to play a fundamental role in the initial development of the plaque. The most widely accepted hypothesis is that what triggers this process is a reaction to the damage of the intima. Therefore, atherosclerosis would represent an inflammatory response of the vessel wall (Ross et al., 1993). The element that characterizes the primary lesions is the presence of an endothelium that is not morphologically damaged yet. This has led to consider that the most important factor in development of the disease is a cellular dysfunction and activation, together with an increase in the endothelial permeability, rather than a direct damage. This process manifests itself with an increased leukocyte and monocyte adhesion, which is highlighted by alterations in the expression of the endothelial adhesion molecules ICAM-1 and VCAM-1 (InterCellular Adhesion Molecule 1, Vascular Cell Adhesion Molecole 1) (O'Brien et al., 1996; Cybulsky et al., 1991; Gimbrone et al., 1997).
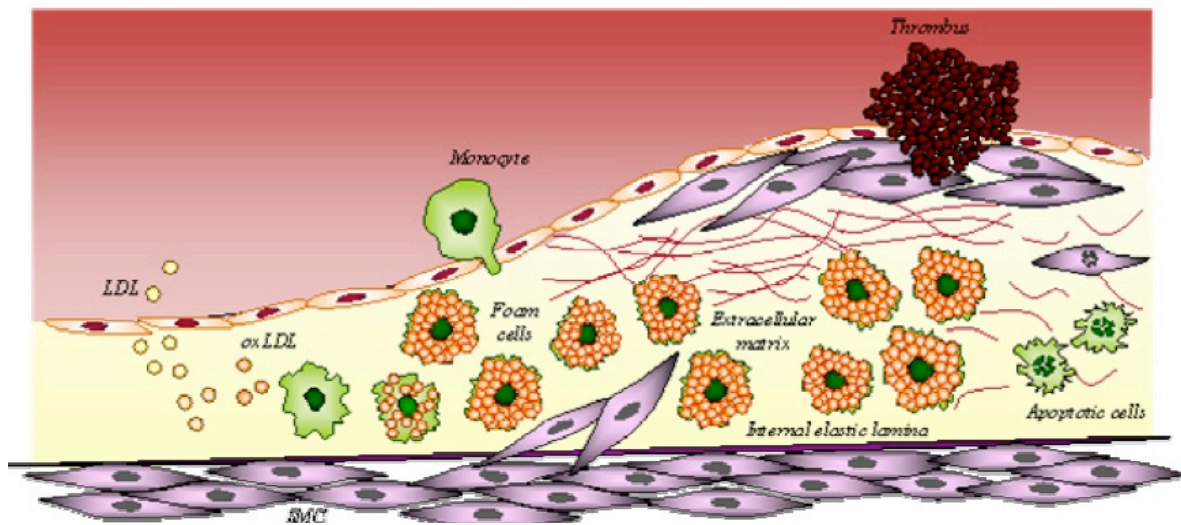
Figure 3: Development and progression of atheromasic lesions (Fortunato et al, 2007).

The main causes of the endothelial dysfunction and damage are the hemodynamic changes that occur in some specific points of the circulatory tree – major branch points and bifurcations – and the harmful effects of hypercholesterolemia.

Effects of hemodynamics on vascular cells.

In support of the role of the blood flow, and of its changing from laminar to turbulent with a loss of tangential force – and, therefore, a low "shear stress" – it is relevant to consider the location of the plaques, which can be more frequently found at the ostial area or at the bifurcations.

The blood flow undergoing these changes, with variable levels of parietal stress, is believed to cause the endothelial dysfunctions and thus predispose the development of these lesions in these predictable locations **(Fig 4)**. Cyclic strain has been shown to stimulate expression of cellular adhesion molecules such as ICAM-1 and intracellular second messenger systems such as the adenylate cyclase-cAMP, diacylglycerol-IP3, and protein kinase

C pathways (Pradhan et al., 2004).
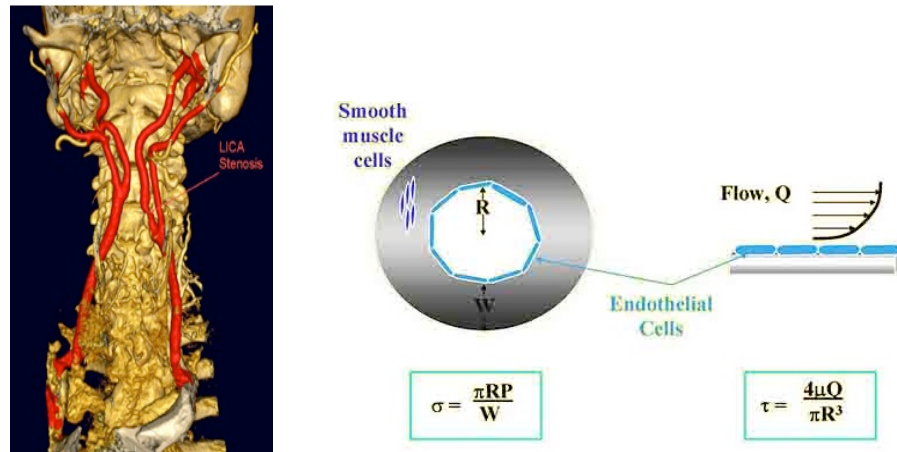
Figure 4: Hemodynamic forces. **A)** Severe stenosis proximal left internal carotid artery as seen in 3D (Rochester Medical Center) **B)** Endothelial cells are subjected to both a tangential, parallel force (shear stress) as well as a circumferential, perpendicular force (cyclic strain). (Pradhan et al., 2004).

This causes the activation of many pro-inflammatory and pro-atherogenic genes, thereby the production of cytokines, adhesion molecules and coagulation proteins, which produce an increase in the endothelial permeability, the cellular turnover and the cellular endocytosis of the LDL that is present in this area.

Hypercholesterolemia.

Hypercholesterolemia can trigger the development of plaque, due to a higher deposition of cholesterol in the subintimal area. Moreover, hyperlipidemia itself determines an endothelial dysfunction owing a greater production of superoxide dismutase and other free radicals of oxygen that deactivate nitric oxide, which is the main relaxing factor in arteries. The oxidative modifications induced by free radicals, and produced by

macrophages and endothelial cells, lead to the formation of oxidized LDL molecules, which in turn contribute to the formation of lesions in different ways:

Oxidized LDL:

1. can be easily phagocytized by macrophages, resulting in the formation of foam cells,

2. are chemotactic for circulating monocytes,

3. increase the adhesion of the monocytes especially by inducing endothelial adhesion molecules,

4. inhibit the viability of the macrophages that are already in the lesion by facilitating the recruitment and the survival of the macrophages in the plaque,

5. stimulate the release of grow factors and cytokines,

6. are cytotoxic to the endothelial cells and the smooth-muscle cells,

7. are immunogenic, as they induce the production of antibodies against the oxidized lipoproteins.

The idea that hyperlipidemia leads to the formation of lesions by means of the oxidative stress on the endothelium is proven by clinical and experimental studies which show how antioxidant proteins and medications that reduce oxidation have a protective effect on atherosclerosis. Moreover, the decrease in cholesterol and the antioxidant therapy improve the endothelial function (Steinberg, 1997)

During the genesis of the plaque, monocytes subsequently adhere to the activated endothelial surface, thanks to the adhesion molecules, and through these cells they migrate to the subendothelial area. Here they differentiate into macrophages and phagocytize the oxidized LDL molecules, thus

becoming foam cells. Macrophages play a multifactorial role in the progression of atherosclerosis thanks to the secretion of proteins such as the interleukins (IL-1) and the tumour growth factor (TNF), which increase the adhesion of the leukocytes. Furthermore, macrophages produce radicals of oxygen, which cause the oxidation of the LDL molecules in the lesion, and elaborate growth factors that can contribute to the proliferation of the smooth-muscle cells. Prematurely during the development of the lesion, the smooth-muscle cells migrate to the intima, where they proliferate and determine the deposition of extracellular material, thus facilitating the enhancement of the plaque (Ridker et al., 2002).

During the early stages of atherogenesis, the intimal plaque is composed of an aggregation of foam cells, some of which may die and release extracellular lipids and cellular debris, which surround the muscle cells. The adipose cellular atheroma gradually changes, as a consequence of the deposition of collagen and proteoglycans. The connective tissue, particularly abundant in the intimal area, produces the fibrous cap, which then develops in the mature fibroatheroma. Some of these lesions subsequently undergo further modifications:

A. accumulate of larger amount of connective tissue, thus becoming fibrous plaques.

B. calcification deposits.

C. develop a central core that is rich in lipids and foam cells, which increase the potential risk of developing serious complications (Ross et al., 1993).

The fibrous cap

The fibrous cap is the outer fibrous part that covers the atherosclerotic plaque. It is the structure that separates the blood flow from the necrotic core of the lesion, therefore it is very important for the stability of the plaque. If there are lesions on its surface, circulating elements – platelets and coagulation factors – can come into contact with the inner elements of the plaque, thus causing the formation of thrombi **(Fig 3).**

The fibrous cap originates from the secretory activity of the smooth-muscle cells. These cells migrate from the media to the sub-endothelial area – during the formation of the plaque – where they produce collagen, elastic fibres and proteoglycans, in order to limit the expansion of the inflammatory process of the plaque towards the vascular lumen (Ross et al., 1993; O'Brien et al., 1996; Cybulsky et al., 1991; Gimbrone et al., 1997; Mauriello et al., 2010)

Therefore, the presence of a thin-fibrous cap represents a condition of unstable plaque prone to rupture. The development of a thin-fibrous cap is determined by a series of phenomena:

1. activation of the leukocytes inside the plaque and production of metalloproteinases,

2. degradation of collagen and proteoglycans, which are produced by the smooth-muscle cells,

3. release of cytokines that can reduce the activity of the smooth-muscle cells.[34]

Histological tests have highlighted that the thin-fibrous cap is associated with higher concentrations of macrophages in the subendothelial area. The

thin-fibrous cap (<65 μm) is a condition of instability of the plaque, because it may cause ruptures on its surface, independently from the size of the necrotic core.

In general, in the areas that present lesions of the fibrous cap that do not determine more severe clinical manifestations, the healing of the ulcerated surface is not complete. These areas present a weaker resistance that can subsequently determine other fractures on the surface, which can be associated with more severe clinical manifestations. This explains the typical manifestations of the carotid plaque. As a premonitory sign we can consider transient ischemic attacks (TIA), which are the epiphenomenon of a microfracture on the surface of the atherosclerotic lesion; in the following days, this may result in a major ischemic event (stroke), due to another rupture of the plaque that had not completely healed (Redgrave et al., 2006; Virmani et al., 2003; Virmani et al., 2006).

Instrumental evaluations. In the ultrasound study, the morphology of the surface of the plaque represents an additional element in the evaluation of the risk associated with a carotid lesion, besides the analysis of the degree of stenosis. Therefore, the identification of alterations on the surface of the plaque, such as the ulcerative lesions (which are identified as introflexions of the surface of the plaque of at least 2 mm per 2 mm of length), is very important in the overall evaluation of the patient, as it allows to identify an additional risk of ischemic events **(Fig 5)**. There are other methods of imaging such as the Computerized Tomography (CT) or the Magnetic Resonance (MR), which allow to identify the structural alterations and the risk of cerebral events due to the presence of a particularly thin-fibrous cap. However, in the clinical practice they are used less than the ultrasound scan (Lovett et al., 2004; Wasserman 2008; Takaya et al., 2006).
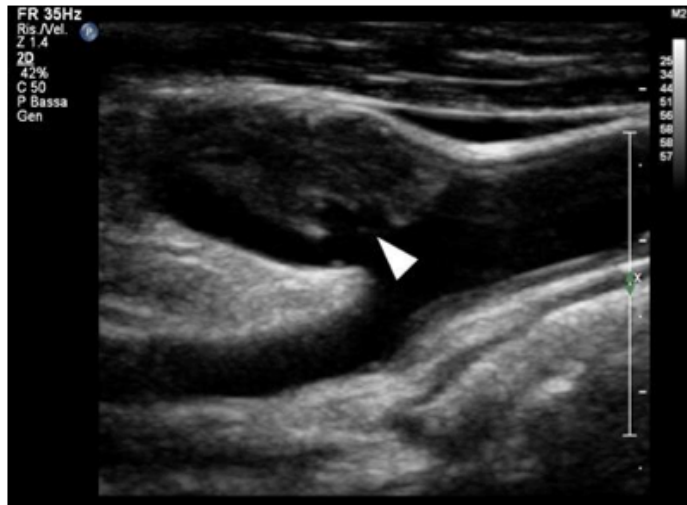
Figure 5: Ulcerated plaque on the surface of the fibrous cap (arrow), identified by means of an ultrasound evaluation. The presence of lesions in the structure of the carotid plaque represents a condition of structural instability and, therefore, of a higher risk of cerebrovascular events

The alterations on the surface of the plaque or the identification of a thin-fibrous cap represent a condition of instability of the plaque and a higher cerebrovascular risk; however, their role is marginal in the decision-making process for the surgical treatment of the carotid lesions. Indeed, the data of most of the clinical trials, from which the current indications originate, refer above all to the evaluation of the degree of stenosis and to the symptomatology that is associated with it.

Plaque classification

The classification of atherosclerotic lesions was initially carried out by macroscopic observation, using descriptive terms such as "Lipid streak" or

atheromatous plaque, fibrous or broken. The terminology varied from study to study so the correlation of data was impossible. In 1994-1995, the American Heart Association (AHA) has established criteria by which plaques are classified according to cellular content and structure, analysing the area of major lesion (Stary et al., 1995) **(Table 1a)**. It is important to differentiate;

–   young stable plaque with a low extracellular lipid content, less dangerous (types I–III)

–   unstable plaque, more dangerous types including plaque with a high extracellular lipid content (types IV and Va), more prone to rupture and acute thrombosis (Richardson et al 1989; Cheng 1993),

–   and older calcified and fibrotic plaque (types Vb and Vc), which are dangerous because of their high degree of stenosis and the risk of rupture (Table 1a, b)**.**

Terms for Atherosclerotic Lesions in Histological Classification		Other Terms for the Same Lesions Often Based on Appearance to the Unaided Eye	
Type I lesion	Initial lesion		
Type II lesion		Fatty dot or streak	Early lesion
IIa	Progression-prone type II lesion		
IIb	Progression-resistant type II lesion		
Type III lesion	Intermediate lesion (preatheroma)		
Type IV lesion	Atheroma	Atheromatous plaque, fibrolipid plaque, fibrousplaque, plaque	Advanced lesions, raised lesions
Va	Fibroatheroma (type V lesion)		
Vb	Calcific lesion (type VII lesion)	Calcified plaque	
Vc	Fibrotic lesion (type VIII)	Fibrous plaque	
Type VI lesion	Lesion with surface defect and/or hematoma/hemorrhage and/or thrombotic deposit	Complicated lesion, complicated plaque	

Table 1a: AHA classification

Culprit lesion	A lesion in a coronary artery considered, on the basis of angiographic, autopsy or other findings, to be responsible for the clinical event. In unstable angina, myocardial infarction and sudden coronary death, the culprit lesion is often a plaque complicated by thrombosis extending into the lumen.
Eroded plaque	A plaque with loss and/or dysfunction of the lumenal endothelial cells leading to thrombosis. There is usually no additional defect or gap in the plaque, which is often rich in smooth muscle cells and proteoglycans.
High-risk, vulnerable and thrombosis-prone plaque	These terms can be used as synonyms to describe a plaque that is at increased risk of thrombosis (or rethrombosis) and rapid stenosis progression.
Inflamed thin-cap fibroatheroma (TCFA)	An inflamed plaque with a thin cap covering a lipid-rich, necrotic core. An inflamed TCFA is suspected to be a high-risk/vulnerable plaque.
Plaque with a calcified nodule	A heavily calcified plaque with the loss and/or dysfunction of endothelial cells over a calcified nodule, resulting in loss of fibrous cap, that makes the plaque at high-risk/vulnerable. This is the least common of the three types of suspected high-risk/vulnerable plaques.
Ruptured plaque	A plaque with deep injury with a real defect or gap in the fibrous cap that had separated its lipid-rich atheromatous core from the flowing blood, thereby exposing the thrombogenic core of the plaque. This is the most common cause of thrombosis.
Thrombosed plaque	A plaque with an overlying thrombus extending into the lumen of the vessel. The thrombus may be occlusive or non-occlusive.
Vulnerable patient	A patient at high-risk (vulnerable, prone) to experience a cardiovascular ischemic event due to a high atherosclerotic burden, high-risk/vulnerable plaques, and/or thrombogenic blood.

Table 1b: This second table above is a summary of the crucial definitions related to the vulnerable plaque (Schaar et al., 2004).

The calcification

The calcification at the level of the arteries is a process that is not clear yet and can appear both at the level of the media and at the level of the intima.

Media. The involvement of the media, which is defined as Monckeberg's calcific sclerosis, is a process that begins in areas that are not generally involved in atherosclerotic manifestations, such as the distal vessels of the limbs, the visceral vessels and the thyroid vessels. The calcification is associated with pathologies characterised by ionic alterations: metabolic dysfunctions, electrolyte disorders, diabetes and chronic kidney failure. The calcification can also be determined by alterations of the nerve stimuli and neuropathies. Another possible cause is the lumbar sympathectomy, after which the area of the sympathectomy shows an increased development of calcifications of the media in the vessels of the ipsilateral foot (88% in 2 years) compared to the contralateral foot (18%).

Intima. The most common condition is the intimal calcification that develops at the level of the atherosclerotic lesions. The most widely accepted hypotheses associate the inflammation in the plaque with the deposition of calcium crystals (besides the effect caused by alterations in the metabolism of phosphorus and calcium). The phlogosis at the level of the atherosclerotic lesion is associated with the release of cytokines, which cause the production of molecules that stimulate the formation of calcified nodules. The Bone Morphogenetic Protein 2 (BMP2), which is secreted by the smooth-muscle cells, plays a fundamental role in this process. The stimuli inside the plaque can be very weak – thus determining microcalcifications – or they can be particularly intense, thus causing a progressive differentiation of the smooth-muscle cells into cells with an osteoblastic/ osteoclastic activity and the formation of bone matrix or even bone tissue. In the atherosclerotic plaques, calcium initially develops in nodules that are at a basal level and, subsequently in microcrystals in the whole plaque (Doherty et al., 2004; Abedin et al., 2004: Demer et al., 2003).

At the level of the vessels, the identification of calcifications can be an indicator of atherosclerosis. In the coronary arteries, calcium is located only in the atherosclerotic plaques: for this reason, methods such as the TC have been introduced for the non-invasive evaluation of these lesions (Calcium Score). At the level of the carotid stenoses, as the ultrasound scan is the most used method of investigation to easily identify the presence of a plaque, the role of the calcification as an indicator of atherosclerosis is not considered. On the contrary, the presence of calcific deposits in the carotid is an indirect indicator of the instability of the plaque. Indeed, the histological evaluation of the carotid plaques has highlighted in many studies that, in general, the calcified plaques can be found in asymptomatic patients, whereas calcifications are scarce or inexistent in patients who have had a neurological symptomatology and, thus, with unstable lesions. Afterwards, analyses on anatomopathological reports have confirmed that

the calcification inside the carotid plaque is associated with a thicker fibrous cap and a less significant development of the lipid core, which both determine the stability of the plaque (Huang et al., 2001).

In the ultrasound evaluation, the presence of calcifications is identified thanks to the presence of a marked hyperechogenicity, which can also determine the development of an acoustic shadowing due to the total reflection of the ultrasound waves. This makes the evaluation of the atheromatous lesion possible; therefore, in these lesions, the evaluation of the flow modification after the acoustic shadow is fundamental for the identification and evaluation of the degree of stenosis.

Another type of calcification is "a plaque with a calcified nodule" which is a heavily calcified plaque with the loss and/or dysfunction of endothelial cells over a calcified nodule. This is the least common of the three causes of thrombosis described here (Virmani et al., 2000, **Table 1b**).

Calcification triggers' mechanism in arteries is still unknow. The identification of a calcified carotid lesion is interesting for the indication of a possible surgical treatment.

The lipid core

The lipid core of the carotid plaque is the most interesting element for it represents the main factor determining the stenosis and, consequently, the cerebral ischemic risk. The core is mainly composed of LDL molecules that cross the vascular endothelial barrier from the blood flow and accumulate in the intima. The macrophages are recruited and activated by the subendothelial deposit and differentiate into foam cells. These cells release oxidizing substances, which determine the formation of the oxidized LDL molecules, which have a chemotactic role as they stimulate the evolution of

the atheromatous lesion. The serum concentrations of cholesterol, with high values of LDL and low values of HDL, are fundamental for the development of the carotid plaque and are related to a larger accumulation of lipids inside the plaque. The presence of an abundant lipid component inside the carotid plaque increases plaque instability, for different reasons (Ross et al., 1993)

1. greater fragility with possible events of internal haemorrhage,

2. increased phlogistic component,

3. presence of a thin-fibrous cap,

4. strong stimulus to the aggregation of platelets in case of lesions.

As a consequence, the methods for the identification of these lesions rich in lipids are very important.

Hypercholesterolemia. The evaluation of the serum concentrations of cholesterol is the most helpful element: the study ACST (Asymptomatic Carotid Surgery Trial) highlights how patients with a carotid stenosis over 70% and values of blood cholesterol over 250 mg/dl present a significantly higher risk of ischemic events than the group of patients with lower cholesterol serum levels. The endarterectomy treatment of these lesions determines a total reduction of the risk of events, in a 5-year period, by 11,7% in patients with high levels of cholesterol and by 4,6% in patients with lower levels (MRC (ACST) 2004).

Instrumental evaluation. The evaluation of the carotid plaques by means of imaging methods helps to identify the internal component of the core. Today the B-Mode ultrasound evaluation is used for the internal description of the plaque, which is defined as hypoechogenic if it appears structurally darker than the adventitial component. This is due to the fact that the lipid core does not determine the reflection of the ultrasound waves and,

therefore, appears as dark. However, the direct evaluation does not allow an objectification of the result; for this reason, it is defined as "dependent operator" and considered as liable to individual variations. The analysis of the structure of the plaque by means of the Grey Scale Measurement (GSM) represents a more objective method. This method takes into account the average variation of the grey scale in the area of the plaque, returning a numeric result, which, thus, is not subjective. (**Fig. 6**)
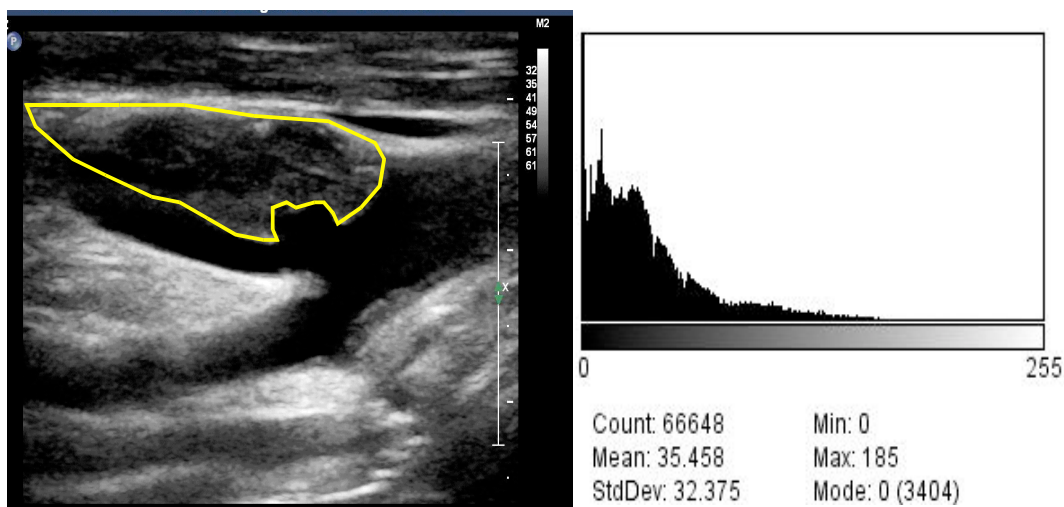
Figure 6: evaluation of the Grey Scale Measurement (GSM). In the area of the plaque, the average of the grey scale is calculated and a numeric value indicating the degree of hypoechogenicity is produced.

Evaluations by means of this method have highlighted that symptomatic plaques generally have lower values of GSM (<50), whereas asymptomatic plaques have higher values, which is an indicator of a structure that is more stable and less prone to possible complications. Moreover, long-term evaluations have highlighted how plaques with low GSM levels can determine ischemic events (Kern et al., 2004; Biasi et al., 1999).

As already mentioned before, also methods such as TC and MR can be used

to analyse the structure of the core, which confirms that lesions that are structurally richer in lipid component present higher long-term cerebrovascualr risks (Takaya et al., 2006; Cappendijk et al., 2008).

Pharmacological therapies. The use of therapies with pharmaceuticals that can determine a reduction of the blood concentrations of lipids and cholesterol, such as the inhibitors of the HMG-CoA Reductase (statins), has resulted in a reduction of the cerebrovascular risks by both having an effect on the lipid levels and reducing the phlogistic condition that characterises atherosclerosis. It has been demonstrated that high doses of statins are effective for the stabilization of the carotid plaque. Ultrasound evaluations in patients with carotid stenosis between 40% and 60%, and receiving Atorvastatin therapy 80 mg/die (for 12 months), have highlighted a significant ultrasound stabilization of the plaque (with an increase of the GSM from 66 to 100) compared to patients receiving low doses of the same medication (GSM from 64 to 85) (Kadoglou et al., 2010).

Other studies have highlighted how the statin therapy can determine a significant reduction in the concentrations of macrophages and inflammation inside the carotid plaque (Tang et al., 2009).

Statins have resulted as being helpful in the treatment of the carotid stenoses, because they reduce the lipid component of the core and stabilize the plaque. However, in presence of lesions that are hemodynamically significant, the effectiveness of the statins in preventing cerebrovascular events has not been demonstrated yet (Treasure et al.,1995; Anderson et al., 1995).

Biomarkers and vulnerable plaque

Previously, atherosclerosis was thought primarily as a "plumbing" problem. The degree of stenosis on an angiogram, symptoms and signs of ischemia provided the main tools to assess atherosclerosis. In the last decades, studies on the pathogenesis of the disease have grown fast (Libby et al. 2005). The

understanding of the pathophysiology of this disease has now entered a new era based on understanding of the biology and a critical reappraisal of the pathobiology of atherothrombosis (Hansson et al. 2006).

Biomarker are measurable and quantifiable biological parameter such as protein, enzyme or hormone concentration, gene phenotype distribution in a population. Biomarker's evaluation is a useful indicator of a normal biological process, pathogenic process, or the pharmacologic response to a therapy. The properties of a biomarker depend on their use. Currently the techniques available for biomarker development are genomics, proteomics, metabolomics, pharmacogenetics, integratomics, bioinformatics and molecular imaging technologies. Several categories of biomarker have been described that are pertinent to cancer, namely screening, diagnostic, prognostic, predictive, pharmacological, surrogate response and safety biomarker. Biomarker assays need to be carefully validated and be robust, reliable and reproducible when applied in clinical contexts (Murukesh et al., 2010). Biomarker's application in cardiovascular disease risk assessment is multiple: screening diagnosis, prognostication, prediction of disease recurrence, and therapeutic monitoring. (Vasan, 2006)

For the prediction of atherothrombotic events, markers of inflammation, fibrinolysis, oxidative stress, and altered lipid metabolism are currently in discussion. Also new emerging biomarker are in consideration, for example MPO, PAPP-A, neuron-specific enolase (NSE) represented in the **table 4** (Hermus et al. 2010).

During plaque formation different pathological processes involved in the progression of atheromasic lesions are associated with plaque vulnerability,

such as inflammation, neoangiogenesis, lipid accumulation, apoptosis, proteolysis and thrombosis. Also morphological characteristics are related with plaque instability such as ulceration **Fig** 7 (Hermus L et al. 2010). Biomarker's studies are based on the concept, that a vulnerable plaque contains predictive information for future cardiovascular events, also in other areas of the vascular tree (Lammeren et al., 2011). Results are promising and plaque markers can be used to develop imaging methods to identify patients at risk and to monitor treatment effect. Plaque biomarker studies use the concept of vulnerable plaque to favour the prediction of vascular patients.

Vulnerable plaque

Vulnerable plaque are characterized by a large lipid core, a thin fibrous cap, a rich infiltrate of macrophagic inflammatory cells and scarce smooth muscle cells. Atherosclerotic plaque prone to rupture have specific structural, cellular, and molecular characteristic listed in **Table 2** and illustrated in **figure 7.** The presence of a thin fibrous cap overlaying a large lipid core increase at high risk for rupture. Plaque rupture usually leads to various degrees of thrombus formation. Thrombosis may result in unstable angina, myocardial infarction, or sudden death, particularly if collateral flow is inadequate.

Early identification of high-risk plaque is critical, but vulnerable plaque is not detectable with the current diagnostic methods. If this plaque could be detected a major advance in healthcare would be achieved. Identification methods available are thermography, spectroscopy, radioisotope scintigraphy, more recently optical coherence tomography and ultrasound imaging. Nowadays the concept of vulnerable plaque is evolving towards patient vulnerability. Vulnerable plaque are not the only cause of symptomatic events, others parameters are involved, i.e. vulnerable blood

(prone to thrombosis) plays an important role in the outcome. Therefore, the term "vulnerable patient" is more appropriate and is now proposed for the identification of subjects with high likelihood of developing cardiac events in the near future (Naghavi et al., 2003).

Stable plaque		Unstable, ruptured plaque
Small lipid core		Large lipid core
Thick fibrous cap		Thin fibrous cap
Low macrophage content		High macrophage content
Low microvessel density		High microvessel density
No Intraplaque hemorrhage		Presence of Intraplaque hemorrhage
No cap rupture, no superimposed thrombus		Cap rupture and superimposed thrombus
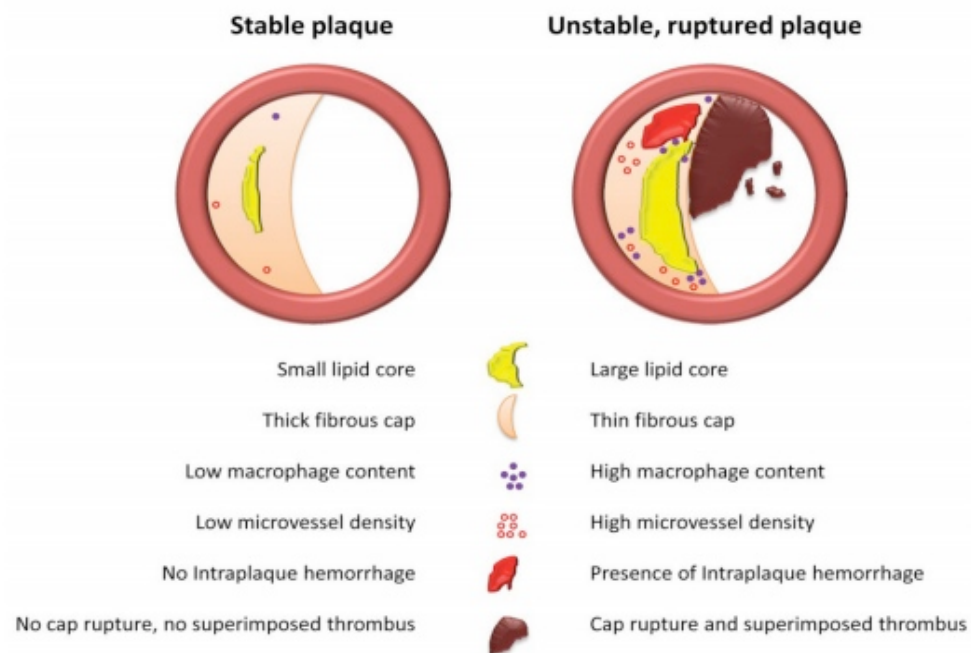
Figure 7: Overview of a stable atherosclerotic plaque and an unstable atherosclerotic plaque (Lammeren et al., 2011).

Features of Rupture-Prone Plaque
Structural
Large lipid-rich core
Thin fibrous cap
Reduced collagen content
Cellular
Local chronic inflammation
Increased macrophage density and activity
T-lymphocyte accumulation near sites of rupture
Increased neovascularization
Reduced density of smooth-muscle cells
Increased number and activity of mast cells
Expression of markers of inflammatory activation
Molecular
Increased tissue-factor expression
Matrix metalloproteinase secretion

Table 2: Features of plaque prone to rupture

Traditional biomarker

Conventionally, biomarker are identified based on large epidemiologic studies demonstrating the significative statistical association between a phenotype and the studied biomarker. Markers for risk are considered a biochemical signature that correlates with the increased risk of the disease development as determined by clinical and epidemiological studies. C reactive protein (CRP) has emerged as an independent predictor of an incident cardiovascular event in more than 15 large prospective studies,

adding a prognostic value to that conveyed by the Framingham Risk Score. In addition the lack of correlation between LDL-cholesterol and CRP allowed the identification of a subgroup of patients with increased incidence of coronary artery disease but a normal lipid profile (Koenig et al., 2005, Ridker et al., 2002). Some of the most common markers of cardiovascular disease are listed in **table 3.**

RISK	Total Cholesterol mg/dl	LDL mg/dl	HDL mg/dl	TG mg/dl	Omocistein umol/l	HsCRP mg/l	BNP pg/ml
LOW	<200	<130	>60	>200	2 -15	<1	<100
MODERATE	200-240	130-160	40-60	200 - 400	31-100	1 - 3	
HIGH	>240	>160	<40	>400	>100	>3	>100
Cardiovascular risk Hyperlipidemia => increased risk					Cardiovascular risk	Inflammation disease	Cardiovascular risk

Table 3: Markers of dyslipidemia and new marker (omocistein, hsCRP and BNP).

Emerging biomarker

Serum biomarker representing inflammatory activity in vulnerable carotid plaque may be used to identify high-risk patients for cerebral ischemic events. In a study on 100 patients, the relationship between 4 biomarkers-Neopterin, PTX3, sCD163, sTREM-1- and neurological symptoms, presence of coronary (CAD) and peripheral (PAD) artery disease was analysed. Serum neopterin and sTREM-1 levels may be related to the presence of atherosclerotic disease, but not to carotid plaque vulnerability (Hermus et al.,. 2011).

Recent analysis of inflammatory markers, including hs-CRP, interleukins 6, 10 and 18, soluble CD40 ligand, P- and E-selectin, NT-proBNP, fibrinogen and cystatin C, in patients with acute coronary syndrome showed that all markers by themselves offer only limited incremental information to clinical risk scores. However, a combination of fibrinogen and NT-proBNP contained predictive information in addition to clinical parameters (Lammeren et al .,2011).

Leukocyte telomere length is also associated with the presence of atherosclerotic carotid plaque but is not a proxy for local plaque telomere length. Plaque telomere length is related to plaque characteristics and development of restenosis following endarterectomy (Huzen et al., 2011).

Biomarker; applications always changing.

Biomarker are promising but also have limitations due to their instability or involvement in different pathways; as an example the role of homocysteine is very controversial. In 1969 Kilmer McCully reported an association between increased homocysteine and premature cardiovascular disease, since then many studies and trials demonstrated that homocysteine is an independent risk factor for cardiovascular disease (McCully et al., 1969; Ueland 2008). But, forty years later, this hypothesis has not been conclusively confirmed or refused.

In fact, in the NORVIT trial, enrolling 3,749 subjects who had a recent myocardial infarction there was a trend towards a worse outcome in the group given the combination of folic acid, vitamin B6, and vitamin B12 (Bønaa et al., 2006).

In the HOPE 2 trial (The Heart Outcomes Prevention Evaluation) that also targeted patients at risk of vascular events, 5,522 subjects were randomized to placebo or the combination of folic acid, vitamin B6, and vitamin B12.

Over a 5-year follow-up period, the homocysteine-lowering therapy did not significantly reduce the composite primary end point of death from cardiovascular causes, myocardial infarction, and stroke. A recently published study from Norway in 3,096 subjects undergoing coronary angiography examined the effect of placebo, vitamin B6 alone, folic acid and vitamin B12 administered together, or the combination of folic acid and vitamins B6 and B12. There was no effect of any vitamin therapy on total mortality or cardiovascular events (Ebbing et al., 2008).

So modifying an established risk factor does not always contribute to decrease the risk of cardiovascular disease. Another example is a trial that determines whether obese patients benefitted from treatment with rimonabant in terms of progression of carotid atherosclerosis. There was no difference in atherosclerosis progression between patients receiving rimonabant for 30 months and those receiving placebo. This finding suggests that a 5% loss of body weight over a 30-month period with rimonabant is not sufficient to modify the progression of atherosclerosis in the carotid artery in obese patients with metabolic syndrome (O'Leary et al., 2011).

Still, promising studies of accurate and inexpensive markers for cardiovascular risk assessment are useful in improving the selection of subjects for prevention therapy. Identifying a biomarker can also lead to a preventive or curative therapy aimed to decrease its level of expression.

A promising example for the application of a biomarker is a study on the effects of Varespladib methyl on inflammation and cardiovascular risk. As mentioned above, secretory phospholipase A2 (sPLA2) is a family of pro-atherogenic enzymes involved in lipoprotein remodelling and activation of inflammatory pathways. In acute coronary syndrome, high sPLA2-IIA levels predict major cardiovascular events. In this trial on 625 subjects, it

has been shown that Varespladib reduced the levels of LDL-C, hs-CRP, sPLA2-IIA and positive trends were noted for unstable angina/myocardial infarction. Based on these data, a 6,500 subject Phase III trial is planned (Rosenson et al., 2011).

Lectin-like oxidized low-density lipoprotein receptor-1 (LOX1) is a potent regulator of systemic atherosclerosis. In this study the authors developed a LOX1-targeted liposomal rho-kinase inhibitor and examined the therapeutic effect on carotid intimal hypertrophy in rats. Liposomes conjugated with anti-LOX1 antibody inhibited carotid intimal hypertrophy. The new liposomal drug delivery system targeting LOX1 could become a therapeutic strategy for atherosclerotic diseases (Saito et al., 2011). Many targeted therapies have been developed following the discovery of specific markers; i. e. bevacizumab for VEGF, statin for lipid/cholesterol

Biological pathway	Example of marker involved	Atherosclerotic plaque development processes
Lipid metabolism	LDL, HDL, TG	LDL lipid accumulation in the core
Inflammation	IL6, hsCRP, SAA, PAPP-A, TNF-alfa	SMC and macrophages accumulation in in the lipid core.
Angiogenesis	VEGF	Formation of new vessels
Proteolysis	MMP-9, MMP-12, CCP's, TIMP's	Release of proteolytic enzymes that degrade the extracellular matrix (cap erosion, rupture, acute neurological events)
Hypoxia	Indirect markers: Cytokines, MMP's Direct marker unknow	promotes angiogenesis, increases production of cytokines and MMPs (causing plaque destabilization)
Apoptosis	Annexin 5, Others unknow	SMC and Macrophages accumulation in the lipid core causing rupture ?
Thrombosis		Instability
Calcification	BMP-2, Osteopontin	increase the plaque fragility

Table 4: Emerging biomarkers

Markers of our study: inflammation biomarker

C-reactive protein

The central role of the inflammation during the various stages of the atherogenesis is now clear. The activity of the macrophages determines the

instability of the plaque owing to the erosion of the fibrous cap and the alterations in the internal microvessels. The phlogistic activity manifests itself also with the presence of various molecules – cytokines, chemokines and interleukins – that act as a stimulus for the leucocytes at the level of the plaque (Ross et al., 1993).

Many studies consider these molecular markers as predictive factors of cardiovascular events. In particular, research focuses on cellular adhesion molecules, cytokines, chemokines, acute-phase molecules such as fibrinogen and C-reactive Protein (CRP) (Libby et al., 2002).

CRP has been widely studied; indeed, the literature includes many publications describing its role as a marker of cardiovascular risk.

CRP is a member of the pentraxin family of proteins; its production in the liver is regulated by serum levels of IL-6, although IL-1 and TNF can also contribute to its release. The half-life of CRP is about 19 hours and it is produced at normal levels in conditions of good health and at higher levels in conditions of disease. The main activity of CRP consists in binding to the macrophage Fc receptors and stimulate the phagocytosis of cells that have died through apoptosis or necrosis. Recent studies have identified areas outside the liver where this protein is produced such as the atherosclerotic lesions (by macrophages and smooth-muscle cells), the kidneys, the neurons and the alveolar macrophages. The lipid peroxidation and the infectious state activate the release of CRP with the release of inflammatory cytokines (Thompson et al., 1999; Yasojima et al., 2001).

CRP as a marker of risk. Many studies have demonstrated the predictive role of CRP for cardiovascular events such as myocardial infarction, coronary heart diseases, sudden death, peripheral artery disease and stroke in apparently healthy subjects (Ridker et al., 2003; Ridker et al., 2000; Pearson et al., 2003; Jialal et al., 2003).

As regards these data, the American Heart Association and Centers for Disease Control and Prevention have indicated that CRP can be used as a marker of risk for cardiovascular pathologies.

The recommendations indicate that:

·   CRP< 1mg/l: low risk

·   CRP between 1 and 3 mg/l: intermediate risk

·   CRP> 3 mg/l: high risk.

However, if the levels are higher than 10 mg/l, CRP cannot be used as a marker of cardiovascular risk, because other inflammatory (infectious or traumatic) processes need to be excluded. In the primary prevention of cardiovascular events, it is necessary to use the "high sensitivity" CRP test (hs-CRP) and the patient must not present any acute inflammatory conditions for at least two weeks.

Some of the conditions associated with higher levels of CRP are: obesity, chronic inflammatory diseases, metabolic syndrome and diabetes mellitus type 2.

CRP as an agent of inflammation. The role of CRP as a risk factor has been established; however, its presence at the level of the atherosclerotic lesions has led to look for any possible activity in the development of the plaque. The limitation of these studies lies in the fact that the evaluation of the activity of this protein is carried out in vitro or on animal models but not yet in vivo on human subjects. A list of the cellular activities related to CRP is presented below.

CRP and macrophages: - CRP stimulates the release of reactive oxygen species,[a]

- it stimulates the release of IL-6 and TNF,[b]

- it increases the release of MMP-1,[c]

- it enhances the phagocytosis of cholesterol.[d]

CRP and endothelial cells: - CRP stimulates the expression of adhesion molecules on monocytes (ICAM-1 and VCAM-1),[e]

- it correlates with vasoreactivity and endothelial dysfunction by inhibiting the production of nitric oxide (NO),[f,g]

- it inhibits the production of prostacyclins, which inhibit the platelet aggregation and the proliferation of smooth-muscle cells,[h]

-it stimulates the expression of PAI-1 (plasminogen activator inhibitor-1), which presents an atherogenic and procoagulant activity.[i]

CRP and sm.-musc. Cells: - CRP stimulates the expression of AT_1R (angiotensin type1 receptor), which presents an atherogenic activity,[j]

– it stimulates the cellular proliferation.[k]

CRP role is well-characterized in the coronary district but its predictive role in vulnerable plaque is still unknown.

*references: a; Tebo et al.,1991; b: Ballouet al., 1992; c: Williams et al., 2004; d:Chang et al., 2002); e: Pasceri et al., 2000; f: Fichtlscherer et al., 2000; g: Venugopal et al., 2002; h: Venugopal et al., 2003; i:. Devaraj et al.,

2003; j: Nickenig et al., 2002;.k: Hattori et al,. 2003

Serum amyloid A-protein

SAA is the most impressive of the acute-phase proteins, increasing within 24 h by up to 1000-fold in response to various injuries including trauma, infection, inflammation, and neoplasia (Urieli-Shoval et al., 1998). SAAs can be divided into two groups; the first group comprises the well-characterized acute phase SAAs that associate with HDL during inflammation, thereby remodelling the HDL particle by displacing apolipoprotein (apo)A-I. The second group consists of the recently discovered constitutive SAAs, mouse SAA5 and human SAA4. SAA4 is found to be associated with a distinct subclass of HDL particles unrelated to those involved in the initial cholesterol transfer from cells (de Beer et al., 1995).

The human SAA gene family is composed of four discrete loci containing two highly homologous genes, SAA1 and SAA2, and two less related genes, SAA3 and SAA4. The gene for SAA4 is constitutively expressed and its protein product is a constituent of normal, non-acute-phase high-density lipoprotein. The liver has been considered the primary site of expression. It was demonstrated that the SAA mRNA and protein are widely expressed in many histologically normal human tissues, including stomach, small and large intestine, tonsil, breast, prostate, thyroid, lung, pancreas, kidney, skin epidermis, and brain neurons. (Urieli–Shoval, 1998).

SAA production is up-regulated by proinflammatory mediators, notably the interleukins IL-1 and IL-6 and the tumour necrosis factor TNF-α [7], and conversely, SAA has been shown to induce the production of cytokines in THP-1 monocytes and in neutrophils.(Niemi et al. 2006) This clustering may be due to the fact that SAA can act as a mast cell chemoattractant

(Niemi et al. 2006). Katri Niemi et al. (2006) showed that SAA can activate human mast cells as indicated by the significant induction of TNF-α and IL-1β production. High levels of SAA activate mast cells to degranulate and to release their stores of cytoplasmic neutral proteases, notably tryptase. SAA4 mRNA (express costituvely) and protein expression in macrophage-derived foam cells of coronary and carotid arteries suggested a specific role of SAA4 during inflammation including atherosclerosis (A Hrzenjak et al., *Protein Engineering 14(12):949-952, 2001*). Further credence for extrahepatic expression of SAA4 mRNA is derived from studies in human lesion material. This raises the possibility of similar proatherogenic properties of human SAA4 as reported for A-SAA (Andelko Hrzenjak et al 2001).

Ridker et al have shown that serum SAA concentration is a significant predictor of the risk of cardiovascular events more effective than the levels of LDL-cholesterol or total cholesterol, indicating a cardiovascular relative risk factor of 3.

SAA is also expressed in normal cerebral tissue; the pyramidal neurons of the cerebral cortex and Purkinje cells of the cerebellum. (Urieli–Shoval, 1998). A-apoSAA mRNA was detected in Alzheimer's disease and in rheumatoid arthritis synovial tissue and cells (Liang et al., 1997; Kumon et al., 1999). SAA plasma concentration increased after cerebral infarction; the concentration of SAA depending on the clinical severity of the ischemic stroke. SAA was found also to be a sensitive early indicator of possible infectious complications after the cerebral infarction (Hzecka et al., 2000).

SAA is expressed in a variety of tissue but at the moment only few studies have analysed its involvement in carotid plaque district in correlation to cerebral injuries.

Pregnancy-Associated Plasma Protein-A

Pregnancy-Associated Plasma Protein-A , a high molecular weight zinc binding metalloproteinase, was first found in 1974 in the third-trimester plasma of pregnant women (Lin et al., 1974). PAPP-A has proteolytic activity when it is not bind to proMBP sub-Unit. The main activity of freePAPP-A is to cleave insulin-like growth factor-1 (IGF-1) from its binding protein-4, thereby increasing the accessibility of free IGF-1 to tissues.

In vitro studies showed that IGF activate macrophages, chemotaxis, LDL cholesterol uptake by macrophages and release of pro-inflammatory cytokines, thus suggesting a pro-atherogenic activity. (Renier et al., 1996; Bayes-Genis et al., 2000).

The study of Sangiorgi et al. suggests that PAPP-A is a specific marker of carotid plaque vulnerability and that an increase of PAPP-A serum level is related to the progress of unstable plaque (Sangiorgi et al., 2006).

However there is contradiction through literature towards the role of PAPP-A; pro-atherogenic or repairing factor? Several lines of evidence indicate that PAPP-A is induced in response to, and within, damaged tissues, as a promoter of repair, in virtue of its IGF-1-dependent actions on vasculogenesis, vasodilation, cell preconditioning, cell survival, and insulin-sensitivity. (Chen et al., 2003). PAPP-A may have important and pivotal roles in local cellular function related to wound healing, bone remodeling, atherosclerotic plaque development, angiogenesis and several aspects of human reproduction (Qin et al., 2002). A study showed that PAPP-A is able to stimulate matrix mineralization; BMP-2 is an inducer of the osteoblast transcription factors RUNX2 and OSX which are crucial for bone formation. OSX sees to operate downstream of RUNX2. The cooperation between PAPP-A and BMP-2 in matrix mineralization could involve Osx, but remains unclear. The data of the study suggests that PAPP-

A, demonstrated to be regulated by BMP-2, is also involved in angiogenesis as new blood vessel formation. (PAPP-A is involved in matrix mineralization of human adult mesenchymal stem cells and angiogenesis in the chick CAM Julie Jadlowiec1, 2, 3, Diana Dongell2, Jason Smith3, Cheryl Conover4 and Phil Campbell)

Some studies reported that circulating PAPP-A is not an early marker of acute myocardial infarction. (Jadlowiec et al., 2005). It is important to underline that the PAPP-A form that becomes elevated in ACS is not complexed with proMBP which is hereby defined as free PAPP-A. In 2010, a study including 267 patients free PAPP-A seems to be superior as a prognostic marker compared to total PAPP-A (Lund et al., 2010). Thus, the concentrations obtained with the assays do not accurately reflect the amount of PAPP-A in acute coronary syndromes. The clinical value is most possibly underestimated when total PAPP-A is measured in ACS patients due to the presence of partial overlap between the distribution of PAPP-A in normal population (complexed form only) and distribution of PAPP-A in ACS patients (complexed and free forms).

The validation results from clinical studies evaluating free PAPP-A serum and tissue level remain to be seen and correlated with angiogenesis and calcification in atheromasic plaque.

Neuron-specific enolase

Several previous studies have indicated that monitoring the levels of neuron- or astroglia-specific proteins in the serum and cerebrospinal fluid could be a useful approach for evaluating the severity of central nervous system injury (e.g. traumatic brain injury, cerebral infraction, intracranial hemorrhage).

The marker proposed is the neuron-specific enolase (NSE), which is a highly soluble intracellular protein principally located in neuronal cytoplasm and in neuroendocrine cells. NSE is readily secreted into the cerebrospinal fluid and blood after tissue injury, and has been shown to have a biological half-life of 48 hours. Kaiser et al. 1989. Marangos et al., 1987).

Leukocytes have been proposed as a useful peripheral model to study mental pathologies (Gladkevich et al. 2004; Iga et al. 2008; Rokutan et al. 2005), since their expression profiles have shown similarities to those observed for brain cells, especially for genes encoding neurotransmitter receptors and transporters, stress mediators, cytokines, hormones, and growth factors (Glatt et al. 2005 ; Sullivan et al. 2006).

Thus our interest to determine if the circulatory levels of PAPP-A and NSE mRNA reflects cerebral injuries occurring during CAS or CEA procedure.

Markers of our study: neoangiogenesis biomarkers

Neoangiogenesis

Neoangiogenesis is the growth of new blood vessels from pre-existing vessels. Growth within the atherosclerotic plaque may destabilize the structure leading to rupture. The vascularization of atherosclerotic plaque is a key element in the development and progression of the lesion. Neovessels may destabilize the plaque structure leading to rupture with clinical consequences; some of the clinical features correlated to plaque neoangiogenesis are represented in sketch X (Virmani R. et al., 2005; Kolodgie et al., 2003). The presence of neovascularization in carotid plaque increases plaque instability and therefore results in an increased risk of developing neurological events (Dunmore et al., 2007; Mofidi et al, 2008),

(table 5)
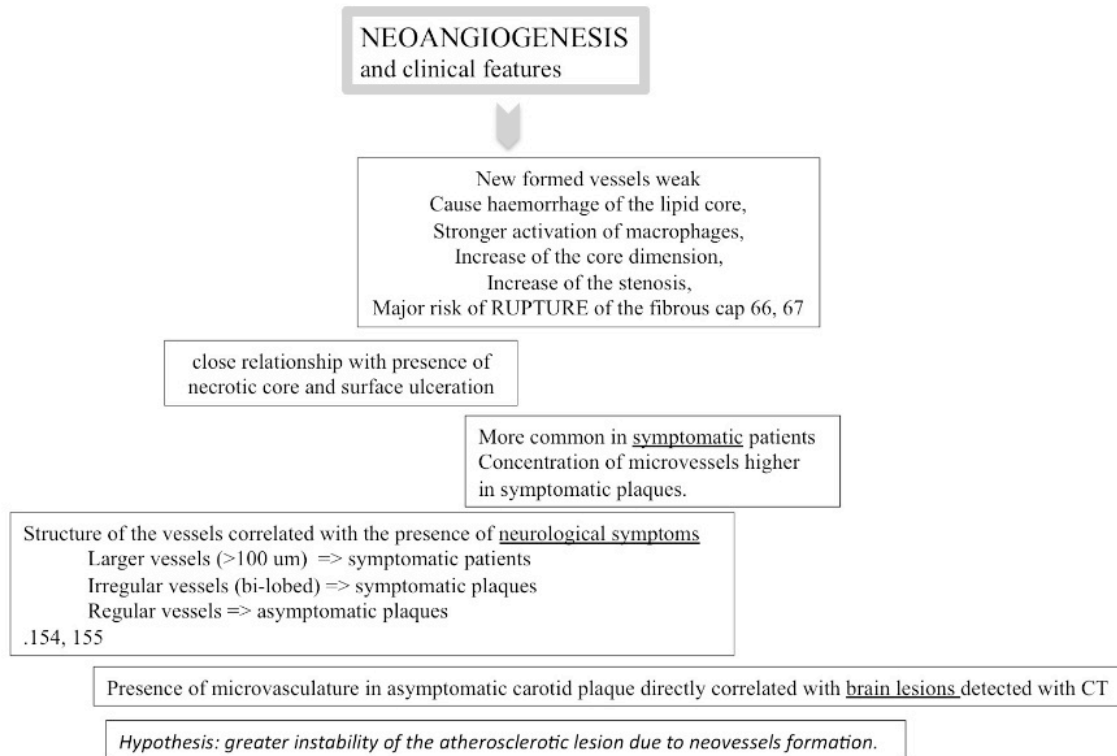
Table 5: Clinical features correlated to plaque neoangiogenesis

Boerhaave (approximately in 1750) suggested that hardening of the arterial wall occurred when the small arteries feeding the muscular layer constricted and hardened (ossified), which is the first description of the vasa vasorum (the vessel within the vessel) directly involved in the angiogenic process (Acierno LJ, 1994). In 1995, Kumamoto et al. was able to show in diseased atherosclerotic epicardial arteries that intimal vessels originated 28 times more frequently from the adventitial vasa vasorum than those originating from the lumen. He was also able to reveal that intimal-medial neovascularization was closely associated with the inflammatory reaction

within the plaque, established early in the atherosclerotic process, and capable of regression. Most authors feel that the intimal-medial neovascularization arises more frequently from the adventitial vasa vasorum. Both adventitial and luminal microvessels are very fragile and prone to leak and rupture creating intraplaque hemorrhages. Kwon reported rapid, extensive development of vasa vasorum angiogenesis in coronary vessels. These were induced by a high fat diet in three months (Kwon et al., 1998; Kantor 1999). Burke and Virmani revealed that plaque rupture in sudden death is related to vasa vasorum angiogenesis in addition to the chronic macrophage inflammatory response (Burke et al., 1999). Thus, later in the atherosclerotic process the angiogenic vasa vasorum may be more responsible for the delivery of the previously discussed harmful molecules and substrates than diffusion through the traditional endothelial lumen surface early in the atherosclerotic process.

Bargers in 1984, was able to show a "malignant like" infiltration of microvessels into the media and intima of the atherosclerotic diseased segments; neovascularization of the vessel wall originate from the adventitial vasa vasorum. In the healthy segments of the same coronary artery there is no involvement of angiogenesis.

The identification of lesions, that are rich of vascular components, represents an additional risk assessment of the vulnerable patient. VEGF is the growth factor mainly involved in the angiogenic stimulus within the plaque but can also be identified in the blood level, representing a possible risk marker. Also instrumental methods, such as CEUS, may allow the identification of atherosclerotic lesions with increased neovascularization, thus quickly identifying lesions at higher risk or rupture.

Vascular Endothelial Growth Factor

The Vascular Endothelial Growth Factor (VEGF) is a molecule that is fundamental for the development of the blood vessels. VEGF is expressed in the embryonic period, during the development of the vascular tree, during the growth stages and in the processes of tissue repair. Angiogenesis is physiologically regulated by VEGF and its inhibitors. When the regulation goes awry, the formation of blood vessels becomes either excessive or insufficient.

The most significant stimulus for the cellular production and release of VEGF, in the adult, is represented by hypoxia; the cells that are responsible for this production can be both normal and tumorous. Many studies have focused their attention on the role of VEGF in the development of solid neoplasms, which need new vascular structures for their growth and, thus, release VEGF to form them.[94]

Only in the past few years, the role of this molecule has been taken into account also with respect to atherogenesis. In the atherosclerotic lesions, the hypoxia and the release of molecules by the macrophages result in the expression of VEGF. Inside the plaque, some small vessels appear and determine the instability of the plaque, as they enhance the recruitment of macrophages and can cause internal haemorrhages. VEGF is expressed by endothelial cells, macrophages and smooth-muscle cells.

Its activity in the plaque is determined by the receptors involved:

VEGFR1: (fms-related tyrosine kinase 1, FLT-1) it determines the pro-inflammatory activity,

VEGFR2: (kinase insert domain-containing receptor, KDR) it regulates angiogenesis.

Its activity is highlighted by experimental studies on animals, during which the administration of recombinant human VEGF increases the size of the atherosclerotic lesions, their vascularization and the number of

macrophages – compared with controls treated with placebo. In other studies on animals, angiostatin, which is an inhibitor of VEGF, reduces the accumulation of macrophages and the size of atherosclerotic lesions. Over the past few years, many studies have demonstrated that the presence of VEGF in atherosclerotic plaque is associated with instability due to both angiogenesis and the degree of the internal inflammation.[95-98]

VEGF targeted therapy. There are medications that are currently used in the treatment of neoplasms and are able to inhibit neoangiogenesis. Their possible role in reducing the progression of the atherosclerotic lesions is demonstrated in animal models, but their application in the clinical practice is still debated. This is due to the fact that, beside the possible benefit of reducing the intraplaque vascularization, there may be adverse ischemic effects in other areas.[99]

A prototypic VEGF inhibitor used in many cancer clinical trials is the monoclonal anti-VEGF antibody, bevacizumab (Murukesh et al., 2010).

The role of VEGF in the atherosclerotic plaque, including the carotid ones, is clear. Studies are trying to confirm the hypothesis that this molecule can be considered as a marker of atherosclerotic risk, in order to identify carotid lesions of high cerebrovascular risk.

Nestin

Nestin is an intermediate filament protein expressed in neural and mesenchymal stem cells, as well as in a variety of progenitors cells (Wagner et al., 2006). It was also seen that Nestin is an angiogenic marker for newly formed microvessels, and numerous Nestin-positive microvessels were described in tumours of control mice (Ramasamy et al. 2011). Moreover, a recent study showed that Nestin is expressed in newly forming blood vessels and also in a high number of endothelial cells after myocardial

infarction (Wagner et al., 2006). A previous study showed that medial vascular smooth muscle cells in the developing arteries potently express Nestin, but its expression is abolished in adult arteries (Oikawa et al., 2010). In adult tissue, Nestin expression may be restricted to newly formed endothelial cells generated during angiogenesis (Teranishi et al., 2007). It is therefore believed that Nestin expression, representing an early endothelial differentiation or an endothelial progenitor phenotype, could be a reliable marker of "progenitor-committed" endothelial cells and/or of a "young" endothelium.

Variants in the Nestin gene are associated with coronary heart disease. The Nestin gene may play a role in the development of both primary and restenotic coronary artery plaque (Meng et al., 2008). Nestin expression in carotid plaque lesions has not yet been studied. Nowadays the known transcription factors regulating Nestin are: Pou, Sox, TTF-1 and WT1 (Wagner et al., 2006; Pelizzoli et al., 2008).

Wilms tumour suppressor

The Wilms tumour suppressor (WT1) encodes a protein with four C-terminal Zn-fingers characteristically found in the transcription factor **(figure 8).**
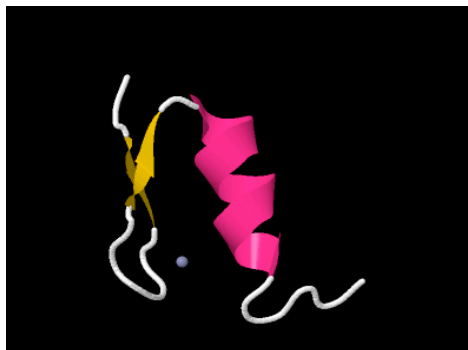
Figure 8: WT1 protein structure.

WT was originally described in the paediatric Wilms' tumour of the kidney,

but its involvement has been demonstrated in a variety of other tumours and tumour cell lines (Hohenstein et al., 2006; Wagner et al., 2008). Some recent studies showed the involvement of WT1 as an activator of the Nestin gene (Hohenstein et al., 2006), and the co-localization of WT1 and Nestin during the different development steps in embryogenesis (Wagner et al., 2006). The functions of WT1 are not only limited to the kidney and promoter of tumour angiogenesis but involve the heart and vascular system as well. Recent findings show the importance of WT1 in heart and coronary vessel development and the identified molecular mechanisms (Sholz et al., 2009).

Therefore the new interest towards WT1 function in neoangiogenesis during plaque formation.

AIM

AIM

In this research our target was to identify local or circulating proteins associated to plaque vulnerability and to the risk of cerebral embolization in order to recognize vulnerable patients for systemic cardiovascular adverse events.

Microembolization during the stenting procedure can cause cerebral lesions. During the CAS procedure stent are mostly associated to distal filters that avoid the diffusion of fragments of emboli detached during the procedure.

The first part of the study wants to establish the correlation between cerebral lesions occurring during CAS and hsCRP, SAA, VEGF, PAPP-A and mRNA NSE.

Indication to CEA is commonly determined by percent of stenosis as well as neurological symptoms and clinical conditions. High plaque embolic potential is defined as 'vulnerability'; however, its characterisation is not universally used for carotid revascularisation. In the second part of the study, we investigated different methods to identify carotid vulnerable plaque, imaging technique and histological parameters as thin fibrous cap thickness, phlogosis and microvessel density, serological markers and molecular markers.

Lastly, since neovessels' density correlates with plaque destabilization, neoangiogenesis represents a crucial step in atherosclerosis. Vasa Vasorum (VV) neovasculogenic potential and involvement in atherosclerosis are now widely accepted, and related to the presence of endothelial progenitor cells. In order to clarify the trigger mechanism of neoangiogenesis in plaques, we studied the morphology of VV in healthy and diseased arteries and their immunohistochemical (IHC) expression of markers of disease and endothelial progenitor cells.

MATERIALS

METHODS

Materials and methods

Carotid artery stenting study

Patients

In the period between June 2009 and December 2009 a series of consecutive patients with ≥70% carotid artery stenosis (North American Symptomatic Carotid Endarterectomy Trial Collaborators, 1991) were submitted to CAS, according to Society for Vascular Surgery recommendations (Hobson et al., 2008). Demographic data, symptoms (amaurosis fugax, transient ischemic attack, minor and major stroke), vascular risk factors (hypertension, coronary artery disease, chronic obstructive pulmonary disease, dyslipidemia, diabetes mellitus, current smoking, chronic renal failure based on a glomerular filtration rate < 60 ml/min) and current therapy (acetylsalicylic acid, anticoagulant, hydroxymethyl glutaryl coenzyme A reductase inhibitor) were all recorded in a database software. All patients gave the appropriate informed consent for the study before the CAS procedure.

Carotid plaque structure analysis.

Carotid plaques were evaluated by duplex scan ultrasound (Philips, IU 22) to determine the role of plaque structure in CAS embolization; the images were digitally stored for later evaluation by an expert operator blinded to the study. The plaques were divided into homogeneous and dishomogeneous, according to gray scale measurement (GSM). GSM was analysed for each plaque with the ImageJ software (http://rsbweb.nih.gov/ij/) using the histogram function that gives a mean gray of pixels of the region of interest. Dishomogeneous plaques were identified with GSM<50 (Biasi et al., 1999), or in the presence of an

ulceration (defined as a surface recess greater than 2 mm deep and 2 mm long).

CAS procedure.

CAS was performed as previously described (Faggioli et al., 2007). Briefly, patients were taken to the angiographic suite after cardiological evaluation and medicated with aspirin 100 mg and clopidogrel 75 mg for 3 days before the procedure. All procedures were performed under local anaesthesia, systemic heparinisation and an 8F groin introducer. Common carotid cannulation was achieved with 40° Boston Scientific® or Medtronic® HS I and II catheters over a Terumo® stiff guide wire. When cannulation was not achievable by these means, several different alternative techniques were used (i.e., buddy wire, coaxial). Brachial or carotid access was not attempted in any case. Routine cerebral protection was performed using Filterwire EZ with 100 μm diameter pores (Boston Scientific®) and stenting by closed-cell (Wallstent, Boston Scientific®). 'Technical success' was defined as the ability to treat the stenosis with less than 30% residual stenosis. Neurological outcome was evaluated both at the end of the procedure and in the following 24 h by a neurologist according to the NIH stroke scale and the modified Rankin scale.

Filter analysis by light microscopy.

At the end of the CAS procedure filters were recovered, gently washed in physiological solution and immediately fixed in 10% neutral, buffered pH 6.9 formalin. Macro photographs of the device in its integrity were taken under a stereomicroscope. After removal of the metallic wire, the filter was cut into two equal portions and flattened; the first sample was mounted onto glass slides using Canada Balsam (Sigma-Aldrich C1795) whereas the second one was stored in formalin for SEM examination. Morphometric analysis was performed under a light microscope (Leitz Wetzlak, Germany) connected with a CCD camera Olympus CX42. Images were acquired using

Image-Pro Plus software (Media Cybernetics) and processed with ImageJ software (http://rsbweb.nih.gov/ij/). An average of 30 fields per filter was acquired and the total area evaluated for each filter was 0,12 mm2 at a magnification of 10X.

The percentage of membrane surface occupied by debris was expressed as percentage of surface involvement (SI). Images were converted to stacks composed by 6 fields each, transformed in montage, converted from colour images to 8-bit greyscale with the scale set at 0.41 pixel/µm. The boundary of the filters was delineated to calculate the total area for each stack (13.2mm2), and then the lower and upper threshold values were set to measure the percentage of the covered area of interest (**Fig. 1B**).
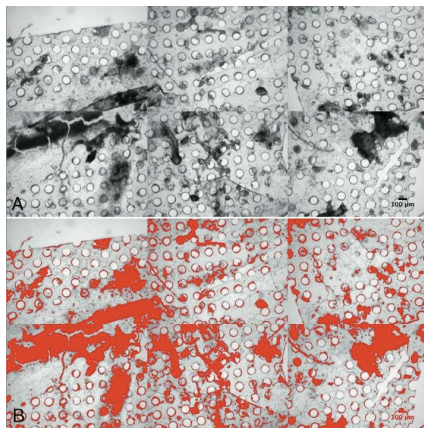
Figure 1: Image stacks to evaluate area covered by debris in filters' membrane.

The number of pores occluded (PO) by thrombo-embolic material, with a minimum mean size of 40 µm, and the total number of non-occluded pores was quantified and expressed as a percentage. For histology and debris characterisation, the apex of some filters with visible adherent material was recovered, dehydrated as before and embedded in paraffin for 1h; 3 µm thick sections were stained with hematoxylin-eosin (HE).

Filter analysis by scanning electron microscopy.

Scanning electron microscopy (SEM) was performed to characterize the dimension and the type of embolic debris adherent to the filter device inner surface.

Filters were embedded in ashless paper filters, washed with phosphate buffer 0.15 M and post-fixed in 1% osmium tetroxide for 15 min at RT. Then the filters were washed for 15 min in distilled water, dehydrated with graded steps of ethanol (70%, 95% and 100% ethanol; 15 min each step) and dried with hexamethyldisilazene (HMDS, Fluka, Steinheim, Germany) for 30 min at RT. The dried filters were accurately flattened and mounted on aluminium stubs (Multilab Type stub pin 1/2'', Surrey, UK), and sputter coated with a 10 nm thick layer of gold in a Balzers MED 010 sputtering device (Balzer Union FL 9496 Fürstentum Liechtenstein). Then samples were observed using a Philips 505 Scanning Electron Microscope at 15 kV. Images were processed with ImageJ. The size of the particles was evaluated by measuring the length of major and minor axis using ImageJ.

Cerebral lesions assessment: DW-MRI.

Diffusion weighted imaging scans were obtained both one to three days before CAS and during the first 24 hours after the procedure. A 1.5T General Electrics Medical Systems (Milwaukee, Wisc) Signa Horizon LX whole-body scanner with a quadrature birdcage headcoil was used. Hyperintense lesions were visually identified on the post-CAS DW-MRI images. Identification was confirmed by the absence of hyperintensity on the corresponding pre-CAS DW-MRI images. The volume and the number of lesions were assessed semi-automatically, with final revision by one of the specialized physicians involved in the study (R.L., C.T.). The volume of the lesions was quantified by defining a threshold for the difference between pre-CAS and post-CAS image intensities, and counting the number of pixels where the difference was greater than this threshold. Classification of new brain lesions was based on the vascular territory in which they occurred. New lesions were defined "ipsilateral (IL)" if located in the

hemisphere ipsilateral to the side of the treated carotid bifurcation; or "non-ipsilateral (CL)" if located in the hemisphere contralateral to it, in the posterior territory, or in both the ipsilateral and contralateral hemisphere.

(For a detailed description of the technical aspects of the DW-MRI please refers to Faggioli et al., 2009)

Carotid endarterectomy specimens

Patients

A series of consecutive patients with either symptomatic or asymptomatic carotid artery stenosis >=70% were submitted to carotid endarterectomy (CEA), according to ESVS and Society of Vascular Surgeons (SVS) recommendations. Symptomatic carotid stenosis, defined as ipsilateral cerebral ischaemic events (major or minor stroke or transient ischaemic attack (TIA) or amaurosis fugax) that occurred in the last 6 months, were evaluated by independent in-hospital neurologists. Epidemiological data, neurological symptoms, vascular risk factors (hypertension, coronary-artery disease, chronic-obstructive pulmonary disease, dyslipidaemia, diabetes mellitus, current smoking and chronic-renal failure) and current therapy (acetylsalicylic acid (ASA), anticoagulant and hydroxymethyl glutaryl coenzyme A reductase inhibitor) were recorded in a database software. Emergency procedures for acute ischaemic symptoms were not included in the study. Preoperative cerebral computed tomography (CT) scan was performed in all cases to identify possible ischaemic lesions. CEUS plaque evaluation was performed in the days immediately before surgery. All patients gave their informed consent for the study before CEA, which was performed in a standard fashion through a laterocervical approach.

CT scan

Cerebral CT was performed in all patients using a multi-slice (16-slice) GE Light Speed scanner (General Electric, Milwaukee, WI, USA). According

to Mofidi et al. the presence of cerebral ischaemic lesions ipsilateral to the side of the carotid plaque was considered a positive CT evaluation. Cerebral ischaemic lesions were defined as areas of low attenuation, involving both grey and white matter or focal areas of encephalomalacia. Cerebral CT evaluation was performed blindly by two different operators within 2 weeks before surgery.

CEUS

Carotid ultrasonography was performed with an ultrasound machine (Philips IU22, Amsterdam, the Netherlands) by a blinded expert operator (with more than 100 carotid ultrasound examinations performed per year), within 2 weeks before surgery. A contrast-specific software operating at low mechanical index was used. The power modulation mode (IU22) was used. The second-generation echo-contrast agent, SonoVue® (Bracco, Milan, Italy), was employed. SonoVue® is based on microbubbles stabilized by phospholipids and filled with sulphur hexafluoride with a median diameter of 2.5 mm. The low solubility and the high resistance of the shell to the mechanical effect of the ultrasound (US) beam allow this contrast agent to act for a long period of time (10 min). The contrast solution is prepared immediately before administration by adding 5 ml of sterile saline solution (0.9% NaCl) to the vial and by vigorously shaking it for at least 20 s. SonoVue® was administered as a bolus at a dose of 5ml and was injected intravenously through a 20-gauge intravenous catheter, followed by a 10-ml-flush of saline water (0.9% NaCl). A linear probe with a transmission frequency of 10-12 MHz was used by a blinded expert operator. Common, internal and external carotid arteries were visualized in the longitudinal and the transverse planes. Images of plaques in B, Colour and Power modes were digitally stored. CEUS evaluation was performed as follows. After presetting real-time, contrast-enhanced imaging modality with coded pulse-inversion technique, image settings were adjusted for maximising the contrast signal. The mechanical index was preset to 0.13

and the frame rate to 12 per s, to reduce microbubble destruction, with image depth at 3-5 cm, according to the patients' anatomical necks characteristics. The longitudinal carotid plaques images in real-time visualisation with the presence of microbubbles in carotid lumen and in the plaques' microvessels were digitally stored for later outline-blinded software analysis. Image storing was performed for at least 10 min, from the moment of injection to the time of decreasing microbubbles concentration in carotid lumen. QLab® (Philips Healthcare, India) software was used for the outline plaques vascularisation analysis, obtaining the maximum level of dB-Enhanced (dB-E) at the peak of microbubble's concentration for each plaque analysed. The stored images sequences were evaluated identifying the carotid plaque, delineating the region of interest and eventually performing the software analysis of microbubbles concentration within the plaques and recording dB-E values (**Fig. 2).**
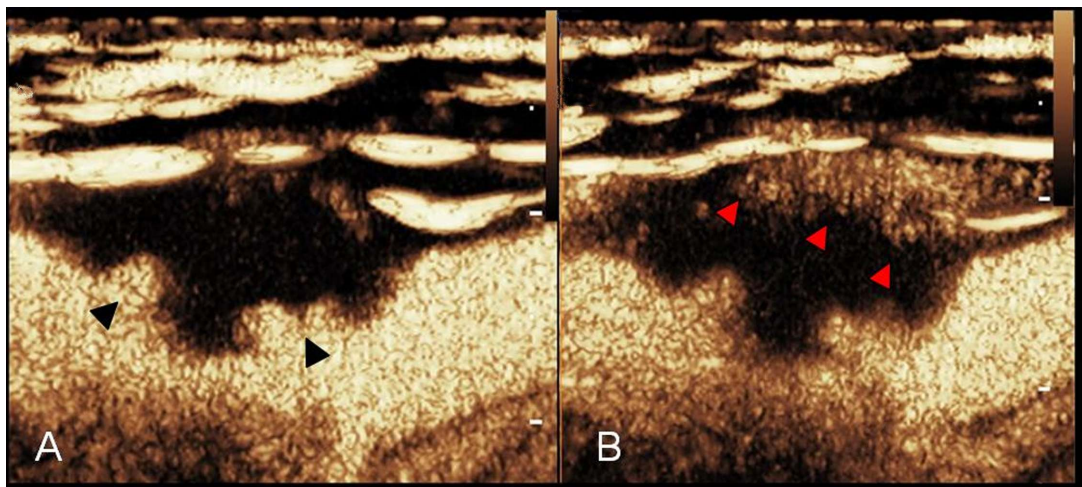
Figure 2: Image sequences of carotid plaque before (A) and after (B) CEUS microvessel detection. Panel B shows the area within the plaque filled with neovessels (red arrows). In panel A, only the border of the plaque is visible (black arrows) showing two ulcers.

Histological analysis of carotid plaque

Carotid plaques were removed in full during surgery to preserve the plaque structure. After 24 h of decalcification, samples were cut in serial sections

and the area with the highest percentage of stenosis was identified and defined as the area of interest for further analysis. Plaque tissue samples were fixed in formalin buffered 10% and embedded in paraffin; 5-mm-thick haematoxylin and eosin-stained sections were observed under a light microscope (LM,Olympus CX42). Carotid atherosclerotic lesions were defined according to the American Heart Association (AHA) classification and grouped as type I to VI ranging from the initial lesion to the complicated lesion. An experienced pathologist performed all histopathological analysis.

Immunohistochemical assay on carotid plaque

Formalin-fixed paraffin embedded 5-mm-thick tissue carotid sections were rehydrated through graded steps of ethanol absolute (Xilol 30min, 100% 10 min, 95% 5 min, 70% 5 min). Antigen retrieval was performed with a heat-mediated method at 1 atm, 120 °C for 20 min in a citrate buffer solution (pH 6) and cooling for 20 min. Endogenous peroxidase activity was blocked with 3% H_2O_2 in absolute methanol for 10min at room temperature (rt), in the dark. Antigene-antibody reaction was developed with the NovoLink Polymer Detection Kit (Novocastra, Newcastle, UK). Sections were incubated overnight in a wet chamber at 4 °C with the tested antibody (represented in **table 1).** Then, sections were incubated with NovoLink® Polymer for 30 min at rt, and subsequently with diaminobenzidine NovoLink® DAB Substrate Buffer) for 30s to 2 min. Cell nuclei were stained with Mayer's haematoxylin (Sigma Chemicals). Negative controls were done without the primary antibody. After dehydratation samples were mounted onto glass slides using Canada Balsam (Sigma- Aldrich C1795). The sections were observed under a light microscope (Leitz Wetzlak, Germany 12 V max, 100W) connected with a charge-coupled device (CCD) camera Olympus CX42. Images were acquired using Image-Pro Plus software (Media Cybernetics

http://www.mediacy.com) and processed with ImageJ free software (http://rsbweb.nih.gov/ij/).

Antibodies	Clone	Dilution	Evaluates	Manufacturer
CD3	SP7 (Rabbit)	1:100	Inflammation T lymphocytes	Neomarker USA
CD68	PG-M1 (Mouse)	1:200	Inflammation Monocytes	Dako A/S, Denmark
dPAPP-A	(PD4 (Mouse)	1:1200	*Macrophages-EC*	HyTest Finland
Mast cell tryptase	AA1 (Mouse)	1:50	Inflammation Mast cells	Dako A/S Denmark
CD31	JC70 (Mouse)	1:50	Vessels density	Dako A/S Denmark
CD34	Q-BEnd-10 (Mouse)	1:100	Vessel density	Dako A/S, C, Denmark
Nestin	10C2	1:400	Immature vessels, ECPs	Millipore USA
WT1	6F-H2 (Mouse)	Pre-diluted	Immature vessels, ECPs	Ventana, Roche
SAA4	EPR2926 (Rabbit)	1:100	*Macrophages-foam cells in Atheroma*	Epitomics USA
a-SMA	1A4 (Mouse)	1:9000	Cellularity (Vascular wall smooth muscle cells)	Sigma, Saint Louis, Missouri, USA

All were monoclonal, **EPC: endothelial progenitors cells

Table 1: Antibodies used during immunohistochemical analysis

Histological evaluation of vulnerability

Vulnerable plaques generally have five histologic hallmarks compared with stable plaques: a larger lipid core (>40% of total lesion area), a thinner fibrous cap, inflammatory cells (NASC 1991; ECST 1991; Bluth et al., 1988; Kern et al., 2004), calcified lesions (Grant et al., 2003) and neoangiogenesis (EI-Barghouty N., 1995). We define vulnerability of the plaque following these last assumptions. Extension of calcification and the lipid core was evaluated on entire circumferential arterial sections dividing the quadrant into four equal fields. The extension was scored in numerical values ranging from 0 to 4 (0=>no calcification or core, 1=>1/ 4 of the field occupied by calcification or core, 2=> 2/4, 3=> 3/4 and 4=> 4/4 all fields occupied). Fibrous cap thickness was measured with a score of 0 (>200 mm) or 1 (<200 mm), and by evaluating intraplaque haemorrhage with a value of 0 if absent or 1 if present. Cellular inflammation infiltrate was characterised with the following immunohistochemical markers: CD68 as a macrophage marker, Tryptase (serine proteinase stored in the mast cell secretory granules) as a mast cell marker and CD3 as a lymphocyte marker. Microvessel density count was obtained with CD34 as a marker of immature and mature endothelial cells (Ecs). **Table 2** summarises these histological features in score.

Histological features	Parameters	Evaluation	Score
Calcification extension	Occupied field of the section	≤2/4	0
		>2/4	1
Lipid core extension	Occupied field of the section	≤2/4	0
		>2/4	1
Thin fibrous cap *(Evaluated with ImageJ software)*	Thickness	>200 um	0
		≤200 um	1
Inflammation score: CD68 CD3 Tryptase	Stained cells positivity 0 to 3+ 0 to 3+ 0 to 3+	Sum of all markers <4+ ≥4+	0 1
Neoangiogenesis (CD34)	Vessels count in ROI *(see text for details)*	<50mm^2 ≥50mm^2	0 1
		Vulnerable plaque if sum of the score ≥ 3	

Table 2: First histological considerations to evaluate the vulnerability of the carotid plaque

Inflammation infiltrate evaluation with ImageJ software, CEUS study

An average of 5 fields per plaque transverse section was evaluated for each section; the area evaluated for each image was 0.12mm2 at a magnification of 10. The positivity for each antibody was arbitrarily semi-quantitatively scored as intense (3), moderate (2), low (1) or absent (0). To quantify the inflammation infiltrate, we summed the score positivity for CD3, CD68 and Tryptase. For a sample with an inflammation score lower than 4? and higher than or equal to 4?, we attributed, respectively, a value of 0 (low) or 1 (high) inflammatory infiltrate.

Neoangiogenesis evaluation with ImageJ software, CEUS study

Neoangiogenesis was expressed as microvessel density, identified by CD34-positive immunostaining. The 5 images were converted to stack, transformed in montage, converted from colour images to 8-bit greyscale and scale was set (1600 px mm 1). The total area in square millimetre was evaluated for each stack, and then we set the lower and upper threshold values to select the stained area for CD34. For each stack, we counted the total number of microvessels, their diameter and the percentage of area occupied by vessels for each photograph. The mean microvessels' density per section was expressed as a function of the total area analysed in the 5 photographs (number of microvessels per mm2).

Sequential double immunofluorescence assay on carotid plaque

To investigate the expression of dPAPP-A and Osterix in the same cells, a double immunofluorescence assay was performed as described above. All washings were performed with PBS solution. Formalin-fixed paraffin-embedded 5-um-thick tissue sections were dewaxed, rehydrated and antigen retrieval was performed as described above. Samples were then washed for

10 min. The sections were treated with goat serum (1:10, Sigma-Aldrich) in 1% BSA in PBS for 30 minutes at RT and incubated first with anti human-Nestin (1:400) in a moist chamber for 60 min, at 37°C. The samples were washed and labelled with a goat anti-mouse Alexa Fluor® 488 (1:250, Invitrogen Corporation, Camarillo, CA) in a moist chamber for 60 min, at 37°C in the dark. After incubation and washing, slides were treated with donkey serum (1:10, Sigma-Aldrich) in 1% BSA in PBS for 30 minutes at RT and incubated with anti WT1 (1:1). Then, the slides were incubated with donkey anti-mouse Alexa Fluor® 647 (1:250, Invitrogen Corporation, Camarillo, CA) in a moist chamber for 60 min, at 37°C in the dark. Finally, after washing, the slides were mounted and nuclei counterstained with DAPI (Pro long anti-fade reagent, Molecular Probes, Milano, Italy). Negative controls were done by omitting the primary antibodies. After 24 hours, samples were observed under a fluorescence microscope (Leica, DMI 6000 B) connected to a CCD camera to capture images.

Vascular healthy tissue specimens and histopathological analysis

Vascular specimens collected from multi-organ donors were kindly provided by the Cardiovascular Tissue Bank, Service of Transfusion Medicine, Policlinico S.Orsola-Malpighi of Bologna. At the end of organ procurement, a vascular surgeon is called to the Tissue Bank to grossly evaluate the status of the vascular specimens, and to exclude atheromasic plaques. Parts of those vascular segments without macroscopic lesions are therefore sent to our Pathology Unit for histopathological analysis, in order to verify their suitability for allograft transplant. Sixteen patients were prospectively selected and evaluated in one-year time length, 9 males and 7 females, mean age 36.27±16.27 (range 16-58). In four cases two different vascular segments were retrieved, with a final number of 20 collected arterial specimens, from femoral artery (12 cases, 60%), abdominal aorta (4 cases, 20%), iliac artery (2 cases, 10%) and renal artery (2 cases, 10%). Histopathological analysis with Haematoxylin and Eosin, Masson's

trichrome stain and Weigert-van Gieson stain for elastic fibers, was performed in all cases by two dedicated pathologists to exclude tissue alterations due to bad preservation and/or misdiagnosed pathological conditions. Histology confirmed a normal architecture in all cases. In particular the adventitia was well preserved, and *vasa vasorum* were well identifiable in the adventitial fat tissue. Intimal endothelial cells were preserved and evaluable in 12 specimens.

Immunohistochemical assay on healthy specimens

Formalin-fixed paraffin embedded tissue sections were processed as described above. Sections were incubated with monoclonal antibodies against CD34, CD31, Nestin, dPAPP-A and SAA4 (see **Table 1**). WT1 antibody detection was automatically performed with BenchMark XT® (Ventana Medical Systems, Inc, Tucson, USA) following the manufacturer's instructions.

Sequential double immunofluorescence assay on carotid plaque

To investigate the expression of Nestin and WT1 in the same cells, a double immunofluorescence assay was performed as described above.

Evaluation of vasa vasorum density with an ocular micrometer and morphology at IHC

We decided to test an alternative and innovative method of count to evaluate microvessel density compared to the method used to count CD34 positive vessels in carotid sections. Microvessel density was calculated through CD34 staining as a marker of both EPCs and mature endothelial cells, and CD31 staining as a marker of fully differentiated vascular and lymphatic endothelial cells.

At 20x magnification we divided vascular adventitia in every IHC slide in 1-mm2 fields, using an Olympus® ocular micrometer (1 length unit = 5 mm, which means that an area of 100 x 100 units is equal to 0.25 mm2). The microvessel "density" per section was obtained by dividing the sum of

all vascular structures observed by the number of counted fields in the section of the total areas analysed in all fields (number of positive vessels per mm2). After microvessel density was determined, we counted the number of vascular structures expressing Nestin and WT1 in each field of all sections. Single-cell positivity and structure without a visible lumen were excluded from the count.

Afterwards, we focused only on the "hot spots", i.e. those areas particularly rich in Nestin- and WT1-positive structures. By means of ocular micrometer we sorted VV by diameter, and we classified them in ≤50 mm, 50 to 100 mm and ≥100 mm, according to the classification used by Giannoni (Giannoni et al., 2009), which is very similar to the definition of "first order" and "second order" VV used by other authors (Kwon et al., 1998; Mulligan-Kehoe et al., 2010). Finally, the different percentages of Nestin- and WT1-positive cells in the "hot spots" were counted in the three different groups of VV.

Atheromasic tissue specimens and histopathological analysis

Patients

To repeat the same analysis performed above in healthy arteries, we analysed atheromasic plaque tissue retrieved from a series of consecutive patients during 2011 having the same characteristics described for the CEA study (symptomatic or asymptomatic carotid artery stenosis >=70%). Epidemiological data, neurological symptoms, vascular risk factors (hypertension, coronary-artery disease, chronic-obstructive pulmonary disease, dyslipidaemia, diabetes mellitus, current smoking and chronic-renal failure) and current therapy (acetylsalicylic acid (ASA), anticoagulant and hydroxymethyl glutaryl coenzyme A reductase inhibitor) were recorded. Histological analysis and immunohistochemical assay of carotid plaque was performed as described above. Sections were incubated with

monoclonal antibodies against CD34, Nestin, dPAPP-A, CD68, SAA4 and WT1 (see Table 1).

Evaluation of microvessel density with an ocular micrometer in carotid plaque at IHC

In carotid plaque sections the CD34 positivity was limited to precise areas called region of interest (ROI). The counting is the same as the evaluation in healthy tissue. The microvessel "density" per section was obtained by dividing the sum of all vascular structures observed by the number of counted fields (ROI) in the section of the total areas analyzed in all fields (number of positive vessels per mm2). After microvessel density was determined, we counted the number of vascular structures expressing Nestin and WT1 in the same corresponding field (ROI) of all sections. Single-cell WT1 or Nestin positive structure without a visible lumen were named "dot" and evaluated separately as negative (=0) or positive (=1). The presence of large vessels structure with a "cavernous" morphology positive to WT1 or Nestin was signalled as negative (=0) or positive (=1). Positivity of macrophages or endothelial cells to dPAPP-A protein was noted as negative (=0), focal cells (=1) and diffuse (=2).

Lipid core and calcification extension was evaluated as previously described (0=>no calcification or core, 1=>1/ 4 of the field occupied by calcification or core, 2=> 2/4, 3=> 3/4 and 4=> 4/4 all fields occupied). Phlogosis and neoangiogenesis presence were scored from 0 to 3 and the location was described as shoulder (1), cap (2), core (3) and diffuse (4). The presence (=0) or absence (=1) of complications, erosion and ulceration of the plaques lesions were signalled. By means of the ocular micrometer we evaluate the minimum and the maximum vessel diameter and fibrous cap thickness per section. Parameters are summarized in **table 3**.

Histological features	Parameters	Corresponding score
Calcification extension *Occupied field of the section*	1/4 2/4 3/4 4/4	1 2 3 4
Lipid core extension *Occupied field of the section*	Idem	Idem
Thin fibrous cap	Thickness	Min um
Vessel diameter *(Evaluated with an ocular micrometer)*	Diameter	Max um
Phlogosis (CD68) or Neoangiogenesis (CD34) description : Score	Stained cells positivity	0 to 3 +
Localization	Shoulder Fibrous cap Core Diffuse	1 2 3 4
Vessel density for CD34, Nestin, WT1 *(Evaluated with an ocular micrometer)*	Vessels count *(see text for details)*	Microvessels density $(n°/mm^2)$
"Cavernous" vessels: WT1 positive Nestin positive "Dot" vessels: WT1 positive Nestin positive	Absence Presence (low signal) Presence (high signal)	0 1 2
Complications Ulceration or erosion	Absence Presence	0 1
dPAPP-A positivity: Macrophages cells Endothelial cells	Negative Focal cells Diffuse	0 1 2

Table 3: Reviewed histological considerations to evaluate neoangiogenesis atheromasic carotid plaque.

Evaluation of circulating markers' concentration

Measurement of circulating hsCRP and SAA.

Serum hsCRP and SAA measurements were used as a surrogate marker of plaque embolic potential. Blood samples were collected 24 hrs prior to CAS and centrifuged at 1800 rpm for 10 min at room temperature (RT). Serum

hsCRP and SAA levels were analysed through nephelometric analysis (Image, Beckman Instrument); following hsCRP determination patients were divided into two groups: Class I, hsCRP<5 mg/l and Class II, hsCRP>5 mg/l. The threshold of 5 mg/l was chosen because higher serum hsCRP levels (>5 mg/l) were previously associated with vulnerable inflammatory plaque at histological evaluation (Garcia et al., 2003) and with complication risk during CAS (Gröschnel et al., 2007). The threshold of 10 mg/l was used for serum SAA levels according to the standard clinical reference range; higher values are associated to chronic infection, such as rheumatoid arthritis (Gillmore et al., 2001).

VEGF and PAPP-A serological evaluation: ELISA assay

Blood samples were collected 24 hrs prior to carotid revascularization in a clot activator tube (Vacuette, z-serum beads clot activator). Samples were placed at room temperature for 30 min to allow clotting, centrifuged at 1800g for 10 min. Serum obtained was immediately aliquoted and stored at -80°C until analysis.

VEGF serum levels were quantified with a Quantikine Human VEGF Immunoassay (Cat#DVE00, R&D systems, Inc, Minneapolis, MN, USA). The kit is a colorimetric solid phase Enzyme-Linked ImmunoSorbent Assay (ELISA) using a 96 wells microplate. Wells are pre-coated with a mouse monoclonal anti VEGF antibody. The optical density of each well was determined within 30 minutes at 450nm. A standard curve was built and GraphPad software generated a four-parameter logistic (4-PL) curve fit. The detection limit of the VEGF levels serum was less than 9.0 pg/ml.

To evaluate the risk associated to higher levels of VEGF, a cut off of 500ng/dl was chosen according to previous evaluations (Larsson et al., 2002; Hasegawa et al., 2005). The cut-off was consistent with the manufacturer (R&D systems) normal control subject group. Elevated VEGF levels were defined as being greater than the 95th percentile value in the

normal control subject group described by R&D Systems. This resulted in a cut-off value for VEGF of 500 pg/ml.

PAPP-A serum levels were quantified with the Active cPAPP-A Elisa (DSL-10-2760, DSL, Inc, Webster, TX, USA). The kit uses a microplate pre-coated with an anti-PAPP-A antibody. As described for the VEGF Elisa assay; the absorbance at 450 nm was read and a standard curve with a four-parameter logistic (4-PL) curve fit was created. The detection limit of the PAPP-A levels serum was less than 0.18 uUI/ml.

NSE and PAPP-A mRNA expression level

RNA Extraction from PAX gene tube

For each patient 2.5 ml of peripheral blood were collected on PAX-gene™ Blood RNA Tubes (PreAnalytiX), stored at room temperature for a minimum of 2 hours, then at −20∘C for a minimum of 24 h, before processing or storing at −80°C. Total RNA was extracted using PAXgene Blood RNA kit (PreAnalytix) following the manufacturer's instructions. RNA was eluted in RNAse free-water. For logistic problems PAX gene tube were not available in all cases; thus RNA from whole blood was extracted using also the Trizol method.

Extraction with Trizol method

Mononuclear cells from whole blood by Ficoll-Histopaque density gradient centrifugation (Ficoll Histopaque 1077, d=1,077 g/ml, Sigma Aldrich, ref 10771) were isolated within 4 hrs from blood collection for optimal RNA extraction. The protocol of the manufacturer's instructions was followed and count the cells were counted.

Cells ($1x10^6$) were homogenized with 800 ul of Trizol reagent (TRI reagent, Ambion Cat #AM9738), collected in an Eppendorf tube and incubated for 5 min at RT. To obtain the phase separation, a proportional quantity of chloroform was added to the sample (0.2ml: 1ml trizol); the

sample are shacked vigorously for 15 seconds and incubated for 2 to 3 min at RT. It was left for 2 min in ice, centrifuged at 12000g, 15 min at 4°C. The centrifugation generates 3 phases: trizol in the lower, waste in the middle and RNA in the upper aqueous phase. The RNA phase was gently collected in a new Eppendorf. 500 ul of isopropyl alcohol (500ul: 1ml trizol) was added and 5 ul of glicogen (2ug/ul) was added on the wall of the Eppendorf. Samples were then incubated at RT for 10 min, centrifuged at 12000g for 10 min, 4°C to allow RNA precipitation. Surnatant was discarded and RNA pellet was washed with 75% ice ethanol (1ml: 1ml trizol), then centrifuged at 7500g for 5 min, air dried for 20 min and dissolved in 15 ul of RNase free water.

Finally eluted RNA (from PAX or Trizol method) is heated 5 min at 65°C (in order to denature RNA and to inactivate RNases) and immediately placed in ice. RNA quality and concentration were assessed by measuring the A260/280 and A260/230 using a Nanodrop ND-420 (Nanodrop Technology). RNA was stored at −80∘C until used.

Reverse transcription assay

Reverse transcription assay was performed using 1 ug of starting total RNA quantity per 25 ul of mix, following the manufacturer's protocol (High capacity cDNA Archive kit, Applied Biosystem). The cDNA was stored at − 20 °C until RT-PCR were performed. RT-PCR was carried following MasterMix Taqman Protocol (TaqMan Univ PCR MasterMix, Applied Biosystem). 4ul of cDNA was amplified using specific primers for NSE, PAPP-A and betaActin described in the table below (Taqman Gene Expression Assay, Applied Biosystem) in the RT-PCR mix.

MIX qPCR	1 sample
Master mix Taqman	10
Probe NSE/betaACT or PAPP-A	1
H20	5
cDNA	**4**
Vol TOT per well	**20ul**

Reactions were run on ABI PRISM 7900HT Sequence Detection System (Applied Biosystems). Cycling conditions were as follows: 10 min at 95∘C, 40 cycles at 95∘C for 15 s and 60∘C for 60 s. Each assay was carried out in triplicate and the transcription level was normalized using beta Actin as a reference gene. A standard curve (used as calculation method) with five dilutions of cDNA (Clontech, Palo Alto, CA) obtained from normal healthy human brain was included in each respective PCR run. Calibration curves were constructed by plotting the threshold cycle versus logarithm of the relative concentration.

Statistical analysis

Continuous variables were expressed as a mean ± standard deviation (SD), categorical variables by relative and absolute frequencies. All correlations were first analyzed with a multiple regression. Analyses of differences between two groups were performed with Fisher's exact test for categorical variables and with unpaired Student's t test or Mann-Whitney U test for continuous variables. Analyses of differences between more than two groups were performed with the Kruskal-Wallis one way ANOVA test. The value of $p<0.05$ was considered significant. Goodness of fit in binary regression model was tested with the Hosmer-Lemeshow analysis. Statistical tests were performed using SPSS® 13.0 for Windows® computer software (SPSS, Chicago, Illinois, USA).

To analyse and represent basic biostatistics, curve fitting and scientific graphing of biological data we used Prism 5® software (GraphPad Software, Inc). We used the non-parametric Spearman correlation coefficient. The best way to interpret the value of r is to square it to calculate r2. Thus for the graphical representation we used a linear regression with an r2 value from the Pearson correlation coefficient.

RESULTS

RESULTS

A total of 84 patients were enrolled from January 2009 to December 2011. No peri-operative complications (neurological events, myocardial infarction, death) were recorded in neither group. Epidemiological data, neurological symptoms, vascular risk factors and current therapy of all patients submitted to CEA or CAS were recorded in our database.

CAS, biomarkers and cerebral lesions

Patients CAS.
Thirtyfour patients either symptomatic or asymptomatic were included in the study. In two cases the CAS procedure was aborted due to technical difficulties and the stent was not deployed. The filters were positioned, subsequently removed and utilized as a control specimen. Mean hsCRP, SAA, VEGF, PAPP-A and HDL serum levels are listed in the **table1**.

|	hsCRP	SAA	VEGF	PAPP-A	Col Tot	LDL	TG	HDL
Mean	15.54±20.36	40.39±8.89	566.4±304.00	1.22±1.26	183.4±32.5	111.7±19.51	134.6±36.25	43.14±8.86

Table 1: Mean serum levels of the studied proteins

Drug therapy CAS
All patients were medicated with aspirin 100 mg and clopidogrel 75 mg for 3 days before and one month after the procedure. Hydroxymethyl glutaryl-coenzyme A-reductase inhibitor (statins) therapy was used by 12 patients. No significant difference was seen in filter percentage of occluded pores (PO), area covered by debris (SI) and SEM evaluation between patients with or without anticoagulant therapy, antiaggregant therapy or statins therapy (data not shown).

*Distribution and description of the material covering the filter*

Filter analysis by light microscopy.

All filters showed the presence of a substantial amount of debris at macroscopic observation. Two of them had extensive deposits of vitreous, yellowish lipid-like material that was dissolved after histological processing (**Fig. 1A**). Microscopic debris were detected in all filters, with a mean percentage of surface involvement (SI) of 29.33%±8.1 and pore occluded (PO) of 27.30%±9.5; control filters showed both a lower SI, 4.15%±2.3, and PO, 0.50%±0.3, compared to filters of treated patients ($p < 0.05$). As we noticed that same statistical correlation in all analysis between PO and SI%, the 2 evaluations were considered interchangeable.
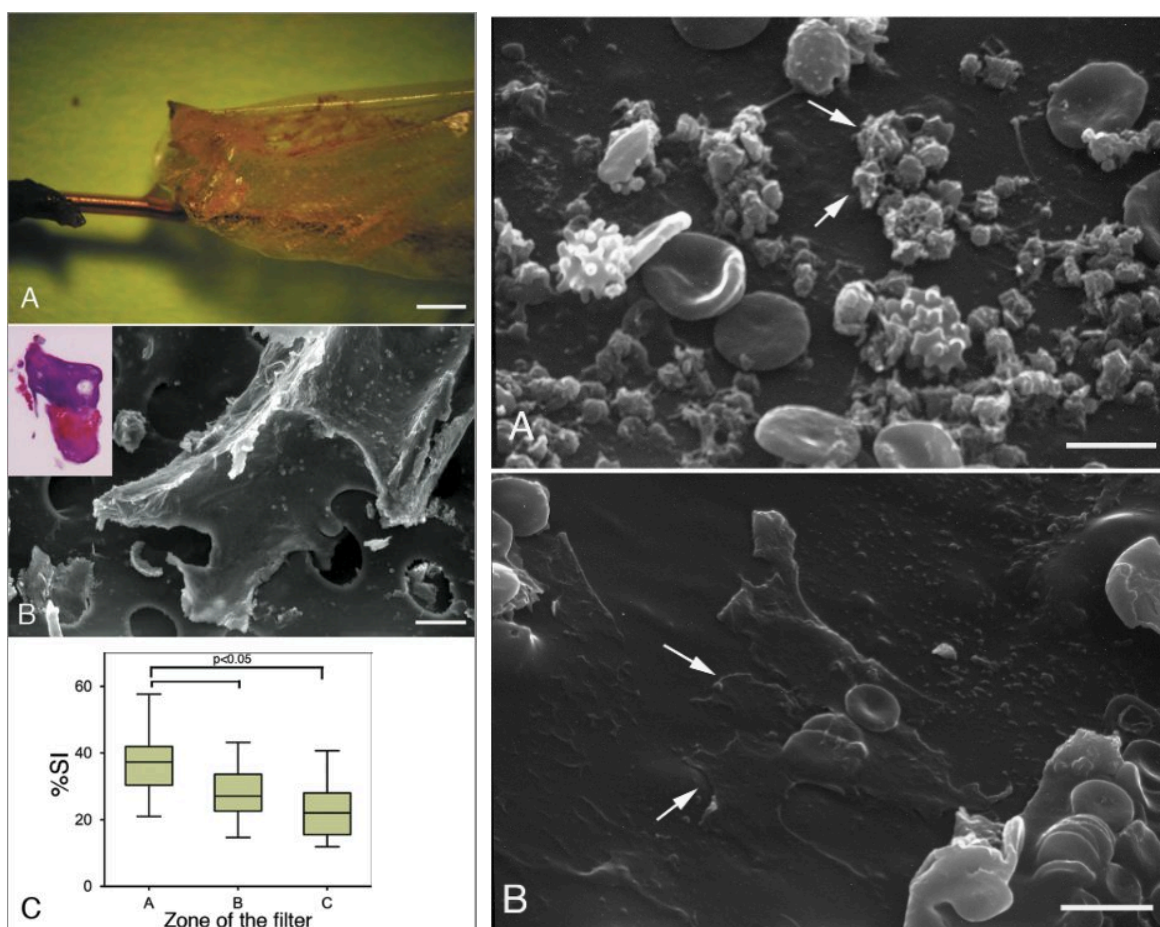
Figure 1: Left panel: a filter used during CAS (A, scale bar 1mm) and the corresponding scanning electron microscopy showing details of the point with accumulation of embolic material (B, scale bar 100 µm). Hematoxylin-eosin staining of a plaque fragment removed from the filter point (B, insert; magnification 40x). Distribution of embolic material (% SI) in three different zones of the filter: distal (zone C), medial (zone B) and proximal (zone A) (graphic C). Right panel: surface filter showing a variety of cells ranging from red blood cells, acanthocytes, aggregates of dendritic, activated platelets (white arrows; A, scale bar 5 µm) and fully spread platelets (white arrows; B, scale bar 10 µm).

Distribution of the material was heterogeneous along the filter membrane with a significantly higher SI (37%± 9.00) at the tip of the filter (zone A) compared to the middle zone (zone B; 28%±7.7) and distal zone (zone C; 23%±8.3) (**Fig. 1C**). Plaque fragments were commonly seen at the tip of the filter (**Fig. 1A, B**). Hematoxylin-eosin staining revealed that the type of material removed from the paraffin embedded filters was composed by thrombo-embolic debris, acellular material, cholesterol clefts and atheromatous plaque fragments (**Fig. 2**).
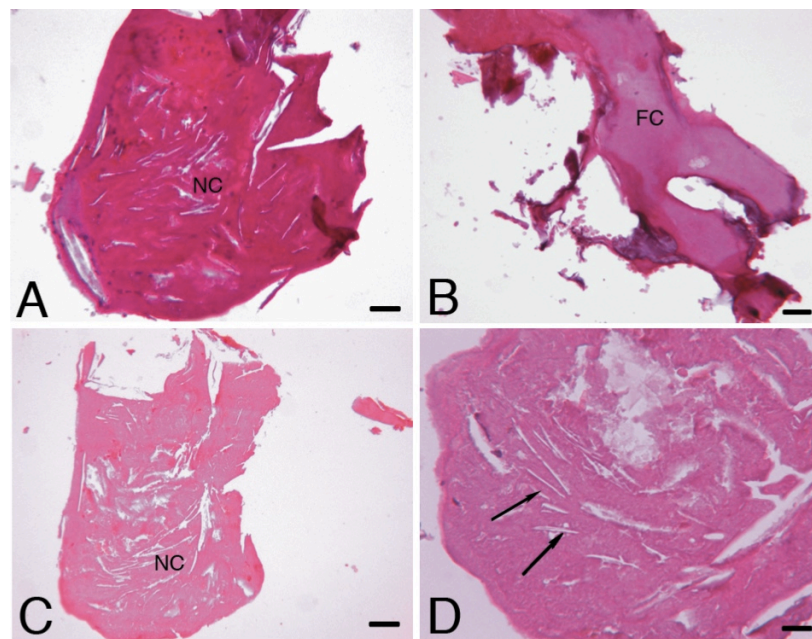
Figure 2: Histological images of debris recovered from the entire filter membrane showing necrotic-lipid core (A and C; FC) and fibrous cap (B; NC) fragments; D) higher magnification of panel C showing amorphous and acellular material rich in cholesterol clefts (arrows). Scale bars: A, B, C = 100 µm; D = 5 µm.

Filter analysis by scanning electron microscopy.

To clarify the composition and the mean size of debris adherent to the inner surface part of the filter, devices were analysed through SEM and histological analysis. Unlike control filters, visibly clean, all areas of the filter were covered with debris ranging from 30µm to 2 mm. All filters were covered with an amorphous film, i.e., biofilm, of protein composition typical for all biomaterial. Pores of 100 µm diameter were occluded by clumps of red blood cells (RBC), embolic and plaque fragments (**Fig. 3**). SEM also revealed the presence of activated platelets with dendritic and spread morphologies (not shown).

No differences were found in volume and composition of embolic debris between patients with homogeneous and dishomogeneous plaque (data not shown).
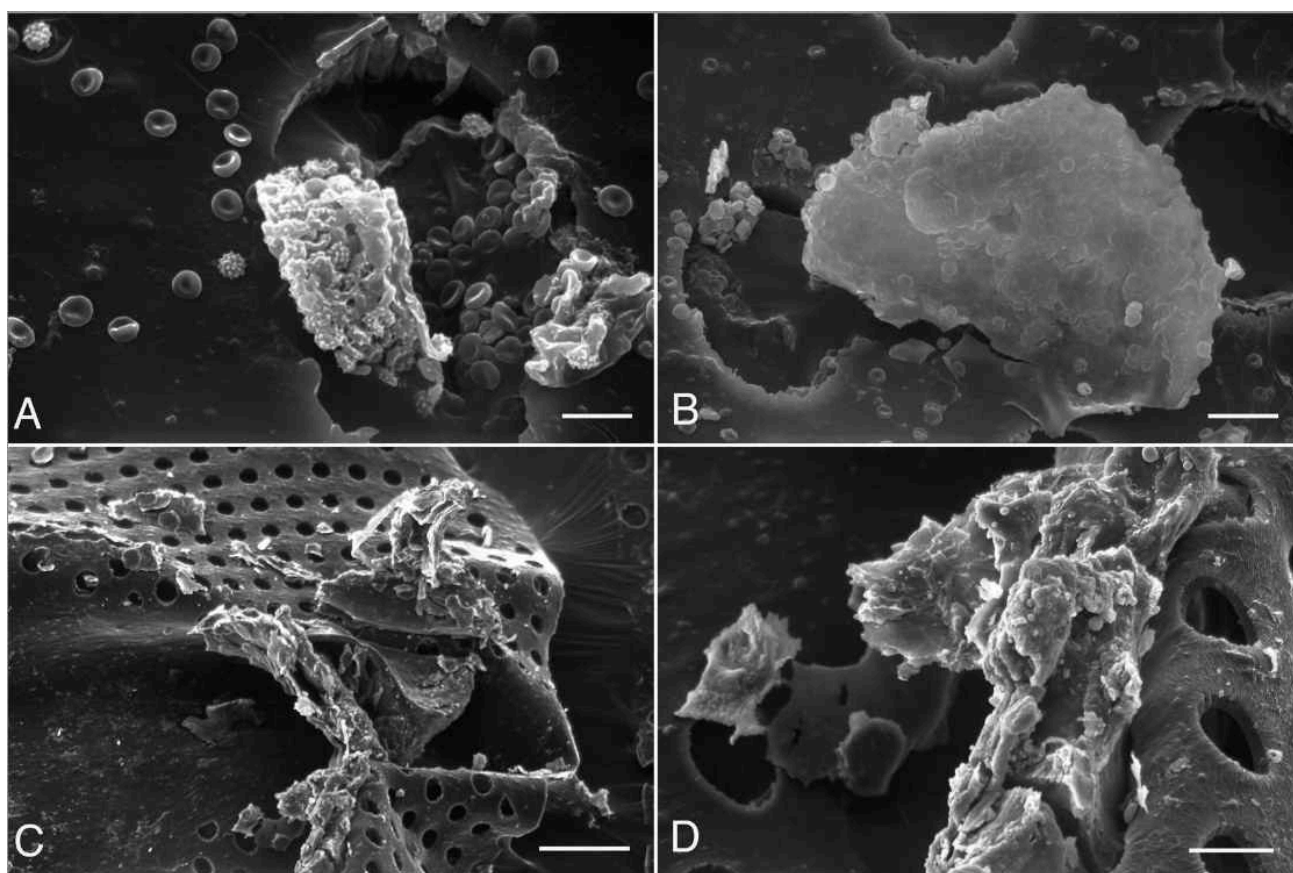
Figure 3: Representative scanning electron microscopic images of thromboembolic materials captured by the filter surface (A, scale bar 25 µm; B, scale bar 40 µm). Details of plaque fragment trapped at the filter's tip (C, scale bar 500 µm; D, scale bar 100 µm)

Markers levels pre-procedural, amounts of debris and cerebral lesions post-procedural

Patients with hsCRP>5mg/l had a greater percentage of PO (and SI) compared with lower levels of hsCRP (32.78%±11.41 vs. 23.9%±6.7, p=0.0019 (33.3%±7.7 vs. 25.4%±7.0, p=0.07 respectively) (**Fig. 4** left upper graph).

According to the type of plaques, patients with dishomogeneous plaque had a significantly higher PO vs those with homogeneous plaque (38.68%± 7.1 vs. 24.06%±5.6 respectively, p=0.036) (**Fig. 4** right upper graph). Patients having higher hsCRP level (≥5mg/l) and dishomogenous plaque had a greater number of occluded pores and a major % of surface (SI) covered with debris (35.7%±11.7 vs. 19.9%±6.7, p=0.049 and 33.3%±7.7 vs. 25.4%±7.0,

p=0.04) respectively compared to patients with homogenous plaque and lower hsCRP (<5mg/l) **(Figure 4A, B).**
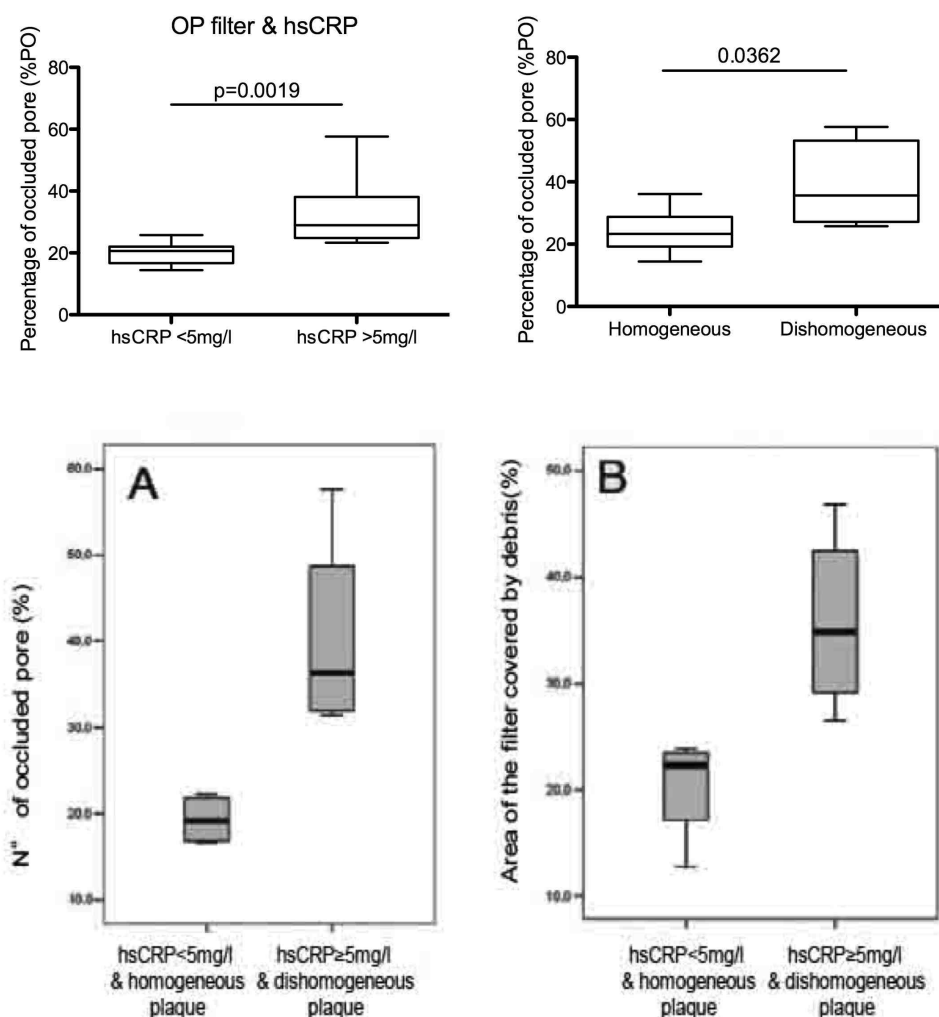
Figure 4: hsCRP level, plaque type and filter protection. Percentage of PO and SI for hsCRP<5mg/l and for hsCRP>5mg/l levels. Percentage of PO (A) and SI (B) in patients with hsCRP<5mg/l homogenous or hsCRP>5mg/l and dishomogenous plaque.

For patients with high SAA (>10mg/l) and VEGF (>500pg/ml) values we found filters with an increased number of pore occluded (PO) by debris. (**Fig 5**, SAA: 22.20±6.90 vs

35.94±13.52%, p=0.023 and VEGF: 22.45±5.68 vs 37.09±11.06%, p= 0.0047). High percentage of occluded pores was also associated with high PAPP-A levels and low HDL levels (trend, **fig. 5**).
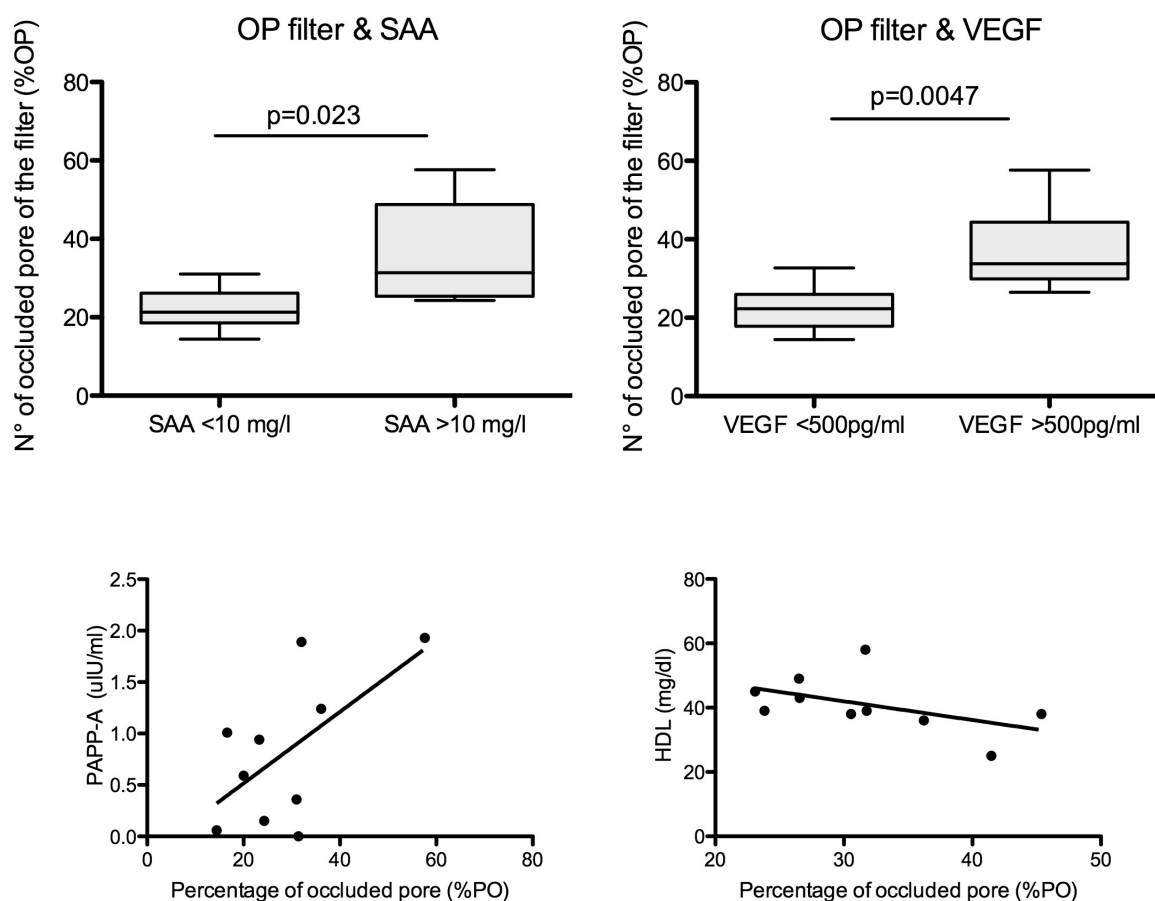
Figure 5: SAA, VEGF. PAPP-A, HDL and percentage of occluded pores of the filter protection

Patients presenting neurological symptoms before the CAS procedure had an increase of the amout of debris covering the filter membrane (**Fig 6**, 22.70±6.9 vs 35.52±6.95%).

After the stenting procedure, ischemic asymptomatic cerebral lesions were observed in all patients. The median number of cerebral lesions was 22 range 0-2550 and the median volume was 500 range 0.0001-12043mm3. Patients with more than 30% of the filter area covered by embolic debris showed a higher number of total cerebral lesions post CAS (**Fig 6**,

15.7±7 vs. 3.4 ±2.1, p=0.03). Patients with hsCRP ≥ 5mg/l showed a higher number of total cerebral lesions (2.5±1.64 vs 17.5± 5, p=0.01) compared to patients with lower hsCRP levels (OR 2.6, CI 1.005-6.8) **(Fig 6).** hsCRP ≥ 5mg/l is also associated to the volume of cerebral lesions ≥1000 mm3 (OR 3.9, C.I. 1.1-13.7, not shown).
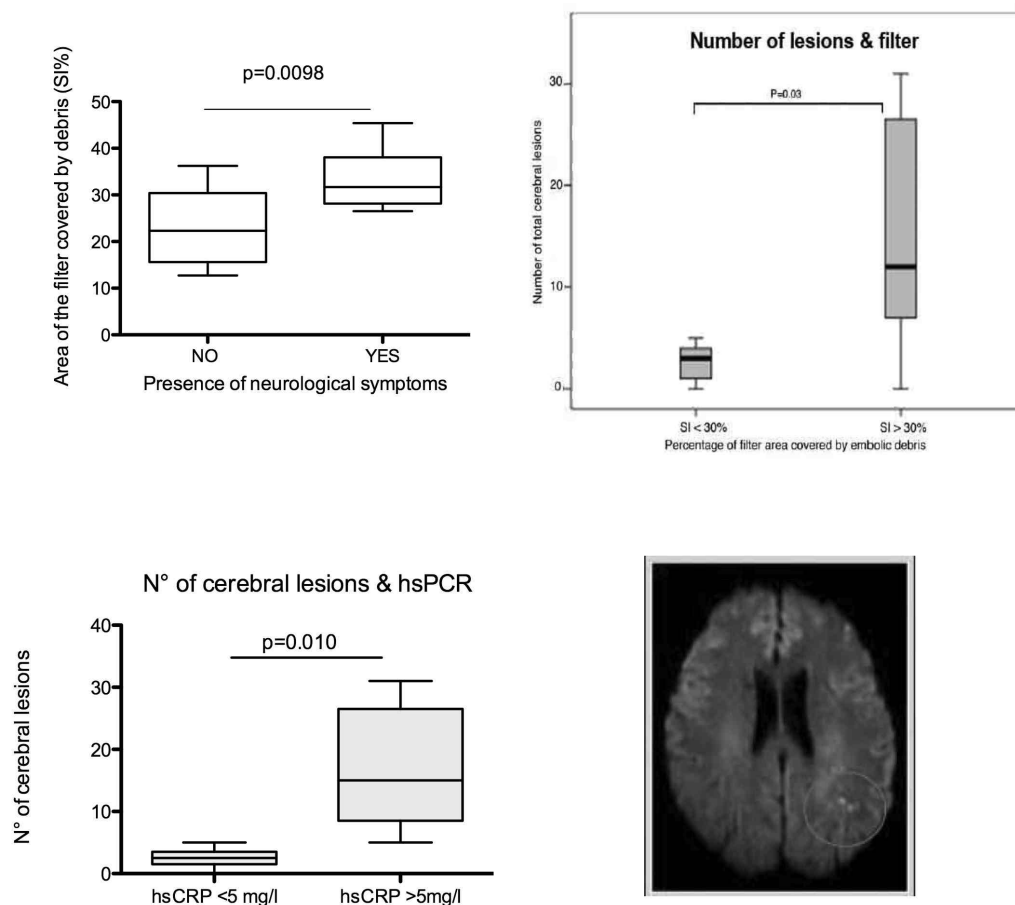
Figure 6: Cerebral lesions post-procedural and hsCRP levels pre-CAS. In the RMx imaging the circle indicates a cerebral lesion.

Patients who had SAA > 10mg/l showed a significave increase of the number of total cerebral lesions compared to patients with lower SAA levels before the procedure (3.4±1.14 vs 18.2±6.35, p=0.012) **(Fig 7).** Serological values of SAA> 10mg/l before the CAS procedure is also associated to a major volume of cerebral lesions (3253.12±567 vs 513.02±202 mm3, p=0.004). Moreover,a perfect positive linear correlation was observed

between the volume of cerebral lesions and SAA serum level pre CAS (Figure, r^2=0.962) **(Fig 7).**
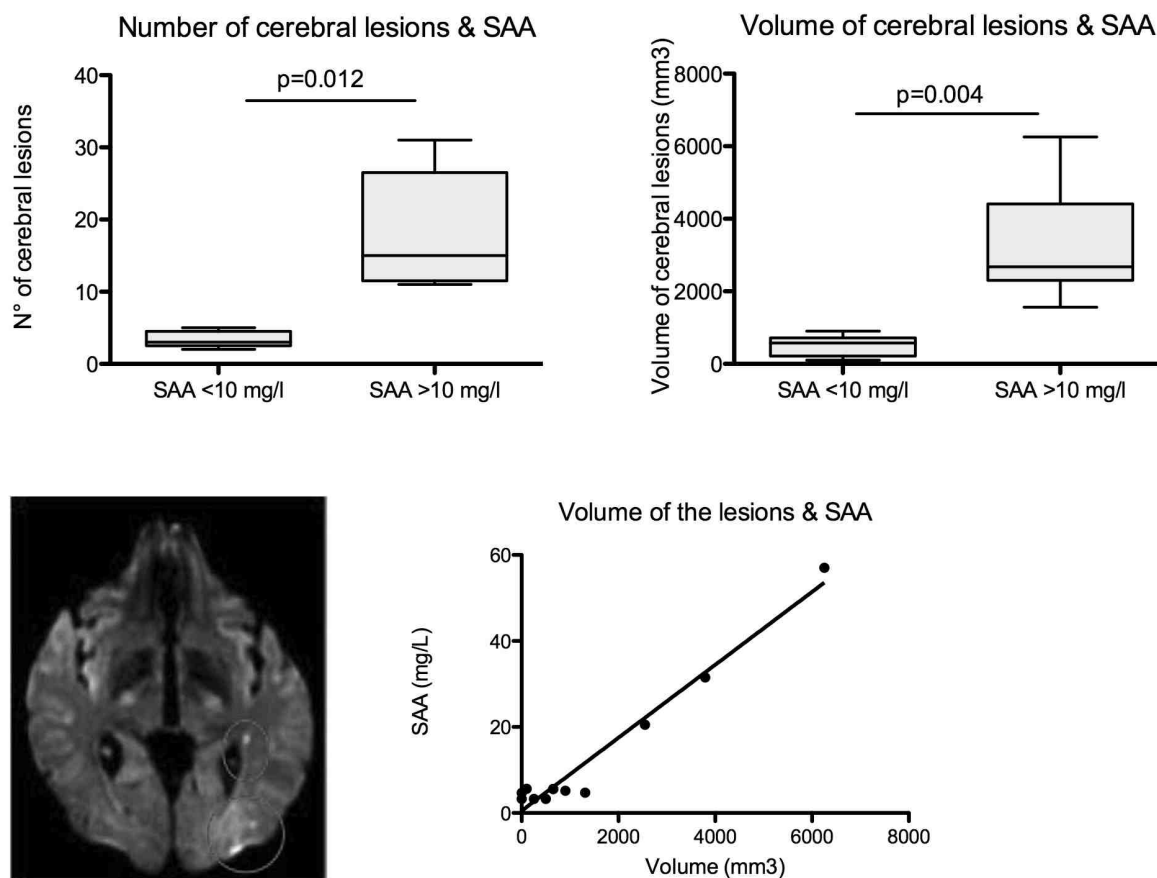
Figure 7: Cerebral lesions post-procedural and SAA levels pre-CAS. RMx showing cerebral lesions in 2 different's loci.

NSE mRNA and mRNA PAPP-A expression levels were not associated to the presence of cerebral lesions. However circulating NSE mRNA levels in blood increased up to 4 times with the increase of SAA and hsCRP serum levels **(Fig 8).** In patients submitted to CAS procedure we found an increase of 32% of the expression of NSE mRNA compared to CEA procedure.
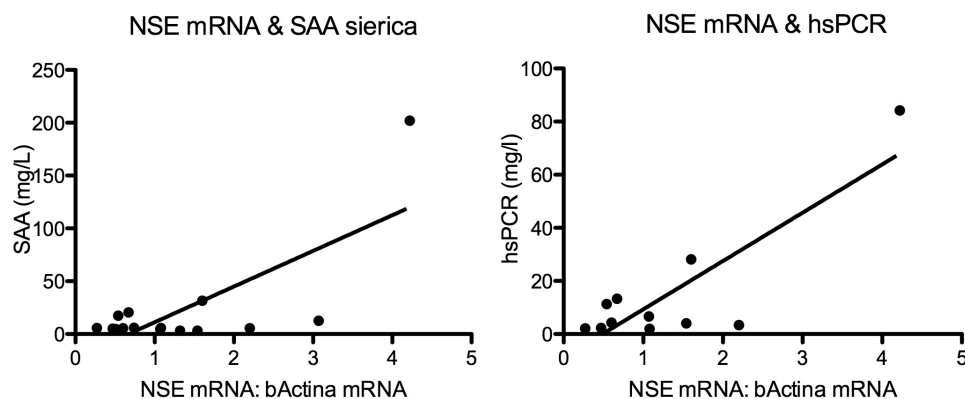
Figure 8: NSE mRNA expression level and inflammation markers

Identification of plaque vulnerability in patients submitted to CEA

Patients

Fifty-two patients either symptomatic or asymptomatic were enrolled for the CEA study. Mean hsCRP, SAA, VEGF, PAPP-A and HDL levels are listed in **table 2**.

	hsCRP	SAA	VEGF	PAPP-A	Col Tot	LDL	TG	HDL
Mean	4.035±2.72	12.8±.1.3	617.4±200	1.5±1.16	163.4±33.5	103.8±27.51	102.3±26.5	50±8.44

Table 2: Mean serum levels of the studied proteins

hsCRP levels were significantly higher in symptomatic patients compared to asymptomatic ones: 19.9 ± 34.2 vs. 4.3 ± 3.2 mg/l, p=0.007. The same relation was observed for VEGF; serum levels were 623.6 ± 133.8 pg/l in symptomatic and 443.2 ± 161.9 pg/l p=0.04, in asymptomatic patients.

We remind that plaques, in this first part of the study on CEA, were evaluated for 5 histological parameters; microvessels density, fibrous cap thickness, inflammation, calcification and lipid core area. The sum of these 5 parameters (0-5) defines the histological plaque vulnerability.

CEUS evaluation, inflammation and plaque vulnerability

Among the 52 CEA patients, a group of 22 patients was submitted to contrast-enhanced ultrasonography (CEUS) analysis. dB-E ranges from 2 to 7.8, mean 4.85±1.9. No statistically significant differences were identified for demographic characteristics, vascular risk factors or current therapy (not shown).

It was seen that patients with ischaemic neurological symptoms pre-CEA (stroke, TIA or amaurosis fugax) had significant higher carotid dB-E compared with asymptomatic ones (7.40±0.5 dB-E vs. 3.5±1.4 dB-E respectively, p=0.006). In particular the presence of an ipsilateral embolic lesion on preoperative CT scans was significantly correlated with higher dB-E on CEUS compared with patients with negative cerebral CT scan (5.96±1.5 dB-E vs. 3.0±1.0 dBE, respectively, p=0.01).

At histological evaluation, the presence of high inflammation infiltrate in the carotid plaque specimens was related to higher dB-E at CEUS evaluation, compared with specimens with lower inflammation. Ten patients had a score inflammation of 4-5 with a dB-E of 7.4±1.2 and 12 patients, score 1-2, had a dB-E of 3.2±0.9 (p=0.03).

Microvessels were identified in the medial border of the lipid core, within the cap, within the lipid core, within the intima and in the shoulder. The percentage of number of vessels per region was 59%in the shoulder, 26% in the cap and 15% in the core. We observed that an elevated vessel density on plaque specimens ($>50mm^2$) corresponds to a higher dB-E ($<50mm^2$: 2.5±0.7 dB-E vs $50mm^2$: 5.5±1.2 dB-E, p=0.04). An increase of dB-E was also noticed in patients presenting a fibrous cap <200um (<200um: 5.96± 1.5 dB-E vs >200um: 3.0± 1 dB-E, p=0.01). Finally, plaques with a vulnerability score of 5 had an increase of the dB-E compared to patients with a vulnerability score of 1 (7.6±0.2 vs. 2.5±0.6, p=0.001) (plaques scored 2 had a dB-E of 4.6± 0.8; scored 3 in none; scored 4 had a dB-E of 7.1±0.5). The dB-E levels were significantly different between vulnerability groups (p=0.001) **(Fig 8).**
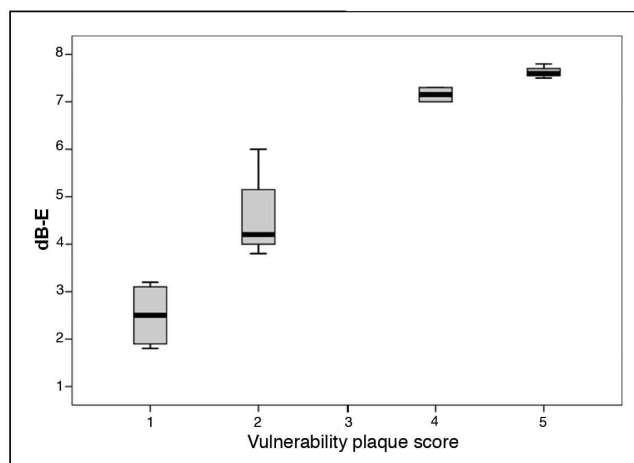
Figure 8: dB-Enhancement evaluation of plaque vulnerability score. Differences between groups are statistically significant at ANOVA analysis (p=0.001).

VEGF, hsCRP serum levels and histological plaque vulnerability

All 22 carotid plaque specimens were suitable for the histological evaluation. Inflammation markers were present in all carotid specimens analysed with different grade of staining (**Fig. 9 A-D**): CD68, marker of macrophages, was highly expressed in all carotid plaques sections compared to mast cells followed by lymphocytes, as shown in figure 9E (p<0.05).
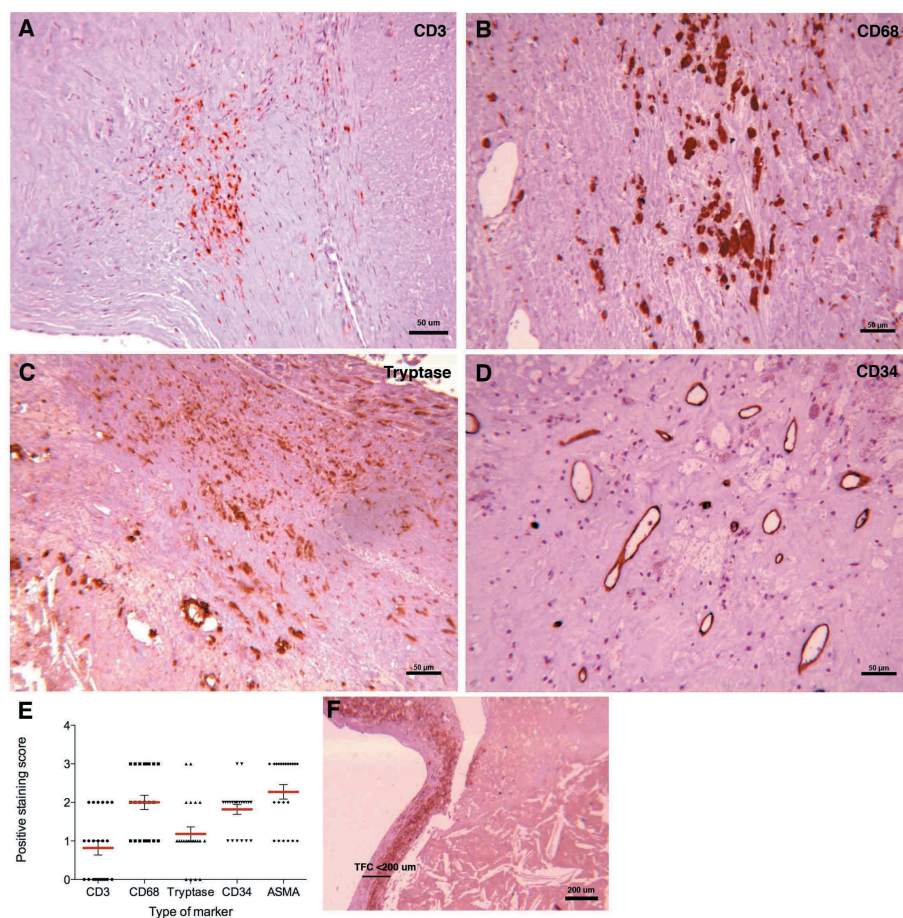
Figure 9: Characterization of plaque vulnerability in the CEA procedure. To evaluate inflammatory infiltrate carotid plaque sections were immunostained with CD3 (A, lymphocytes in the shoulder area), CD68 (B, macrophages in the fibrous cap), Tryptase (C, mast cells in the fibrous cap). Microvessels in proximity of the core stained with CD34 (D). Distribution of grade of staining for each marker (E).

Patients with vulnerable plaques (vulnerability score 3 to 5) had higher hsCRP and VEGF serum levels compared with patients with non vulnerable plaques (score 0 to 2) (hsCRP: 21.3 ± 24.2 mg/l vs. 3.0 ± 1.7 mg/l, p=0.004 and VEGF: 660.8 ± 284.0 pg/ml vs. 429.9 ± 262.9 pg/ml, p=0.01). The presence of inflammation infiltrate in the carotid plaque specimens was related to higher dB-E at CEUS evaluation, compared with specimens with no inflammation (7.4 ± 1.2 dBE vs. 3.2 ± 0.9 dB-E, respectively, p= 0.03) (not shown).

Moreover patients with pre-operative neurological symptoms presented high score of plaque vulnerability (score 2 to 3) at histological analysis (p=0.02). HsCRP >5mg/l was associated with the presence of vulnerable plaques with Odd Ratio (OR) 2.5, Confidential Interval (CI) 95%1.1-5.5, p=0.01; the presence of VEGF>500 pg/l was associated with the presence of vulnerable plaques with OR 3.0, CI 95%1.1-7.7, p=0.01.

Thin fibrous cap

Neurological symptoms were detected in 57.14% and 67% of them presented erosion and/or ulceration of the plaque surface. Neurological symptoms were also associated positively to the thickness of the fibrous cap (TC negative: 207.9±72.07um vs TC positive 98.63±52.67) **(Fig 10).** The fibrous cap was thinner in patients with higher level of VEGF (p=0.0001 r^2=0.5601), NSE mRNA expression level (p=0.032, r^2=-0.711) and a trend was observed for the level of triglycerides. Inversely patients with major level of HDL presented a thicker fibrous cap (trend) **(Fig 11).**
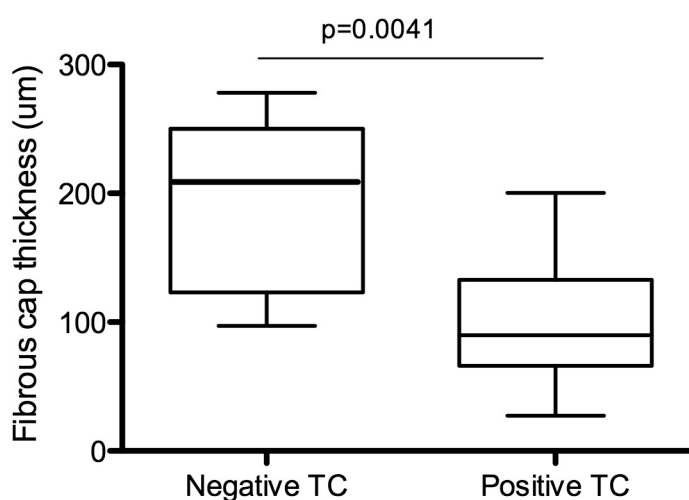
Figure 10: Association between fibrous cap thickness of the plaque and the presence of pre-operative neurological symptoms in patients submitted to CEA.
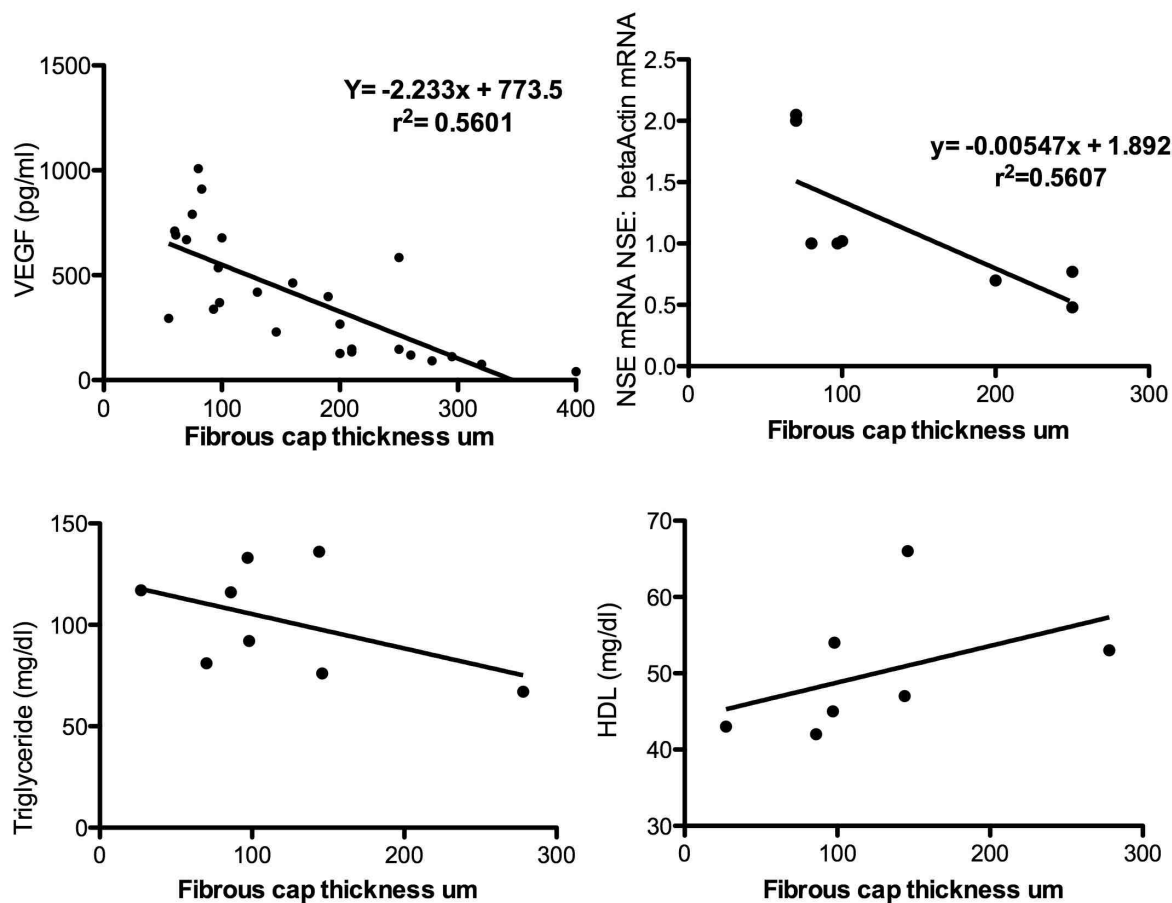
Figure 11: Correlation between the thickness of the fibrous cap and VEGF, NSE mRNA expression level, triglycerides and HDL blood level.

Vascular healthy tissue specimens and histopathological analysis

CD31 and CD34

The mean number of CD31-positive vascular structures in the adventitia of the 20 cases was 181.60±94.52 (median 152, range 67-425), the mean counted fields were 12.86±4.23 mm2 (median 12, range 6-21 mm2), the mean final "density" of CD31-positive structures was 13.63±3.50/mm2 (range 8.11-22.67/mm2, Fig. 1A). The mean number of CD34-positive

vascular adventitial structures was 146.30±72.27 (median 133, range 34-329), the mean counted fields were 11.53±3.98 mm2 (median 11, range 4-18 mm2), the mean final "density" of CD34-positive structures was 12.20±3.04/mm2 (range 7.68-20.89/mm2, **Fig. 12A**). The mean ratio between CD34 and CD31 "densities" was 0.94±0.24, very close to 1.
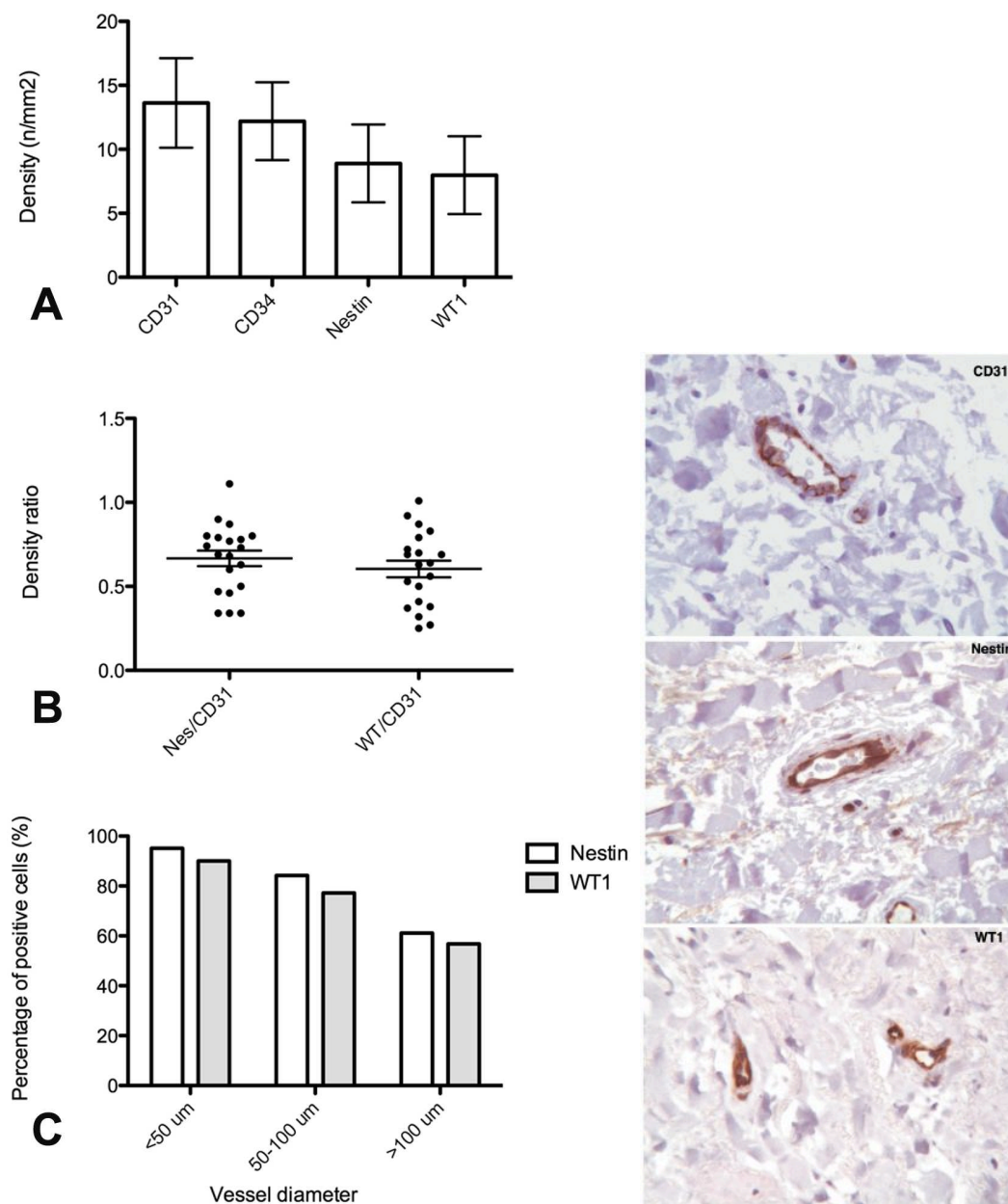
Figure 12: Immunohistochemistry results. A) Histogram representing mean densities of positivity expressed as number of positive vessels/mm2 of CD31, CD34, Nestin and WT1; B) Scatter plot illustrating the distribution of the Nestin/CD31 and WT1/CD31 ratios in all cases (see text for details); C) Histogram with the percentage of Nestin- and WT1-positive cells in the three groups of vasa vasorum sorted by diameter. Right panel; an example of immunohistochemical pattern of positivity for CD31 (upper), Nestin (center), and WT1 (lower) in small-sized vessels (25x magnification).

Nestin and WT1

The mean number of Nestin-positive vascular structures in the adventitia of the 20 cases was 117.10±59.13 (median 114, range 19-242), the mean counted fields were 12.83±4.20 mm2 (median 14, range 5-19 mm2), the mean final density of Nestin-positive structures was 8.90±3.04/mm2 (range 3.04-15.87/mm2, **Fig. 12A**). The ratio between Nestin density and CD31 density ranged from 0.34 to 1.29, with a mean Nestin/CD31 ratio of 0.69±0.26, which briefly means that a mean of 69% of CD31-positive vessels showed concomitant positivity for Nestin as well (**Fig. 12B**).

The mean number of WT1-positive adventitial vessels was 105.85±51.63 (median 95, range 23-209), the mean counted fields were 13.24±3.82 mm2 (median 14, range 2-20 mm2), the mean final density of Nestin-positive structures was 7.98±3.04/mm2 (range 2.88-14.73/mm2, **Fig. 12A**). The ratio between WT1 density and CD31 density ranged from 0.25 to 1.27, with a mean WT1/CD31 ratio of 0.63±0.27, which means that a mean of 63% of VV showed concomitant positivity for WT1 and CD31 (**Fig. 12B**).

As expected, the ratio between Nestin and WT1 "densities" is very close to 1:1. Indeed the mean Nestin/WT1 ratio in all 20 cases was 1.15±0.25.

Comparison between IHC and vessel morphology

Since not all VV showed positivity for Nestin and WT1, we focused on the "hot spots", i.e. the areas of major positivity. Of note, Nestin-positive and WT1-positive vascular structures of ≤50 μm in diameter were positive for those antibodies in the large majority of cells (95% and 90% of cells respectively for Nestin and WT1). Positive VV with diameter ranging from

50 to 100 μm had a mean of 84% and 77% of Nestin- and WT1-positive cells respectively. Positive vessels ≥100 μm in diameter expressed only 61% and 57% of Nestin and WT1 respectively (**see also Fig 12C**).

There is an increase in Nestin and WT1 expression, in terms of number of positive cells, and it is inversely correlated to the size and calibre of the micro-vessels. In particular in this study we observed higher positivity for Nestin and WT1 in small arteries (recognizable by the muscular layer), less than 50 μm in diameter, especially in "nests", relatively distant from vascular media, in which several small arteries were visible together with small veins of similar size and peripheral nervous structures (**Fig. 12 and 13**). Conversely, vessels of more than 100 μm in diameter, both arteries and veins, were generally negative for Nestin and WT-1, or showed only few scattered positive cells.
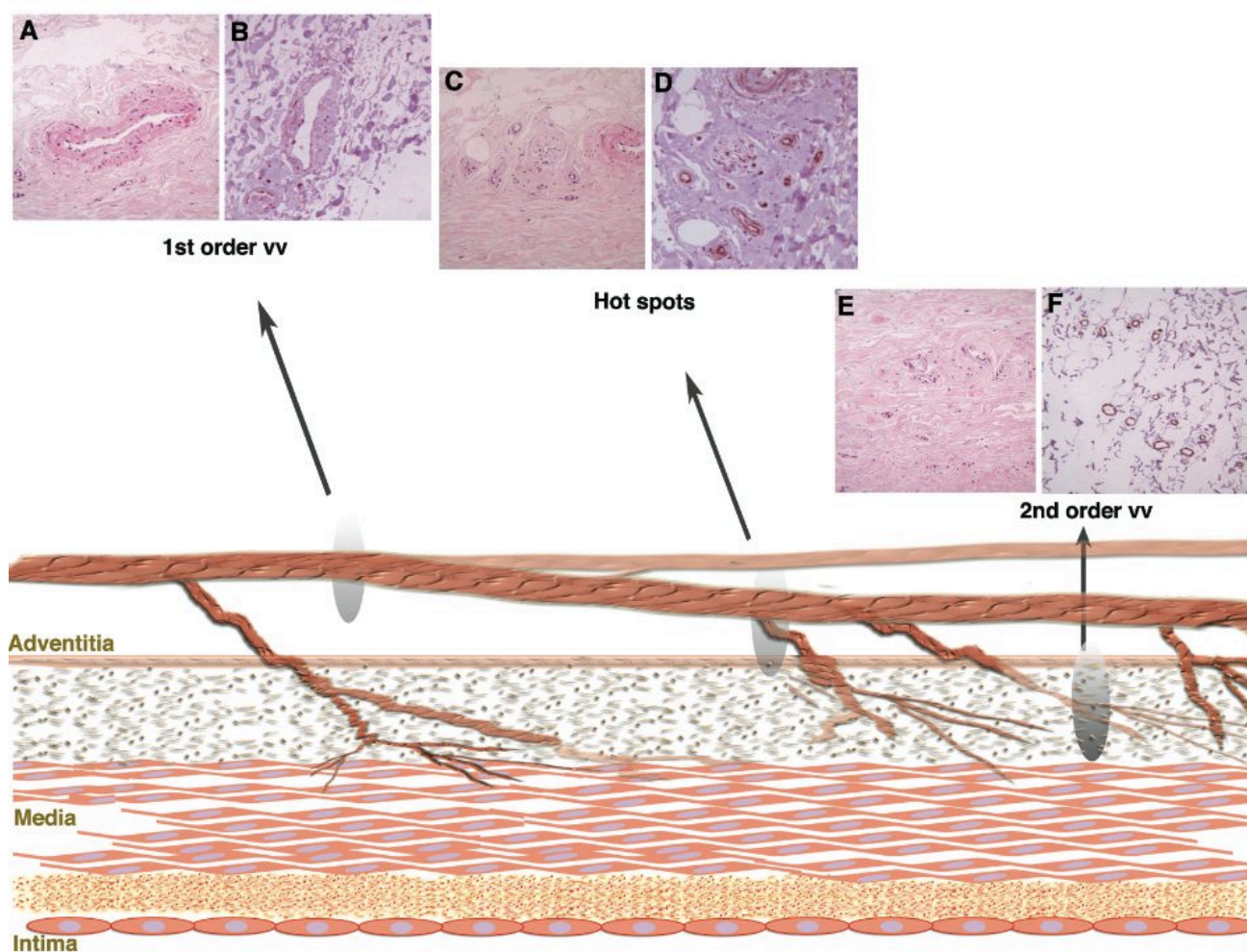
Figure 13: A representation of a first-order vasa vasorum, its second-order vasa vasorum, and a hypothetical "hot spot" in the branching. Inserts A,C, E show the histological

appearance of each level (Haematoxylin-Eosin stain, 10x magnification), inserts B, D, F show Nestin immunoreactivity (10x magnification).

Localization of Nestin and WT1 at immunofluorescence

Since in the IHC assay we noticed that the Nestin expression pattern closely resembled the pattern of WT1 and the ratio between Nestin and WT1 "densities" is very close to 1:1, we investigated by double immunofluorescence whether these two proteins had an overlapping localization. Nestin and WT1 signals co-localized in the endothelial cells from adventitial VV, including the "hot spots". WT1 signal was strongly expressed by endothelial cells mainly in vessels of ≤50 μm in diameter. The expression was confined in the perinuclear and nuclear area (**Fig. 14A**), but a cytoplasmic pattern was also observed (**Fig 14D**). Nestin expression was restricted to the cytoplasm (**Fig. 14B and C**). The merge of WT1 and Nestin revealed that they were mostly expressed in the same cell population (**Fig.14E**) and, surprisingly, cytoplasmic expression of WT1 overlaps nestin expression. This phenomenon was mainly observed in endothelial cells from vessels of *>100μm* in diameter.
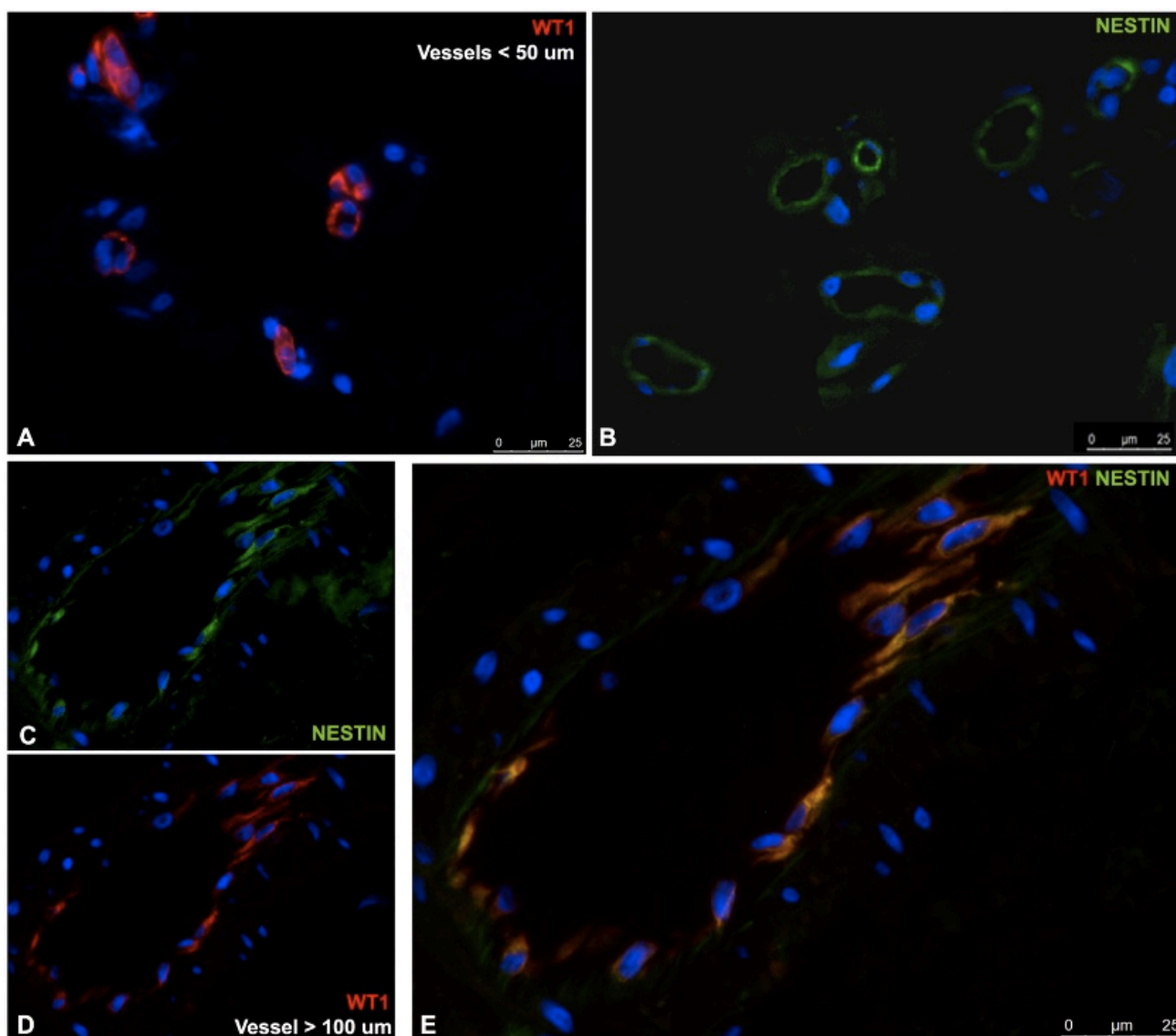
Figure 14: Double-label immunofluorescence micrographs representing WT1 (red) detectable in the nucleus of vessels <50 um (A) or in the cytoplasm of vessels with a diameter >100 um (D) and Nestin (green), detectable only in the cytoplasm (B, C). The merged image (E) shows the colocalization in the cytoplasm of Nestin and WT1 proteins in a vessel of > 100um. Nuclei (blue) were counterstained with DAPI. Scale bars: 25 um.

Vascular atheromatous tissue specimens and a new histopathological analysis: a neoangiogenesis study

In this analysis the number of positive vessels was evaluated in the same positive region of interest for each markers. To simplify the results presentation we express one field as 1 mm2 (corresponding in the ocular micrometer to four fields of 0.25um2).

CD34, Nestin and WT1

The mean number of CD34-positive vascular adventitial structures in atherosclerotic plaques of the 23 cases analysed was 100.65±68.68 (median 87, range 11-283), the mean counted fields were 2.35±1.72 mm2 (median 2, range 0.25-8.25 mm2), the mean final "density" of CD34-positive structures was 43.27±14.68/mm2 (median 42.28, 22-88.56/mm2, Fig.).

The mean final "density" of Nestin-positive structures was 32.68±12.65/mm2 (median 30.84, 12-58/mm2, **Fig 15).** The mean final "density" of WT1-positive structures was 17.95±9.80/mm2 (median 17.00, 4-40/mm2, **Fig 15**.).

Neoangiogenesis histological score (0-3) was perfectly linear with the n° of fields evaluated, n° of positive cells and density of each markers (CD34-WT1-Nestin, data not shown). All measurements were highly repeatable; the number of fields and the number of positive cells counted for each marker were highly comparable (**Fig 15**). Neoangiogenesis score was strongly associated to the degree of inflammation in the atheromateous plaque (p=0.016, data not shown).

0.25um2	Nº field counted		CD34	Nestina	WT1
	Healthy		46,1	51,3	52,95
	ds		15,93	16,78	15,29
	Atheromasic		9,39	8,78	8,70
	ds		6,87	7,04	7,29
0.25um2	Nºpositive vessels		CD34	Nestina	WT1
	Healthy		146,3	117,1	**105,85**
	ds		72,27	59,13	51,63
	Atheromasic		100,65	68,74	**37,35**
	ds		68,68	47,54	31,05
	Density Nº of vessels/mm2		CD34	Nestina	WT1
	Healthy		12,19	8,9	**7,98**
	ds		3,04	3,04	3,04
	Atheromasic		43,27	32,68	**17,95**
	ds		14,68	12,65	9,8

1mm2	Nº field counted		CD34	Nestina	WT1
	Healthy		11,53	12,83	13,24
	ds		3,98	4,20	3,82
	Atheromasic		2,35	2,20	2,17
	ds		1,72	1,76	1,82
1mm2	Nºpositive vessels		CD34	Nestina	WT1
	Healthy		36,58	29,28	26,46
	ds		18,07	14,78	12,91
	Atheromasic		25,16	17,18	9,34
	ds		17,17	11,89	7,76

Figure 15: Graphical representations of the parameters studied for neoangiogenesis analysis in atheromateous palques.

Nestin and WT1 "dis-correlation"

In atheromateous arteries the Nestin expression pattern didn't match the pattern of WT1 as in healthy arteries. WT1 signal intensity was weaker in atheromateous vessels **(Fig 16).**
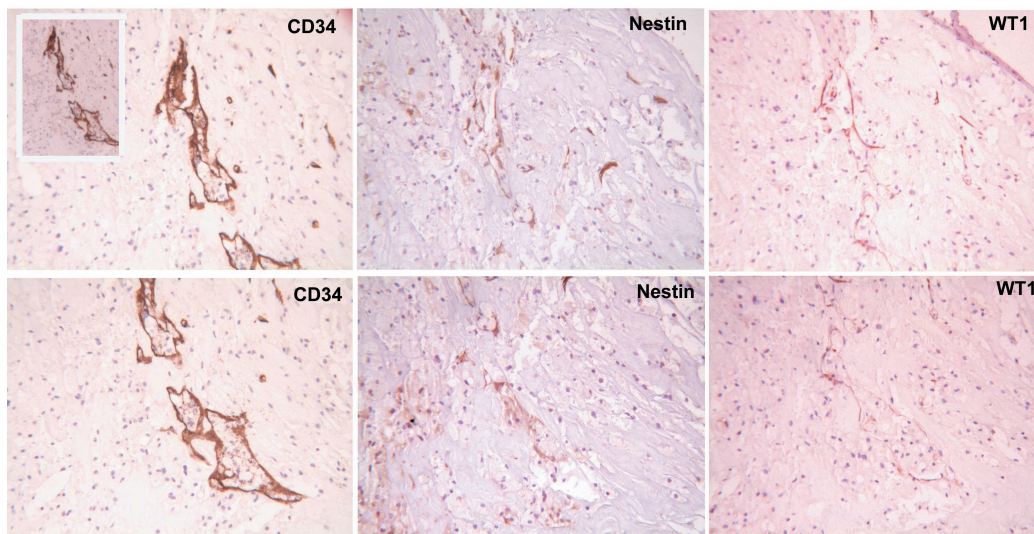
Figure 16: Example of immnostaining for each marker. Magnification 25X

The ratio between Nestin and WT1 "densities" is not close to 1 but to 0.5 (**Figure 17**). In healthy arteries 90.7% of vessels positive to Nestin expressed WT1, in atheromateus plaques only 55.9% of Nestin positive vessels expressed WT1 ($p < 0.05$). There is no significative difference between Nest/CD34 density ratio in healthy and atheromateous arteries; in both cases the ratio is close to 0.8. There was a significative difference of density ratio CD34/WT1 between healthy and atheromateous plaques; in healthy arteries 67.2% of vessels positive to CD34 expressed WT1, in atheromateus plaques only 43.8% of CD34 positive vessels expressed WT1 ($p < 0.05$) **(Fig 17).**

The four-panel figure shows bar charts comparing Healthy and Atheromasic vessels:

- Top left: Density ratio NEST/CD34 — Healthy (77.5 % of vessels CD34+ are Nest+) ≈ 0.75; Atheromasic (71.8% of vessels CD34+ are Nest+) ≈ 0.75.
- Top right: Density ratio WT1/NEST — Healthy (90.7% of vessels NEST+ are WT1+) ≈ 0.9; Atheromasic (55.9% of vessels NEST+ are WT1+) ≈ 0.56, marked with *.
- Bottom left: Density ratio CD34/WT1 — Healthy (67.2 % of vessels CD34+ are WT1+) ≈ 0.67; Atheromasic (43.8% of vessels CD34+ are WT1+) ≈ 0.44.

	CD34+/Nest+	CD34+/WT1+	Nest+/WT1+
Healthy vessels %	75,5	67,2	90
Atheromasic vessels %	71,8	43,8	55,9

Figure 17: Density ratio of each markers. The arrow represents the decrease of ratio density between WT1 and Nestin.

The immunohistochemical analysis also revealed different patterns of CD34 staining. Microvessel morphology ranged from small regular vessel, flattened, irregular lobulate-shaped vessel or big angiomatoid vessel (**Fig 18).**
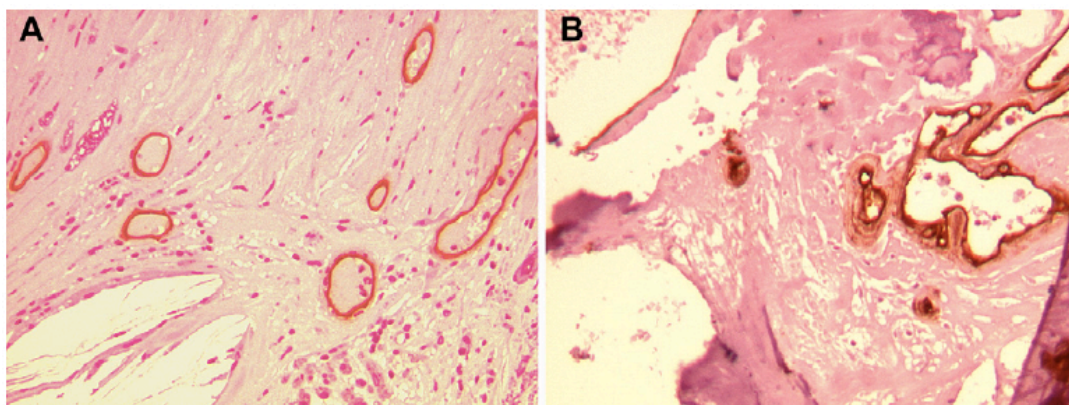
Figure 18: CD34 immunostaining of intraplaque microvessels. A) Small, regularly-shaped microvascular pattern; B) Cavernous, angiomatoid microvascular pattern**.**

Dots vessels

We noticed in 7 lesions (30.4% of cases) the presence of small vessel composed by one single endothelial cell with or without a lumen. The presence of dots vessels in atheromateous lesions was significantly associated to neoangiogenesis score (6 cases having a score 3, p=0.004). Dots positive areas are diffuse among the lesion; 6 cases correspond to a diffuse neoangiogenesis (6 cases with a score 4, p=0.007, not shown). Plaques containing dots structure also correspond to lesions with a higher number of fields and number of positive vessels to CD34+, Nest and WT1 (p<0.05). Five cases (71.42%) had a strong positivity (2+) to Nestin while none dots was WT1 positive (**Fig 19**). A weaker intensity of staining (1+) was observed in one cases for Nestin and 4 cases for WT1. Dots didn't express at all Nestin in one cases and neither WT1 in 3 cases. The presence of dots vessels was also associated to the absence of macrophages postive to dPAPP-A (trend p=0.06) and to an increase of SAA serum levels (6.82±2.3 vs 90.03±48 mg/l, trend p=0.06) **(Fig 19).**
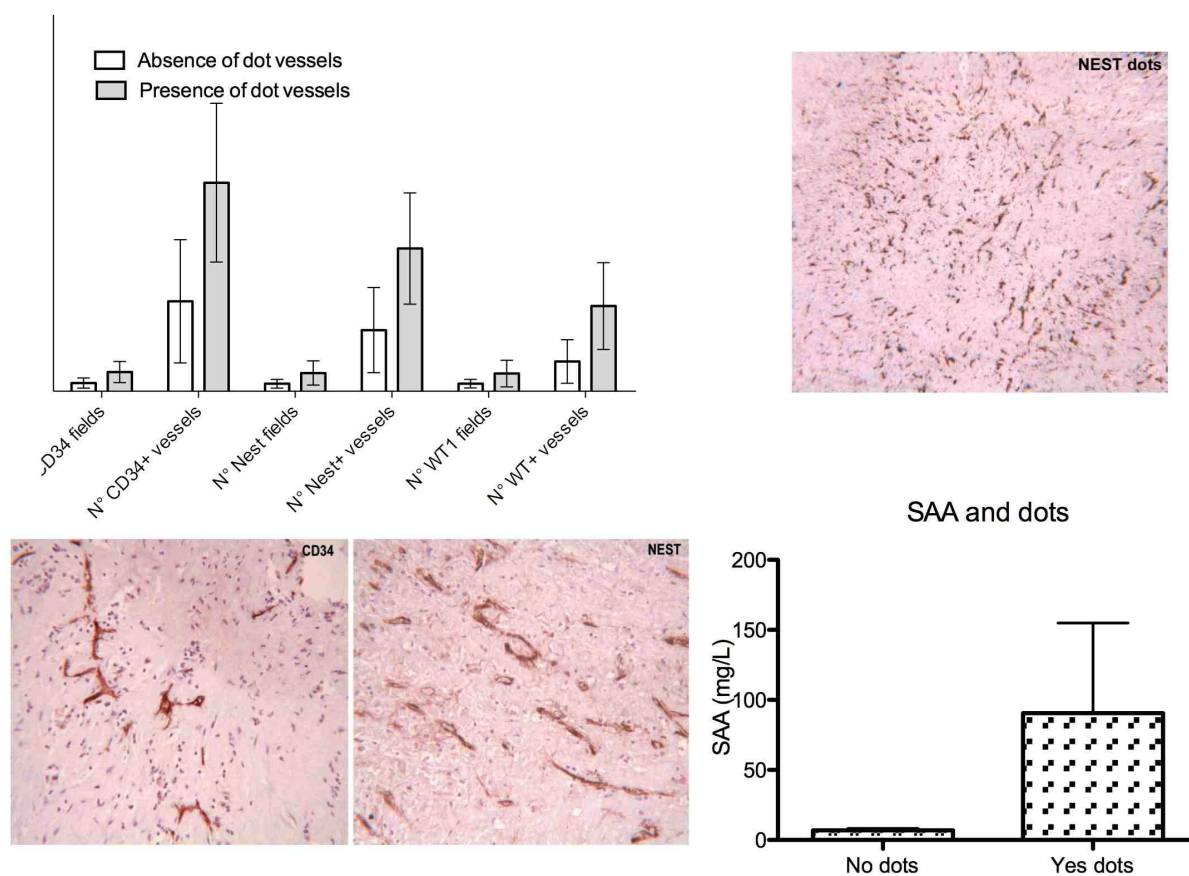
Figure 19: Association between the presence of dot vessels and neoangiogenesis (all p value<0.05 *Mann-Whitney U and Wilcoxon W tests*). Fields are expressed in 0.25um^2 for a better graphical representation. Images of dots vessels, 10 X magnification. The right bottom graph represents the relation between SAA serum levels and dots presence in plaques.

Complications in atheromateous plaques

Calcification was more frequent in female; 85.7 % of female presented a calcified score of 2 or 3. Only 42.85% of males had high calcification score (p<0.0001).

Complications and erosion of the atheromateous palques were related to age, symptomatic patients, to the presence of neurological symptoms and to TIA. After 75 years, 91% of the patients presented plaques with complications that increased up to 30% compared to patients

under 75 years (p=0.0397). The main complication involved was the erosion of the plaque (**Figure 20**). Symptomatic patients presented major complications of the carotid plaques (14.28% vs 57.14%, p=0.015). The same relationship was seen between patients who underwent a TIA and the presence of complicated plaques (p=0.005).
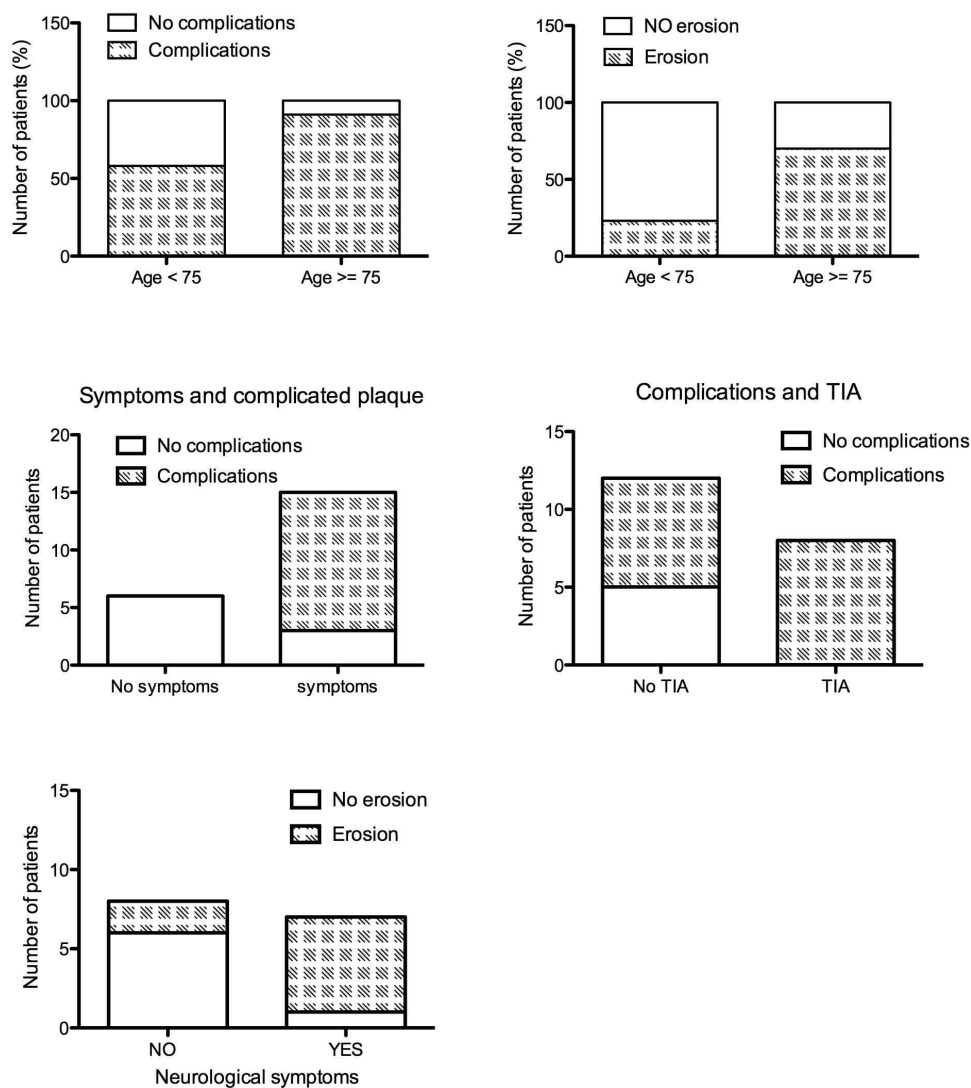
Figure 20: Association between plaque structure, age and symptoms.

Calcified nodules

We noticed the presence of plaque with calcified nodules in 7 cases. So we decided to compare histological, serological and clinical characteristics of these seven cases to another

group of 7 atheromateous plaque without calcified nodules and with a low calcification score (0 or 1). No differences were found for age, gender, AHA lesion classification, diabetes, IRC, ASA, statine terapy, PAPP-A or VEGF serum levels, symptoms, TIA, presence of neurological symptoms and ipertension **(Table 3).**

	No nodules (calcification score 0-1) 7	Calcified nodules 7	p value
Age	70.86±8.9	69.75±10.89	ns
Gender Male Female	5 2	6 1	ns
Neurological symptoms Yes No	3 4	5 7	ns
Dislipidemia Yes No	6 1	6 1	ns
Diabetes Yes No	2 5	1 6	ns
Smoke Yes No	3 4	1 6	p<0.05
Chronic-obstructive pulmonary disease Yes No	3 4	1 6	ns
Stenosis	87.8%± 9.1	76.75	ns
Hydroxymethyl glutaryl coenzyme A reductase inhibitor user Yes No	5 2	5 2	ns
VEGF pg/ml	366.9 ±200	376.2 ±210	ns
hsCRP mg/l	2.86 ±1.19	14.19 ±6.16	p<0.05
SAA mg/l	4.32 ±1.18	31.44±19.9	p<0.05
PAPP-A	1.51±1.87	1.16±1.35	ns

Table 3: Clinical characteristics of patients presenting a plaque with calcified nodules.

Significative differences were noticed for smoker, histological and serological markers levels, lipid core area and complications of the lesions (erosion and/or ulceration). Data are summarized in **figure 21.**

Patients with calcified nodules had a decrease of 42.11% of phlogosis histological score compared to atheromateous plaque (score 11+ vs 19+, p<0.05). Serum inflammation proteins levels were also decreased; mean hsCRP and SAA in patients presenting calcified nodules were respectively 2.86±1.19 mg/l and 4.32±1.18 mg/ml vs 14.19±6.16 and 31.44±19.90 mg/ml in atheromateous patients (p=0.024). Only 57% of the calcified nodules had a high lipid core area score (2-3) compared to 95% in atheromateous plaques. (p=0.02).

The presence of complications was seen in 83% of the atheromateous plaques while only 17% of the calcified nodules presented complications of the plaque structure (p=0.02).

Compared to atheromaterous plaque, immunohistochemical analysis showed an intense positivity to dPAPP-A of the area surrounded calcified nodules. The immunofluorescence analysis revealed that dPAPP-A was negative or weakly expressed in healthy arteries (data not shown).
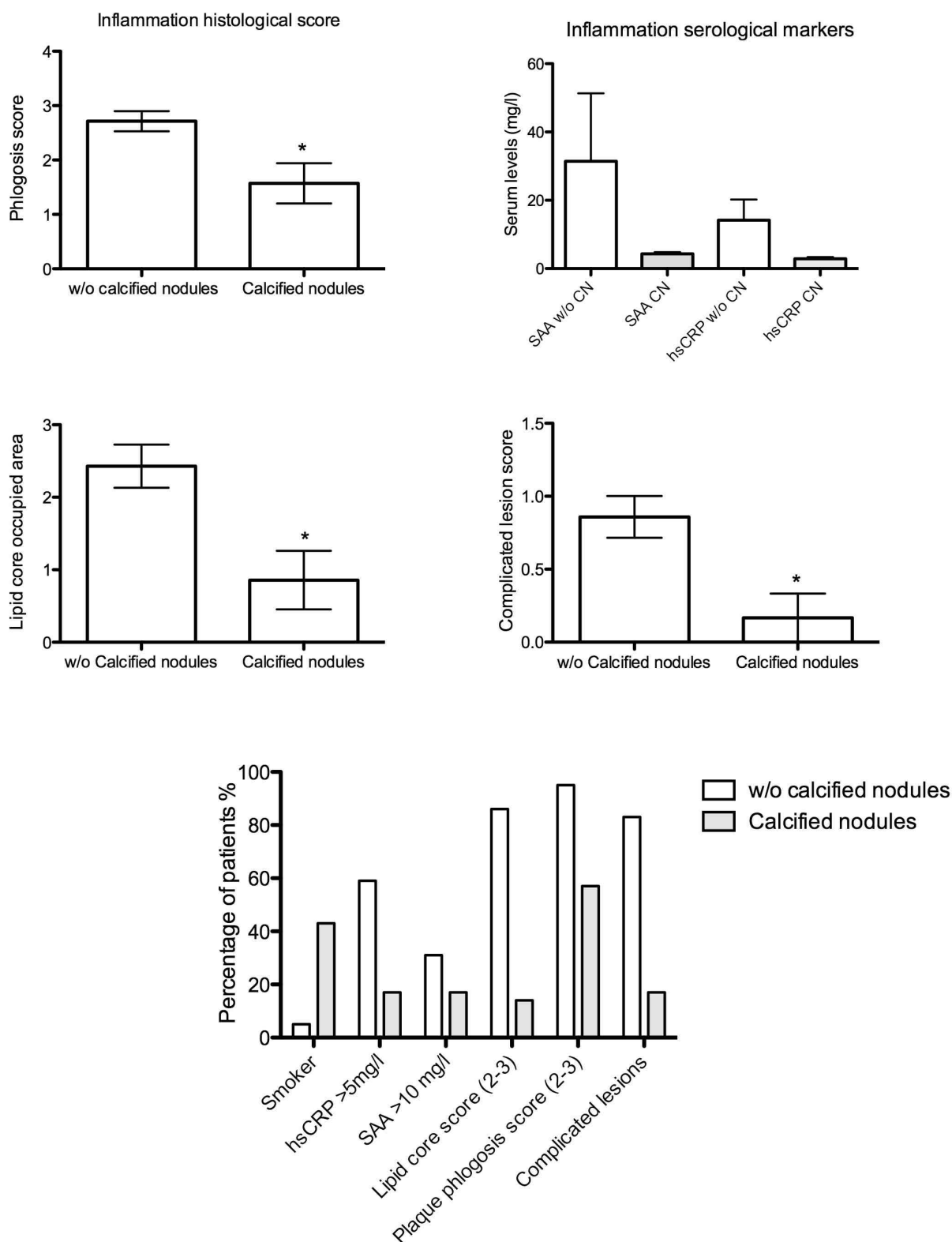
Figure 21: Summary of the significatives differences between patients presenting an atherosclerotic plaque with or w/o calcified nodules (Fisher test, p<0.05).

DISCUSSION

DISCUSSION

Cerebral lesions risk and serological markers levels

The risk of embolization from carotid plaque is of paramount importance both in indication to revascularization and during the carotid endovascular procedure. However, methods to objectively identify this risk are presently not available. Several methods have been suggested, (i.e. GSM, Magnetic Resonance imaging, Computed Tomography etc.) In fact no study has correlated the amount of embolic debris in CAS procedure and serological markers such as CRP. In this study we examined filters obtained by the CAS procedure, evaluating the amount and the pattern of debris, indicative of the vulnerability of the plaque treated. According to our data, not all plaques behave similarly; patients with CRP above 5 mg/l, SAA above 10 mg/l and VEGF above 500 pg/ml showed a significantly increased number of pores occluded (PO), indicative of debris greater than the size of pore filter, i.e., 100 μm. As know HDL removes excess cholesterol from walls' arteries; in fact patients showing higher HDL blood levels presented a filter with lower PO and thus less accumulation of thromboembolic material on the membrane.

These findings and their correlation with the embolic potential of the plaque is supported by the relationship existing with echographic characteristics of the plaques: dishomogenous plaques showed a significantly greater percentage of both pore occluded, which further supports the clinical findings of their higher embolic potential. In this sense, it is not surprising that patients with elevated CRP and dishomogenous plaque had an even greater percentage of PO. Ultrastructural appearance of the debris and histological analysis showed features consistent with the plaque origin of the emboli; it should be outlined that in the CAS technique employed in this study, filters are opened only during stent deployment and dilatation. We can therefore

reasonably exclude other possible origins of embolic material, as confirmed by the analysis of the control filters. Moreover, the amorphous material retrieved from the filter membrane originated from dislocated fragments of the necrotic core during the procedure. These results confirm the data obtained in previous studies evaluating the nature of embolic debris captured during the procedure (Angelini et al., 2002; Hayashi et al., 2009).

An increase of post procedural cerebral lesions was detected in patients having hsCRP >5 mg/l and SAA >10 mg/l values. During the CAS procedure fragments of plaque get detached and pass through the pores of the filter protection causing an increase of cerebral lesions. The number and the volume of cerebral lesions are predictable by hsCRP and SAA serum levels before the procedure.

Thus high hsCRP, VEGF and SAA levels are correlated with the amount of embolic material seen in cerebral filters demonstrating the relationship between carotid plaque structure, inflammation and the embolic potential in CAS.

Identification of vulnerable plaque

CEUS with dB-E can be used as a marker for vulnerable plaque. dB-E was associated significantly with different histological parameters of the atherosclerotic plaque; thinner fibrous cap, greater inflammatory infiltrate and greater microvessels' density. An increase of dB-E was also associated to either symptomatic patients or to the presence of preoperative ipsilateral embolic lesions. Correlated to the recognition of vulnerable plaque, we observed that patients having neurological symptoms pre-operatively had also high VEGF and hsCRP levels. Furthermore a high plaque vulnerability score (between 3 and 5) was associated to higher hsCRP and VEGF serum levels compared with patients with non-vulnerable plaques. Plaques containing a thin fibrous cap were found in patients presenting pre-operative neurological symptoms (TIA, Stroke, AF), strengthening the relation

between TFC and risk of embolization of vulnerable plaque with a fibrous cap thinner. Interestingly, there was an inverse linear correlation between VEGF, PAPP-A mRNA, triglycerides serum levels and fibrous cap thickness of the carotid plaque: the fibrous cap was thinner in patients with higher level of these 3 markers. Patients having higher HDL levels had a thicker fibrous cap; as said before HDL removes excess cholesterol from walls' arteries, thus reducing the availability of LDL up-take inside the lesions. As shown in previous studies, HDL appears to a have a protective effect against the risk of plaque rupture and embolization (Assmann et al., 2004).

PAPP-A level: a technical issue

PAPP-A mRNA level expression in blood was more sensitive than serological analysis of PAPP-A protein expression level; mRNA increased up to 30 times in certain patients while PAPP-A serum level increased maximum 3 times. Increased mRNA expression level correlated with serological SAA levels (and active PAPP-A), glycaemia levels and with the area of the filter covered by debris. We repeated the same ELISA assay twice to evaluate active PAPP-A concentration in the serum but with scarce results. PAPP-A concentrations were extremely low and the concentration curve was flat. Many studies evaluating serological PAPP-A obtained opposite results; in some cases PAPP-A was correlated to cardiovascular disease (Qin et al., 2002) and in others there was not any correlation with the disease Dominguez-Rodriguez et al., 2005). mRNA PAPP-A evaluation could be more sensitive and precise than the evaluation of protein concentration in the serum.

PAPP-A bound to the membrane of cells has got proteolytic activity, although internalized PAPP-A has little or no protease activity. In our histological analyses we saw that dPAPP-A was found in some macrophages, some endothelials' cells and rare SMCs.

Our results correlate with a model proposed by Conover et al., in which activated macrophages in developing plaque secrete pro-inflammatory cytokines that differentially stimulate ECs and SMCs to express and secrete PAPP-A, which can act in an autocrine and paracrine manner to amplify atherosclerotic disease progression through its ability to enhance local IGF action. (Conover et al., 2008).

A positive correlation was found between macrophages dPAPP-A positive cells in patients with dyslipidemia (not shown). This is concordant with in-vitro studies showing that IGF activates LDL cholesterol uptake by macrophages suggesting a pro-atherogenic activity. (Renier et al., 2000).

HsCRP and SAA

hsCRP and SAA are marker of inflammation; both have a standard reference range but with a different means. In particular, hsCRP is a recognized marker in the prevention of cardiovascular disease. Regarding SAA, the reference range refers only to an accumulation of the amyloid proteins but not to an increase of the risk of cardiovascular disease. Here we showed a perfect linear positive correlation between increased levels of SAA before CAS procedure and cerebral lesions occurring during the procedure. Until now SAA levels were only correlated to cerebral infarction, it is the first time that SAA levels are associated directly with the number and the volume of cerebral lesions. Serological SAA may be the etiologic factor for ischemic stroke, so efficient treatment of chronic infectious inflammatory processes is of utmost importance. Until now we considered hsCRP as the best marker for cardiovascular disease but it is worthy to introduce SAA as a new standard pre-operatory blood test in addition to hsCRP.

The gene for SAA4 is constitutively expressed and its protein product is a constituent of normal, non-acute-phase high-density lipoprotein (Urieli–Shoval, 1998). We observed that SAA4 is not expressed in normal arteries, but in carotid lesions SAA4 positivity is very strong (data not shown). This

suggests a tissue-specificity of the SAA4 isoforms towards SAA1 and SAA3. SAA4 is a specific marker of carotid atheromatous lesions.

SAA emerged as an interesting histological and serological marker in this study. SAA serum levels are also associated to neoangiogensis, particularly to the presence of dots vessels. Patients presenting plaques with a high neoangiogenesis score and showing dots vessels structure had an increase of pre-operative SAA serum levels. SAA serum levels are related to the plaque structure as a potential marker of plaque vulnerability

Plaque containing calcified nodules showed basal serum levels of SAA and hsCRP; in these complications, histological inflammation and neoangiogenesis are almost absent.

Circulating molecular markers: peripheral model to study local damage?

Higher expression level of NSE and PAPP-A mRNA post procedural were correlated to the increase of circulating inflammation markers (hsCRP and SAA) and also to the presence of a thinner fibrous cap (TFC). However NSE was neither sensitive nor specific in predicting patients with cerebral lesions. The major concentrations of NSE are found in the gray matter (composed of a majority of neurons) opposite to the white matter as the pyramidal tract and corpus callosum that contain the lowest concentration of NSE. NSE is therefore a specific marker for lesions occurring in the gray matter. So NSE is not specific for the cerebral white matter, but injuries can occur with the same probabilities in the gray matter. If cerebral lesions are concentrated in the gray matter NSE expression levels will not be significantly affected. This data is consistent with precedent studies that have shown the inefficacy of NSE as a cerebral lesions' marker (Fridriksson et al., 2000). The optimum resides in proteins expressed in both areas and overall having a molecular structure able to cross the blood brain barrier. NSE mRNA expression level is correlated with inflammation levels of hsCRP and SAA pre-procedural. We thought that this increase is due to leucocytes infiltration into cerebral brain lesions (Glatt et al. 2005; Sullivan et al. 2006) and subsequent release

of leucocytes in the peripheral blood thus correlating with hsCRP and SAA levels. So NSE levels reflect a general state of inflammation that might be caused by brain injury but is not proportionally related to the number and volume of lesions. The same hypothesis is related to PAPP-A mRNA expression levels; blood mRNA expression of PAPP-A might increase because leucocytes infiltrate into the atheromateous lesion and are subsequently released into the blood. Thus reflecting the local concentration of mRNA PAPP-A in atheromateous plaques. Peripheral circulating leucocytes are very promising for the analysis of local concentration in tissue. This is concordant with previous studies on circulating mRNA as tumour marker (Somma et al 1999, D'Alessandro et al., 2008).

Neoangiogenesis and atherosclerosis development

A "classic" model describes the first-order Vaso Vasorum (VV) to derive from major arteries, running longitudinally along the vessel wall. Second-order VV originating from first-order VV form a plexus around the adventitia and the vascular media. These two orders of VV are different in size, function and anatomic sites: the VV <50 mm in diameter that we described in this study are likely to represent the second-order VV (described in animal models as vessels of 60-70 mm in size), while the vessels ≥100 mm should represent the first-order VV (more than 150 mm in pig coronary arteries) (Kwon et al., 1998; Moreno et al., 2006; Ritman et al., 2007; Mulligan-Kehoe et al., 2010). We have chosen to maintain a "grey zone", from 50 to 100 mm in diameter, because it is sometimes difficult to evaluate vascular size, due to cut effects which can induce an overestimation of capillary diameter. The results we obtained seem to support this view, as the 50-100 mm VV showed intermediate IHC expressions, but were more similar to the <50 mm VV group.

Nestin is a progenitor cell and angiogenic marker, also involved in early development steps in embryogenesis (Wagner et al., 2006; Green et al.,

2009) and WT1, a transcription factor of Nestin, which acts also as a critical regulator of organogenesis (Hohenstein et al., 2006). Here we saw that both proteins are expressed in adult arteries as well. The variability among VV is reflected by the different expression of Nestin and WT1 that we found analysing the adventitia of healthy arteries. Indeed a more pronounced expression of Nestin and WT1 was found in VV <50 mm in diameter (which show more than 90% of positive cells) rather than VV >100 mm in diameter (which are often negative and, when positive, show a mean of 60% of positive cells). Furthermore, those small-sized VV positive for Nestin and WT1 are recognizable in areas (that we called "hot spots"), characterized by several small-sized VV, arteriolar in morphology, often together with peripheral nervous structures (identifiable with the *nerva vasorum*). Due to their location (deeper layer of adventitia, relatively far from media) and morphology ("network" of small vessels with nervous structures), we can hypothesize that the "hot spots" may represent points where second-order VV originate from a branching of first-order VV (see **Fig. 13**). The "hot spot" could therefore represent a valid model for the vasculogenic niche, i.e. a specific domain with a specific architecture and a specific location, containing several Nestin- and WT1-positive vascular structures.

As previously said, Nestin gene transcription is regulated by WT1 (Wagner et al., 2006; Pelizzoli et al., 2008). Our results show that Nestin and WT1 are expressed in the same cell population in healthy arteries. Interestingly, WT1 is both expressed in the cytoplasm and in the nucleus. For a long time the presence of WT1 in the cytoplasm was attributed to an antibody-staining artefact (Hohenstein et al., 2006) and there was no evidence of WT1 cytoplasmic expression at IHC. Our finding correlates with recent studies showing the presence of WT1 in the cytoplasm. The cytoplasmic isoform WT1 (+KTS) has a high affinity for RNA, while the nuclear isoform (–KTS) binds DNA. These and other observations have led to the

proposal that the –KTS form of WT1 acts as a transcriptional regulator, while the +KTS form, in the cytoplasm, plays a role in RNA processing (Green et al., 2009). The cytoplasmic colocalization of WT1 and Nestin strengthens the role of WT1 as a post-transcriptional activator of Nestin protein. It would be interesting to compare WT1 sub-cellular localization in normal arteries versus pathological arteries to assess a correlation with neovascularization during atherogenesis. Indeed recent studies showed how an increase of WT1 in the cytoplasm is associated with different processes in cell differentiation (Wagner et al., 2008). In our series WT1 was mainly cytoplasmic in the larger vessels, while nuclear expression increased in the smaller vessels ("second-order" VV).

We want to point out that in atherosclerotic plaque the count of positive cells was performed only for the region of interest. So the increase in the number of positive cells or field between healthy and atherosclerotic plaque is not relevant in this analysis.

As in healthy arteries, atheromatous lesion vessels still expressed Nestin as well as CD34. In healthy arteries 90.0% of vessels Nest$^+$ are WT$^+$ but in atheromatous lesion only 55.9% of Nest$^+$ are WT$^+$. Moreover "dots" vessels' structure in atheromatous plaque strongly express Nestin and CD34 but weakly express WT1 (phenotypes CD34$^+$/NEST$^+$). Nestin expression is not anymore only depending on WT1; within the atherosclerotic lesions Nestin expression is driven by the activation of additional transcriptional factors. WT1 is well studied as a tumour suppressor and recently the implication of WT1 in the vascular response to myocardial ischaemia and its oncogenic potential was seen as a promoter of tumour angiogenesis (Scholz et al., 2009). Angiogenesis is regulated by the balance of proangiogenic VEGF(165) and antiangiogenic VEGF(165)b splice isoforms. Mutations in WT1 suppress antiangiogenic VEGF(165)b and cause abnormal gonadogenesis, renal failure, and Wilms' tumors (Amin et al., 2011). We suggest that, as in tumour, a mutation of WT1 could lead to a loss of

repression (or function) on angiogenesis, thus to an abnormal neovascularisation.

EPCs, contiguous to the VV in the adventitia of healthy arteries (hot spot) have a Nest$^+$/WT$^+$ phenotype. In the atheromatous lesions, under a biochemical or mechanical stimulus, EPCs proliferate in the media and promote neovascularization of the media leading to the formation of new vessels Nestin$^+$/WT$^-$. Additionally new vessels can also sprout from the endothelial cells from II order vessels advancing in the media. According to some authors, the main source for angiogenesis in diseased arteries is the proliferation of VV, and in particular second-order VV located in adventitia (Kwon et al., 1998; Mulligan-Kehoe et al., 2010). However the Nestin$^+$/WT$^-$ phenotype suggests the formation of vascular structures from circulating or tissue-resident endothelial stem cells, which proliferate into "de novo" endothelial cells in the media.

In both cases, our "hot spots" represent the main manifestation of this proliferative potential: Nestin positivity is to be considered as a characteristic of a "young" endothelium, still progenitor committed, and not as an expression of real stem cell potential. Furthermore, the nuclear localization of WT1 could be associated with an increasing transcriptional activity in the "hot spots". These committed progenitor cells play a key role in neovascularization during atherogenesis. Patients with elevated SAA serological levels presented plaque with this particular structure named vessels "dots". The presence of dots in atherosclerotic plaque is associated to an active neovascularization process.

Plaque remodelling has been the target of medical therapies, such as statins, aiming at the possibility of transforming an unstable plaque into a more stable plaque, reducing the cerebrovascular risk (Watanabe et al., 2005).

The formation of new blood vessels around an atherosclerotic lesion plays a major role in plaque rupture, and the use of antiangiogenic drugs stabilizing plaques could prevent the arising of cardiovascular events.

Calcified plaques

A subgroup of patients presenting calcified nodules was identified among atheromateous lesions. We saw that plaque presenting calcified nodules correlates with different clinical, serological and histological features compared to atheromateous plaque without nodules. They are not associated to the neoangiogensis and inflammation process. Serum levels of hsCRP and SAA are not related to plaque vulnerability or any clinical symptoms in plaque with calcified nodules. Previous studies of our group showed the presence of mesenchymal vascular wall cells resident in the healthy arteries having adipogenic, chondrogenic, leiomyogenic and osteogenic potential (Pasquinelli et al., 2010). Moreover in PAOD diabetics patients data suggested that resident endothelials progenitors cells resident near Vasa Vasorum under injury cause a dysfunction of angiogenesis in the media. (Orrico et al, 2012).

Observations	hsCRP	SAA	VEGF	mRNA NSE
Serum values	**>5mg/l**	**>10mg/l**	**>500pg/ml**	In patients submitted to CAS; levels increased 32%. mRNA NSE increased with inflammatory proteins levels
SEM and OM analysis of filters	Increase of the debris accumulation	Increase of the debris accumulation	Increase of the debris accumulation	
Cerebral damage after CAS	Increased n° and Volume of cerebral lesions	Increased n° and Volume of cerebral lesions		
Type of plaque: GSM CEA analysis	Dishomogeneous High vulnerability score (3-5)	Dishomogeneous High vulnerability score (3-5)	Thinner fibrous cap vulnerability score (3-5)	Thinner fibrous cap

CEUS analysis (high dB-E signal)	High vulnerability score (4-5) and inflammation score	CT scans+: Ipsilateral ischemic lesion preoperative	Higher vessel density	Fibrous cap <200um
Thinner fibrous cap	Increase serum levels of VEGF, NSE, PAPP-A serum levels increase.		Neurological symptoms.	
"dots" vessels	High neoangiogensis score, CD34+/Nest+/WT-		Increase serum levels of SAA, dPAPP-A$^+$ macrophages	

Table 1: Main findings of this study

Main findings of this study:

The **table 1** above summarizes our main findings

- First study to show that pre-procedural serum levels of SAA are directly related to the number of cerebral lesions post stenting.

- SAA4 protein isoform appears to be a tissue specific histological marker of atheromatous lesions; a quantitative analysis is necessary to prove the statistical significance.

- Circulating protein and mRNA reflect the local structure of the atheromateous plaques.

- The presence of a thin fibrous cap is associated to neurological symptoms and to circulating protein levels

- Atherosclerotic plaque vessels showed a different phenotype compared to healthy plaque Nest+/WT-

- Nestin driven neoangiogensis in atheromateous palque is activated by an alternative transcriptional factor alternative to WT1

Based on this findings two questions arise:

- Are committed progenitor cells located in adventizia responsible for abnormal neovascularization during atherogenesis?

- What event triggers the new phenotype of neovessels in atheromateous plaques?

Previous data of our group showed that osteoprogenitors cells are contiguous to Vasa Vasorum where they are inactive and under an unknown stimulus, cells migrate in the media producing bone matrix (Pacilli 2011). This mechanism is concordant to our hypothesis on neovessels' formation during atherogenesis. Our ongoing research is now oriented versus the mechanisms that trigger the bone formation and the neovessels' formation. Understanding the unknown early stages of atherogenesis is of fundamental importance for the development of a drug that is targeted to inhibit the possible progenitors' cells involved.

Conclusion

This study identifies patients at major risk of embolization and cerebral lesions. Ultrastructural analysis pointed out how debris dislocates from the carotid plaque during the procedure and passes through the pores of the filter leading to the formation of cerebral lesions. These data show that the stenting procedure is not indicated in patients with hsCRP, SAA and VEGF higher than the threshold values. CEUS with dB-E can be used as a marker for neovascularization and vulnerable plaque.

Limits of the study

This study included a limited amount of patients. Carotid plaque analysis is limited to patients who undergo vascular surgery, which limits the domain of patients suitable for risk assessment. Plaque analysis takes place at one point in time, while it is known that atherosclerotic plaque composition changes over time. We continue now to perform analysis on the area near the atheromateous lesion.

BIBLIOGRAPHY

Bibliography

Abedin M., Tintut Y. and Demer L. L.: Vascular Calcification: Mechanisms and Clinical Ramifications. Arterioscler Thromb Vasc Biol 2004;24:1161-1170

ACAS Executive Committee. Endarterectomy for asymptomatic carotid artery stenosis. Executive Committee for the Asymptomatic Carotid Atherosclerosis Study. Jama 1995;273(18):1421-8. North American Carotid Endarterectomy Trial Collaborators Beneficial effect of carotid endarterectomy in symptomatic patients with high grade stenosis. N Engl J Med. 1991;325:445–453

Acierno LJ: Atherosclerosis (arteriosclerosis). In The History of Cardiology Edited by: Acierno LJ. New York: Parthenon Publishing Group Inc; 1994:109-126.

Amin EM, Oltean S, Hua J, Gammons MV, Hamdollah-Zadeh M, Welsh GI, Cheung MK, Ni L, Kase S, Rennel ES, Symonds KE, Nowak DG, Royer-Pokora B, Saleem MA, Hagiwara M, Schumacher VA, Harper SJ, Hinton DR, Bates DO, Ladomery MR. WT1 mutants reveal SRPK1 to be a downstream angiogenesis target by altering VEGF splicing. Cancer Cell. 2011 Dec 13;20(6):768-80.

Anderson T. J. et al.: The effect of cholesterol-lowering and antioxidant therapyon endothelium-depent coronary vasomotion. N Eng J Med 1995; 332:488

Angelini A., Reimers B., Della Barbera M., Saccà S., Pasquetto G., Cernetti C., Valente M., Pascotto P., Thiene G. (2002). Cerebral protection during carotid artery stenting. Collection and histopathologic analysis of embolized debris. Stroke 33, 456-461.

Assmann G, Gotto AM Jr. HDL cholesterol and protective factors in atherosclerosis. Circulation. 2004 Jun 15;109 (23 Suppl 1):III8-14

Ballou SP, Lozanski G. Induction of inflammatory cytokine release from cultured human monocytes by C-reactive protein. Cytokine. 1992;4:361–368.

Bartel DP. MicroRNAs: genomics, biogenesis, mechanism, and function. Cell. 2004, 116(2):281-97

Bayes-Genis A, Conover CA, Schwartz RS. The insulin-like growth factor axis: a review of atherosclerosis and restenosis. Circ Res 2000;86:125–30.

Bhatt A, V. Jani. The ABCD and ABCD2 Scores and the Risk of Stroke following a TIA: A Narrative Review, ISRN Neurology, 2011, Article ID 518621.

Biasi G.M., Sampaolo A., Mingazzini P., De Amicis P., El-Barghouty N. and Nicolaides A.N. (1999). Computer analysis of ultrasonic plaque echolucency in identifying high risk carotid bifurcation lesions. Eur J Vasc Endovasc Surg. 17, 476-9.

Bijuklic K, Wandler A, Hazizi F, Schofer J. The PROFI Study (Prevention of Cerebral Embolization by Proximal Balloon Occlusion Compared to Filter Protection During Carotid Artery Stenting) A Prospective Randomized Trial. J Am Coll Cardiol. 2012 Jan 19. [Epub ahead of print]

Bluth E. I., Wetzner S. M., Stavros A. T. et al.: Carotid duplex sonography A multicenter recommendation for standardized imaging and Doppler criteria. RadioGraphics 1988; 8: (3) 487-506

Bønaa KH, Njølstad I, Ueland PM, Schirmer H, Tverdal A, Steigen T, et al. NORVIT trial investigators Homocysteine lowering and cardiovascular events after acute myocardial infarction. The New England journal of medicine. 2006;354(15):1578–88. doi:10.1056/NEJMoa055227. [PubMed]

Burke AP, Farb A, Malcom GT, Liang Y, Smialek JE, Virmani R: Plaque rupture and sudden death related to exertion in men with coronary artery disease. JAMA 1999, 281(10):921-926

Cappendijk V. C., Kessels A. G. H., Heeneman S. et al.: Comparison of Lipid-Rich Necrotic Core Size in Symptomatic and Asymptomatic Carotid Atherosclerotic Plaque: Initial Results. J Magn Reson Imaging 2008;27:1356–1361.

Chang MK, Binder CJ, Torzewski M, Witztum JL. C-reactive protein binds to both oxidized LDL and apoptotic cells through recognition of a common ligand: Phosphorylcholine of oxidized phospholipids. Proc Natl Acad Sci U S A. 2002;99:13043–13048.

Chen BK, Leiferman KM, Pittelkow MR, et al. Localization and regulation of PAPP- expression in healing human skin. J Clin Endocrinol Metab. 2003; 88: 4465–4471

Chen WJ, Yin K, Zhao GJ, Fu YC, Tang CK. The magic and mystery of MicroRNA-27 in atherosclerosis. Atherosclerosis. 2012 Jan 18. [Epub ahead of print].

Cheng GC, Loree HM, Kamm RD, Fishbein MC, Lee RT. Distribution of circumferential stress in ruptured and stable atherosclerotic lesions: a structural analysis with histopathological correlation. Circulation 1993; 87:1179-1187

Cipollone F, Felicioni L, Sarzani R, Ucchino S, Spigonardo F, Mandolini C, Malatesta S, Bucci M, Mammarella C, Santovito D, de Lutiis F, Marchetti A, Mezzetti A, Buttitta F. A unique microRNA signature associated with plaque instability in humans.. Stroke. 2011 Sep;42(9):2556-63. Epub 2011 Aug 4

Conover CA, Harrington SC, Bale LK. Differential regulation of pregnancy associated plasma protein-A in human coronary artery endothelial cells and smooth muscle cells.. Growth Horm IGF Res. 2008 Jun;18(3):213-20. Epub 2007 Oct 23.

Cotran, Kumar, Collins "Robbins" VI Ed.: Le basi patologiche delle malattie. Piccin nuova libreria p 583-595.

Cybulsky M. I., Gimbrone M. A.: Endothelian expression of mononuclear leukocyte adhesion molecule during atherogenesis. Science 1991; 251:788.

D'Alessandro V, Muscarella LA, Copetti M, Zelante L, Carella M, Vendemiale G. Molecular detection of neuron-specific ELAV-like-positive cells in the peripheral blood of patients with small-cell lung cancer. Cell Oncol. 2008;30(4):291-7.

De Beer MC, Yuan T, Kindy MS, Asztalos BF, Roheim PS, de Beer FC. J Lipid Res. 1995 Mar;36(3):526-34. Characterization of constitutive human serum amyloid A protein (SAA4) as an apolipoprotein.

Demer L. L. and Tintut Y.: Mineral Exploration: Search for the Mechanism of Vascular Calcification and Beyond: The 2003 Jeffrey M. Hoeg Award Lecture. Arterioscler Thromb Vasc Biol 2003;23:1739-1743

Devaraj S, Xu DY, Jialal I. C-reactive protein increases plasminogen activator inhibitor-1 expression and activity in human aortic endothelial cells: implications for the metabolic syndrome and atherothrombosis. Circulation. 2003;107:398–404.

Doherty T. M., Fitzpatrick L. A., Inoue D. et al.: Molecular, Endocrine, and Genetic Mechanisms of Arterial Calcification Endocrine Reviews 2004; 25(4):629–672

Dominguez-Rodriguez A, Abreu-Gonzalez P, Garcia-Gonzalez M, Ferrer J, Vargas M. Circulating pregnancy-associated plasma protein A is not an early marker of acute myocardial infarction Clin Biochem. 2005 Feb;38(2):180-2.

Dunmore B. J., McCarthy M. J., Naylor R. et al.: Carotid plaque instability and ischemic symptoms are linked to immaturity of microvessels within plaques. J Vasc Surg 2007;45:155-9

Ebbing M, Bleie Ø, Ueland PM, Nordrehaug JE, Nilsen DW, Vollset SE, et al. Mortality and cardiovascular events in patients treated with homocysteine-lowering B vitamins after coronary angiography: A randomized controlled trial. The Journal of the American Medical Association. 2008;300(7):795–804. doi:10.1001/jama.300.7.795.

EI-Barghouty N., Geroulakos G., Nicolaides A. et al.: Computer-Assisted Carotid Plaque Characterisation. Eur J Vasc Endovasc Surg 1995; 9:389-393

European Carotid Surgery Trialists' Collaborative Group. MRC European Carotid Surgery Trial: interim results for symptomatic patients with severe (70–99%) or with mild (0–29%) carotid stenosis. Lancet 1991; 337: 1235–43

Faggioli G, Ferri M, Rapezzi C, Tonon C, Manzoli L, Stella A. Atherosclerotic aortic lesions increase the risk of cerebral embolism during carotid stenting in patients with complex aortic arch anatomy. J Vasc Surg. 2009 Jan;49(1):80-5. Epub 2008 Oct 22.

Faggioli G.L., Ferri M., Gargiulo M., Fratesi F., Manzoli L. and Stella A. (2007). Measurement and impact of proximal and distal tortuosity in carotid stenting procedures. J Vasc Surg. 46, 1119-24.

Ferri N, Paoletti R, Corsini A. Biomarkers for atherosclerosis: pathophysiological role and pharmacological modulation. Curr Opin Lipidol. 2006 Oct;17(5):495-501. Review

Fichtlscherer S, Rosenberger G, Walter DH, Breuer S, Dimmeler S, Zeiher AM. Elevated C-reactive protein levels and impaired endothelial vasoreactivity in patients with coronary artery disease. Circulation. 2000;102:1000–1006.

Fortunato G, Di Taranto MD.Polymorphisms and the expression of genes encoding enzymes involved in cardiovascular diseases.Clin Chim Acta. 2007;381:21-5. foto

Fridriksson T, Kini N, Walsh-Kelly C, Hennes H. Serum neuron-specific enolase as a predictor of intracranial lesions in children with head trauma: a pilot study. Acad Emerg Med. 2000 Jul;7(7):816-20.

Garcia B.A., Ruiz C., Chacon P., Sabin J.A. and Matas M. (2003). High-sensitivity C-reactive protein in high-grade carotid stenosis: Risk marker for unstable carotid plaque. J Vasc Surg. 38, 1018-24.

Gillmore JD, Lovat LB, Persey MR, Pepys MB, Hawkins PN. Amyloid load and clinical outcome in AA amyloidosis in relation to circulating concentration of serum amyloid A protein. Lancet. 2001 Jul 7;358(9275):24-9.

Gimbrone M. A., Nagel T.,and Topper J. N.: Biochemical activation: an emerging paradigm in endothelian adhesion biology. J Clin Invest 1997; 99:1809.

Goldstein LB, Adams R, Becker K, Furberg CD, Gorelick PB, Hademenos G, Hill M, Howard G, Howard VJ, Jacobs B, Levine SR, Mosca L, Sacco RL, Sherman DG, Wolf PA, del Zoppo GJ. Primary prevention of ischemic stroke: A statement for healthcare professionals from the Stroke Council of the American Heart Association. Stroke. 2001 Jan;32(1):280-99

Grant E., Benson C. B., Moneta G. L. et al.: Carotid Artery Stenosis: Gray-Scale and Doppler US Diagnosis—Society of Radiologists in Ultrasound Consensus Conference. Radiology 2003; 229:340–346

Green L.M., Wagner K.J., Campbell H.A., Addison K. and Roberts S.G.E. (2009). Dynamic interaction between WT1 and BASP1 in transcriptional regulation during differentiation. Nucleic. Acids. Res. 37, 431-440.

Gröschel K., Ernemann U., Larsen J., Knauth M., Schmidt F., Artschwager J. and Kastrup A. (2007). Preprocedural C-Reactive Protein Levels Predict Stroke and Death in Patients Undergoing Carotid Stenting. Am. J. Neuroradio. 28, 1743-1746.

Hansson GK, Libby P. The immune response in atherosclerosis: a double-edged sword. Nat Rev Immunol 2006;6:508 –19.

Hasegawa Y, Takanashi S, Okudera K, Kumagai M, Hayashi A, Morimoto T, Okumura K. Vascular endothelial growth factor level as a prognostic determinant of small cell lung cancer in Japanese patients. Intern Med. 2005;44(1):26-34

Hattori Y, Matsumura M, Kasai K. Vascular smooth muscle cell activationby C-reactive protein. Cardiovasc Res. 2003;58:186–195.

Hayashi K., Kitagawa N., Morikawa M., Hiu T., Morofuji Y., Suyama K. Nagata I. (2009). Observation of the embolus protection filter for carotid artery stenting. Surg. Neurol. 72, 532-537.

Hermus L, Lefrandt JD, Tio RA, Breek JC, Zeebregts CJ. Carotid plaque formation and serum biomarkers. . Atherosclerosis. 2010 Nov;213(1):21-9. Epub 2010 May 19.

Hermus L, Schuitemaker JH, Tio RA, Breek JC, Slart RH, de Boef E, Zeebregts CJ. Novel serum biomarkers in carotid artery stenosis: useful to identify the vulnerable plaque? Clin Biochem. 2011 Nov;44(16):1292-8. Epub 2011 Sep 12).

Hohenstein P. and Hastie N.D. (2006). The many facets of the Wilms' tumour gene, WT1. Hum. Mol. Genet. 15, R196-201.

Hrzenjak A, Artl A, Knipping G, Kostner G, Sattler W, Malle E. Silent mutations in secondary Shine-Dalgarno sequences in the cDNA of human serum amyloid A4 promotes expression of recombinant protein in Escherichia coli. Protein Eng. 2001 Dec;14(12):949-52.

Huang H.,Virmani R., Younis H. et al.: The Impact of Calcification on the Biomechanical Stability of Atherosclerotic Plaques. Circulation 2001;103:1051-1056

Huzen J, Peeters W, de Boer RA, Moll FL, Wong LS, Codd V, de Kleijn DP, de Smet BJ, van Veldhuisen DJ, Samani NJ, van Gilst WH, Pasterkamp G, van der Harst P. Circulating leukocyte and carotid atherosclerotic plaque telomere length: interrelation, association with plaque characteristics, and restenosis after endarterectomy. Arterioscler Thromb Vasc Biol. 2011 May;31(5):1219-25. Epub 2011 Mar 3.

Jadlowiec J, Dongell D, Smith J, Conover C, Campbell P. Pregnancy-associated plasma protein-a is involved in matrix mineralization of human adult mesenchymal stem cells and angiogenesis in the chick chorioallontoic membrane. Endocrinology. 2005 Sep;146(9):3765-72. Epub 2005 May 26.

Jialal I, Devaraj S. Role of C-reactive protein in the assessment of cardiovascular risk. Am J Cardiol. 2003;91:200–202.

Kadoglou NP, Sailer N, Moumtzouoglou A, Kapelouzou A, Gerasimidis T, Liapis CD: Aggressive lipid-lowering is more effective than moderate lipid-lowering treatment in carotid plaque stabilization. J Vasc Surg 2010;51:114-21

Kaiser E, Kuzmits R, Pregant P, Burghuber O, Worofka W. Clinical biochemistry of neuron specific enolase. Clin Chim Acta. 1989 Jul 31;183(1):13-31.

Kantor B, Kwon HM, Ritman EL, Holmes DR, Schwartz RS: Images in Cardiology Imaging the coronary microcirculation: 3D micro-CT of coronary vasa vasorum. Int J Cardiovasc Intervent 1999, 2(1):79.

Kern R., Szabo K., Hennerici M. and Meairs S.: Characterization of Carotid Artery Plaques Using Real-time Compound B-mode Ultrasound. Stroke 2004; 35:870

Koenig W. Predicting risk and treatment benefit in atherosclerosis: the role of C-reactive protein. Int J Cardiol 2005; 98:199–206.

Kolodgie F. D., Gold H. K., Burke A. P. et al.: Intraplaque Hemorrhage and Progression of Coronary Atheroma. N Engl J Med 2003;349:2316-25

Kumamoto M, Nakashima Y, Sueishi K: Intimal neovascularization in human coronary atherosclerosis: Its origin and pathophysiological significance. Human Pathology 1995, 26:450-456.

Kumon Y, Suehiro JA, Hashimoto K, Nakatani K, Sipe JD. Local expression of acute phase serum amyloid A mRNA in rhreumatoid arthritis synovial tissue and cells. J Reumatol 1999; 26:785-90.

Kwon H.M., Sangiorgi G, Ritman E.L., McKenna C., Holmes D.R. Jr, Schwartz R.S. and Lerman A. (1998). Enhanced coronary vasa vasorum neovascularization in experimental hypercholesterolemia. J. Clin. Invest. 101, 1551-6.

Kwon HM, Sangiorgi G, Ritman EL, McKenna C, Holmes DR Jr,Schwartz RS, Lerman A: Enhanced coronary vasa vasorum neovascularization in experimental hypercholesterolemia. J ClinInvest 1998, 101(8):1551-1556.

Lammeren G, L Moll F, Borst GJ, de Kleijn DP, P M de Vries JP, Pasterkamp G. Atherosclerotic plaque biomarkers: beyond the horizon of the vulnerable plaque. Curr Cardiol Rev. 2011 Feb;7(1):22-7.

Larsson A, Skoldenberg E, Ericson H. Serum and plasma levels of FGF-2 and VEGF in healthy blood donors. Angiogenesis 2002; 5:107–110.

Li S, J Guo, J Wu, Z Sun, M Han, S Shan, Z Deng, BB Yang, RD Weisel, R Li. microRNA-17 accelerates cardiac matrix remodeling after myocardial infarction by targeting TIMP-1 and TIMP-2. Canadian Journal of Cardiology 2011. vol 27 #180, p124.

Liang JS, Sloane JA, Well JM, Abraham CR, Fine RE,Sipe JD. Evidence for local production of acute phase response apolipoprotein serum amyloid A in Alzheimer's disease brain. Neurosci Lett 1997; 225:73-5.

Liapis CD, Kakisis JD, Kostakis AG. Stroke 2001 Dec 1;32(12):2782-6. Carotid stenosis: factors affecting symptomatology

Libby P, Ridker PM, Maseri A. Inflammation and atherosclerosis. Circulation. 2002;105:1135–1143

Libby P, Theroux P. Pathophysiology of coronary artery disease. Circulation 2005;111:3481– 8.

Lovett J. K., Gallagher P. J., Hands L. J. et al.:Histological Correlates of Carotid Plaque Surface Morphology on Lumen Contrast Imaging. Circulation 2004;110:2190-2197

Lund J, Wittfooth S, Qin QP, Ilva T, Porela P, Pulkki K, Pettersson K, Voipio-Pulkki LM. Free vs total PAPP- A as a predictor of 1-year outcome in patients presenting with non-ST-elevation acute coronary syndrome. Clin Chem. 2010 Jul;56(7):1158-65. Epub 2010 May 6.

Marangos PJ, Schmechel DE. Neuron specific enolase, a clinically useful marker for neurons and neuroendocrine cells. Annu Rev Neurosci. 1987;10:269-95.

Mauriello A, Sangiorgi GM, Virmani R, Trimarchi S, Holmes DR Jr, Kolodgie FD, Piepgras DG, Piperno G, Liotti D, Narula J, Righini P, Ippoliti A, Spagnoli LG. A pathobiologic link between risk factors profile and morphological markers of carotid instability. Atherosclerosis 2010; 208:572–580.

McCully KS. Vascular pathology of homocysteinemia: implications for the pathogenesis of arteriosclerosis. Am J Pathol 1969;56:111–28.

Meng W, Patterson CC, Belton C, Hughes A, McKeown PP. Variants in the nestin gene and coronary heart disease. Circ J. 2008 Sep;72(9):1538-9.

Mofidi R, Powell TI, Crotty T, Mehigan D, Macerlaine D, Keaveny TV. Angiogenesis in carotid atherosclerotic lesions is associated with timing of ischaemic neurological events and presence of computed tomographic cerebral infarction in the ipsilateral cerebral hemisphere. Ann Vasc Surg 2008;22:266e72.

Moreno P.R., Purushothaman K.R., Sirol M., Levy A.P. and Fuster V. (2006). Neovascularization in human atherosclerosis. Circulation. 113, 2245-52.

MRC Asymptomatic Carotid Surgery Trial (ACST) Collaborative Group: Prevention of disabling and fatal strokes by successful carotid endarterectomy in patients without recent neurological symptoms: randomised controlled trial. Lancet 2004; 363: 1491–502

Muller JE, Tawakol A, Kathiresan S, Narula J. New opportunities for identification and reduction of coronary risk: treatment of vulnerable patients, arteries, and plaques. J Am Coll Cardiol. 2006 Apr 18;47(8 Suppl):C2-6

Mulligan-Kehoe M.J. (2010). The vasa vasorum in diseased and nondiseased arteries. Am. J. Physiol. Heart. Circ. Physiol. 298, H295-H305.

Murukesh N,C. Dive, G. C Jayson. Biomarkers of angiogenesis and their role in the development. Br J Cancer. 2010 January 5; 102(1): 8–18.

Naghavi M, Libby P, Falk E, Casscells SW, Litovsky S, Rumberger J, Badimon JJ, Stefanadis C, Moreno P, Pasterkamp G, Fayad Z, Stone PH, Waxman S, Raggi P, Madjid M, Zarrabi A, Burke A, Yuan C, Fitzgerald PJ, Siscovick DS, de Korte CL, Aikawa M, Airaksinen KE, Assmann G, Becker CR, Chesebro JH, Farb A, Galis ZS, Jackson C, Jang IK, Koenig W, Lodder RA, March K, Demirovic J, Navab M, Priori SG, Rekhter MD, Bahr R, Grundy SM, Mehran R, Colombo A, Boerwinkle E, Ballantyne C, Insull W Jr, Schwartz RS, Vogel R, Serruys PW, Hansson GK, Faxon DP, Kaul S, Drexler H, Greenland P, Muller JE, Virmani R, Ridker PM, Zipes DP, Shah PK, Willerson JT. From vulnerable plaque to vulnerable patient: a call for new definitions and risk assessment strategies: Part II. Circulation. 2003 Oct 14;108(15):1772-8.

Nickenig G, Harrison DG. The AT1-type angiotensin receptor in oxidative stress and atherogenesis: part I: oxidative stress and atherogenesis. Circulation.2002;105:393–396.

Niemi K, Baumann MH, Kovanen PT, Eklund KK. Serum amyloid A (SAA) activates human mast cells which leads into degradation of SAA and generation of an amyloidogenic SAA fragment. Biochim Biophys Acta. 2006 Apr;1762(4):424-30. Epub 2006 Jan 27.

North American Symptomatic Carotid Endarterectomy Trial Collaborators. Beneficial effect of carotid endarterectomy in symptomatic patients with high-grade stenosis. N Engl J Med 1991; 325: 445–53.

O'Brien KD, McDonald TO, Chait A, Allen MD, Alpers CE. Neovascular expression of E-selectine, intercellular adhesion molecule-1, and vascular cell adhesion molecule-1 in human atherosclerosis and their relation to intimal leukocyte content. Circulation 1996; 93:672.

O'Leary DH, Reuwer AQ, Nissen SE, Després JP, Deanfield JE, Brown MW, Zhou R, Zabbatino SM, Job B, Kastelein JJ, Visseren FL; AUDITOR investigators. Effect of rimonabant on carotid intima-media thickness (CIMT) progression in patients with abdominal obesity and metabolic syndrome: the AUDITOR Trial. Heart. 2011 Jul;97(14):1143-50. Epub 2011 May 24.

Oikawa H., Hayashi K., Maesawa C., Masuda T. and Sobue K. (2010) Expression profiles of nestin in vascular smooth muscle cells in vivo and in vitro. Exp. Cell. Res. 316, 940-50.

Orrico C, Pasquinelli G, Foroni L, Muscarà D, Tazzari PL, Ricci F, Buzzi M, Baldi E, Muccini N, Gargiulo M, Stella A. Dysfunctional vasa vasorum in diabetic peripheral artery obstructive disease with critical lower limb ischaemia. Eur J Vasc Endovasc Surg. 2010 Sep;40(3):365-74. Epub 2010 Jun 1.

Pacilli, A. Characterization of vascular wall progenitor cells and their role in therapeutic angiogenesis and Monckeberg's sclerosis. Doctoral thesis, 2011, http://amsdottorato.cib.unibo.it/3511/

Pasceri V, Willerson JT, Yeh ET. Direct proinflammatory effect of C-reactive protein on human endothelial cells. Circulation. 2000;102:2165–2168

Pasquinelli G, Pacilli A, Alviano F, Foroni L, Ricci F, Valente S, Orrico C, Lanzoni G, Buzzi M, Luigi Tazzari P, Pagliaro P, Stella A, Paolo Bagnara G. Multidistrict human mesenchymal vascular cells: pluripotency and stemness characteristics. Cytotherapy. 2010 May;12(3):275-87

Pearson TA, Mensah GA, Alexander RW, Anderson JL, Cannon RO, Criqui M, Fadl Y, Fortmann SP, Hong Y, Myers GL, Rifai N, Smith SC, Taubert K, Tracy RP, Vinicor F. Markers of inflammation and cardiovascular disease-application to clinical and public health practice. Circulation. 2003;107:499–511.

Pelizzoli R., Tacchetti C., Luzzi P., Strangio A., Bellese G., Zappia E. and Guazzi S. (2008). TTF-1/NKX2.1 up-regulates the in vivo transcription of nestin. Int. J. Dev. Biol. 52, 55-62.

Pradhan S, Sumpio B. Molecular and biological effects of hemodynamics on vascular cells. Front Biosci. 2004 Sep 1;9:3276-85.

Qin QP, Laitinen P, Majamaa-Voltti K, Eriksson S, Kumpula EK, Pettersson K 2002 Release patterns of pregnancy associated plasma protein A (PAPP-A) in patients with acute coronary syndromes. Scand Cardiovasc J 36:358-61.

R Rosamond W, Flegal K, Friday G et al; American Heart Association Statistics Committee and Stroke Statistics Subcommittee.Heart disease and stroke statistics--2007 update: a report from the American Heart Association Statistics Committee and Stroke Statistics Subcommittee.Circulation. 2007;115:e69-171.

Ramasamy K., Dwyer-Nield L.D., Serkova N.J., Hasebroock K.M., Tyagi A., Raina K., Singh R.P., Malkinson A.M. and Agarwal R. (2011) Silibinin Prevents Lung Tumorigenesis in Wild-Type but not in iNOS−/− Mice: Potential of Real-Time Micro-CT in Lung Cancer Chemoprevention Studies. Clin. Cancer. Res. 17, 753-61.

Redgrave J.N.E., Lovett J. K., Gallagher P. J., Rothwell P.M. Histological Assessment of 526 Symptomatic Carotid Plaques in Relation to the Nature and Timing of Ischemic Symptoms: The Oxford Plaque Study. Circulation 2006;113:2320-2328

Renier G, Clément I, Desfaits AC, Lambert A. Direct stimulatory effect of insulin-like growth factor-I on monocyte and macrophage tumor necrosis factor-alpha production. Endocrinology. 1996 Nov;137(11):4611-8.

Richardson PD, Davies MJ, Born GV. Influence of plaque configuration and stress distribution on fissuring of coronary atherosclerotic plaques. Lancet 1989; 2:941-944. CrossRefMedline

Ridker PM, Hennekens CS, Buring JE, Rifai N. C-reactive protein and other markers of inflammation in the prediction of cardiovascular disease in women. N Engl JMed 2000; 342:826-43.

Ridker PM, Rifai N, Rose L, Buring JE, Cook NR. Comparison of C-reactive protein and low-density lipoprotein cholesterol levels in the prediction of first cardiovascular events. N Engl J Med 2002; 347:1557–1565.

Ridker PM. Clinical application of C-reactive protein for cardiovascular disease detection and prevention. Circulation. 2003;107:363–369

Ritman E.L. and Lerman A. (2007). The dynamic vasa vasorum. Cardiovasc. Res. 75, 649-58.

Rosenson RS, Hislop C, Elliott M, Stasiv Y, Goulder M, Waters D. Effects of Varespladib Methyl on Biomarkers and Major Cardiovascular Events in Acute Coronary Syndrome Patients. J Am Coll Cardiol. 2011 Mar 29;57(13):1501.

Ross R.: The pathogenesis of atherosclerosis: a perspective for the 1990s. Nature 1993; 801-809

Saito A, Shimizu H, Doi Y, Ishida T, Fujimura M, Inoue T, Kiwada H, Tominaga T. Immunoliposomal drug-delivery system targeting lectin-like oxidized low-density lipoprotein receptor-1 for carotid plaque lesions in rats. J Neurosurg. 2011 Oct;115(4):720-7. Epub 2011 Jun 17.

Sangiorgi G, Mauriello A, Bonanno E, Oxvig C, Conover CA, Christiansen M, Trimarchi S, Rampoldi V, Holmes DR Jr, Schwartz RS, Spagnoli LG. Pregnancy-associated plasma protein-a is markedly expressed by monocyte-macrophage cells in vulnerable and ruptured carotid atherosclerotic plaques: a link between inflammation and cerebrovascular events. J Am Coll Cardiol. 2006 Jun 6;47(11):2201-11. Epub 2006 May 15.

Sassen S, E. A. Miska, C. Caldas. MicroRNA—implications for cancer. Virchows Arch. 2008 January; 452(1): 1–10

Sayed D, M Abdellatif. MicroRNAs in development and disease. Physiol Rev. 2011 Jul;91(3):827-87

Schaar JA, Muller JE, Falk E, Virmani R, Fuster V, Serruys PW, Colombo A, Stefanadis C, Ward Casscells S, Moreno PR, Maseri A, van der Steen AF. Terminology for high-risk and vulnerable coronary artery plaques. Report of a meeting on the vulnerable plaque, June 17 and 18, 2003, Santorini, Greece. Eur Heart J. 2004 Jun;25(12):1077-82.

Scholz H, Wagner KD, Wagner N. Role of the Wilms' tumour transcription factor, Wt1, in blood vessel formation. Pflugers Arch. 2009 Jun;458(2):315-23. Epub 2008 Dec 4.

Setacci C, G. de Donato, E. Chisci, F. Setacci, A. Stella, G. Faggioli, B. Reimers,C. Cernetti, M.J. Lopera Quijada, B. Cappi and G. Sangiorgi. Deferred Urgency Carotid Artery Stenting in Symptomatic Patients: Clinical Lessons and Biomarker Patterns from a Prospective Registry Eur J Vasc Endovasc Surg 35, 644e651 (2008).

Somma MC, Fusco A. Enolasi Neurono-Specifica (NSE). Caleidoscopio Italiano 1999.

Stary HC, Chandler AB, Dinsmore RE, Fuster V, Glagov S, Insull W Jr, Rosenfeld ME, Schwartz CJ, Wagner WD, Wissler RW. A definition of advanced types of atherosclerotic lesions and a histological classification of atherosclerosis: a report from the Committee on Vascular Lesions of the Council on Arteriosclerosis, American Heart Association. Circulation 1995; 92:1355-1374.

Steinberg D. Lewis A. Conner Memorial Lecture. Oxidative modification of LDL and atherogenesis. Circulation 1997 Feb 18;95(4):1062-71.

Takaya N, Yuan C, Chu B, Saam T, Underhill H, Cai J, Tran N, Polissar NL, Isaac C, Ferguson MS, Garden GA, Cramer SC, Maravilla KR, Hashimoto B, Hatsukami TS. Association between carotid plaque characteristics and subsequent ischemic cerebrovascular events: a prospective assessment with MRI--initial results. Stroke. 2006 Mar;37(3):818-23. Epub 2006 Feb 9

Tang TY, Howarth SP, Miller SR, Graves MJ et al.: The ATHEROMA (Atorvastatin Therapy: Effects on Reduction of Macrophage Activity) Study. Evaluation using ultrasmall superparamagnetic iron oxide-enhanced magnetic resonance imaging in carotid disease. J Am Coll Cardiol. 2009 Jun 2;53(22):2039-50.

Tebo JF, Mortensen RF. Internalization and degradation of receptor bound C-reactive protein by U-937 cells: induction of H2O2 production and tumoricidal activity. Biochim Biophys Acta. 1991;1095:210–216.

Teranishi N, Naito Z, Ishiwata T, Tanaka N, Furukawa K, Seya T, Shinji S, Tajiri T. Identification of neovasculature using nestin in colorectal cancer. Int J Oncol. 2007 Mar;30(3):593-603.
The Heart Outcomes Prevention Evaluation (HOPE) 2Investigators Homocysteine lowering with folic acid and B vitamins in vascular disease. The New England journal of medicine. 2006;354:1567–1577. [PubMed]

Thompson D, Pepys MB, Wood SP. The physiological structure of human C-reactive protein and its complex with phosphocholine. Structure. 1999;7:169–177

Treasure C. B., et al.: Beneficial effects of cholesterol-lowering therapy on thr coronary endothelium in patients with coronary arthery disease. N Eng J Med 1995; 332:481

Ueland PM. Citation classic: importance of chemical reduction in plasma and serum homocysteine analysis. Clin Chem 2008;54:1085– 6.

Vasan RS. Biomarkers of cardiovascular disease: molecular basis and practical considerations. Circulation. 2006 May 16;113(19):2335-62.

Venugopal SK, Devaraj S, Jialal I. C-reactive protein decreases prostacyclin release from human aortic endothelial cells. Circulation. 2003;108: 1676–1678.

Venugopal SK, Devaraj S, Yuhanna I, Shaul P, Jialal I. Demonstration that C-reactive protein decreases eNOS expression and bioactivity in human aortic endothelial cells. Circulation. 2002;106:1439–1441.

Virmani R, Burke AP, Kolodgie FD, Farb A. Pathology of the Thin-Cap Fibroatheroma: A Type of Vulnerable Plaque. Journal of Interventional Cardiology 2003; 16:267

Virmani R, Burke AP, Kolodgie FD, Farb A.: Pathology of the Vulnerable Plaque.Journal of the American College of Cardiology 2006; 47:C13.

Virmani R, Kolodgie FD, Burke AP, Farb A, Schwartz SM. Lessons from sudden coronary death: a comprehensive morphological classification scheme for atherosclerotic lesions. Arterioscler Thromb Vasc Biol. 2000 May;20(5):1262-75.

Virmani R. et al.: Atherosclerotic Plaque Progression and Vulnerability to Rupture: Angiogenesis as a Source of Intraplaque Hemorrhage. Arterioscler Thromb Vasc Biol 2005;25;2054-2061

Wagner N., Panelos J., Massi D. and Wagne K.D. (2008). The Wilms' tumor suppressor WT1 is associated with melanoma proliferation. Pflugers. Arch. 455, 839-47.

Wagner N., Wagner K.D., Scholz H., Kirschner K.M. and Schedl A. (2006). Intermediate filament protein nestin is expressed in developing kidney and heart and might be regulated by the Wilms' tumor suppressor Wt1. Am. J. Physiol. Regul. Integr. Comp. Physiol. 291, R779-87.

Wang X, Connolly TM. Biomarkers of vulnerable atheromatous plaques: translational medicine perspectives. Adv Clin Chem. 2010;50:1-22.

Wasserman B. A., Sharrett A. R., Lai S. et al.: Risk Factor Associations With the Presence of a Lipid Core in Carotid Plaque of Asymptomatic Individuals Using High-Resolution MRI: The Multi-Ethnic Study of Atherosclerosis (MESA). Stroke 2008;39;329-335

Watanabe K, Sugiyama S, Kugiyama K, Honda O, Fukushima H, Koga H, Horibata Y, Hirai T, Sakamoto T, Yoshimura M, Yamashita Y, Ogawa H. Stabilization of carotid atheroma assessed by quantitative ultrasound analysis in nonhypercholesterolemic patients with coronary artery disease. J Am Coll Cardiol. 2005; 46: 2022–2030.

Williams TN, Zhang CX, Game BA, He L, Huang Y. C-reactive protein stimulates MMP-1 expression in U937 histiocytes through Fc[gamma]RII and extracellular signal-regulated kinase pathway: an implication of CRP involvement in plaque destabilization. Arterioscler Thromb Vasc Biol.2004;24:61–66.

Yanagawa B., F Lovren, M Peterson, A Quan, L Errett, D Latter, D Bonneau, S Verma. Novel gene expression changes in bicuspid aortic valves. Canadian Journal of Cardiology 2011. vol 27 #711;p324.

Yasojima K, Schwab C, McGeer EG, McGeer PL. Generation of C-reactive protein and complement components in atherosclerotic plaques. Am J Pathol. 2001;158:1039–1051.

RINGRAZIAMENTI:

Vorrei ringraziare innanzitutto il prof. Andrea Stella che mi ha affidato questo progetto di ricerca approvandone il suo continuo svolgimento.

Come non ringraziare il prof. Gianandrea Pasquinelli per avermi introdotto nel gruppo di ricerca dove ho completato il mio percorso di apprendimento aiutandomi con i suoi consigli, il suo sostegno e soprattutto la sua fiducia.

Un grazie alle dott.sse Francesca Papadopulos che dai primi giorni in laboratorio ha saputo coinvolgermi in tutte le attività.
Non posso inoltre non ricordare tutte le mie domande e i miei dubbi posti continuamente al dott.ssa Annalisa Pacilli (wikiAnna), che sapeva rispondermi, spiegarmi pazientemente e consigliarmi in qualsiasi momento, e su qualsiasi argomento! Grazie!
E come non ringraziare la dott.ssa Elisa Brighenti (maestro Shifu XM) per la sua carica positiva e il dott. Carmine Onofrillo (Onofrix), la dott.ssa Laura Rocchi, la dott.ssa Marianna Penzo, la Dott.ssa Sabrina Valente e la Dott.ssa Daniela Pollutri, per i consigli.....e le risate!
Il nascere e lo svolgimento di questo lungo progetto è dipeso da due colleghi dotati di grande professionalità ma anche ironia! IL dott. Rodolfo Pini che è stato sempre presente e il dott. Francesco Vasuri ormai parte integrante delle mie giornate!
La fase linguistica della tesi è stata attuata grazie all'aiuto della dott.ssa Teresa Filizzola che nonostante gli impegni lavorativi ha dedicato il suo tempo libero alla correzioni di alcuni parti della tesi ma soprattutto a diversi articoli!
Quando stringeva il tempo nella preparazione della tesi, sono stati presenti degli aiuti fondamentali! Mia madre che ha preso parte a

tutto lo svolgimento scientifico di fianco a mio padre...e mia zia, la dott.ssa Mariella Fittipaldi e mio zio, Federico.
Niente sarebbe stato possibile senza i saggi consigli di mia nonna e della mia famiglia.
A tutti gli amici sempre vicini dal primo anno...vi ringrazierò uno a uno...a VOCE!